Identifying functional interactors of the retinal transcription factor, *Vsx2* during early retinal development

By

Amanda M. Leung

Dissertation

Submitted to the Faculty of the

Graduate School of Vanderbilt University

In partial fulfillment of the requirements

For the degree of

DOCTOR OF PHILOSOPHY

In

Cell & Developmental Biology

August 11th, 2023

Nashville, Tennessee

Approved by:

Christopher Wright, D. Phil

Tonia Rex, Ph.D.

Ken Lau, Ph.D.

James Patton, Ph.D.

Pampee Young, M.D., Ph.D.

Edward Levine, Ph.D.

TABLE OF CONTENTS

Page

LIST OF TABLES

Page

LIST OF FIGURES

CHAPTER 1

INTRODUCTION

Clinical Relevance of *VSX2*

VSX2, previously known as *CHX10*, is a paired-like CVC domain containing homeobox gene important in the proper development of the visual system. *Vsx2* has conserved roles in visual system development from worms to humans (Chen and Cepko, 2000; Iseri et al., 2010; Percin et al., 2000; Smirnov et al., 2022; Svendsen and McGhee, 1995). Mutations in *VSX2* lead to anophthalmia/microphthalmia, congenital blindness, cataracts, retinal detachment, coloboma and more recently congenital stationary night blindness (Iseri et al., 2010; Percin et al., 2000; Smirnov et al., 2022); making *VSX2* an important factor for retina and eye development. Patients afflicted with *VSX2* mutant alleles are usually found in consanguineous families as inherited autosomal recessive mutations. It is undeniable that *VSX2* is crucial for proper eye development, primarily through its role as a regulator of retinal development.

Description of the Retina

The retina is a thin, multilayered epithelial tissue, derived from the embryonic diencephalon, located at the back of the eye. Through an intricate connection of cells, the retina allows for light energy to be converted into shapes and patterns that are interpreted by the brain as vision. The most basal layer of the retina known as the inner limiting membrane serves as the boundary between the retina and an aqueous medium, the vitreous body, that constitutes the majority mass of the eyeball. On the apical side of the retina is a highly pigmented, epithelial monolayer of cells called the retinal pigmented epithelium (RPE). The RPE facilitates the light transmission function of the retina and supports the health of the photoreceptors through the

renewal of photoreceptor outer segments, the commencement location of light transmission (Yang et al., 2021). (Fig 1a)

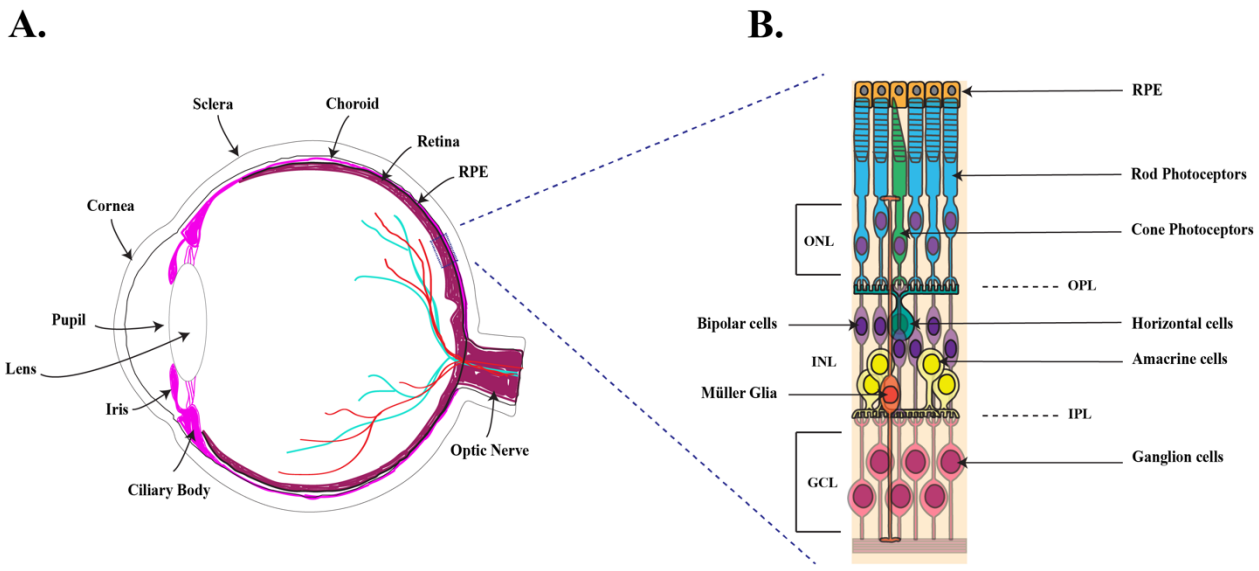

Figure 1. Eye Structure and Retinal Layers. A) Fully formed eye structure with arrow pointing to the location of the retina within the eye connecting to a B) inset box showing the cross section through the retina and detailing the layers and cell types within.

The retina is comprised of seven different cell types: six different types of neurons and one type of glia. These different cell types are well organized into three distinct nuclear layers, separated by two plexiform layers where synaptic connections are made. The different cell types are born in a distinct chronological sequence that is conserved across vertebrates. The cell types are generated in an overlapping sequence as follows: ganglion cells, cones, horizontal cells and amacrine cells, followed by rods, bipolar cells and Müller glia (Miale and Sidman, 1961; Prada et al., 1991; Rapaport et al., 2004; Vail et al., 1991). All the cell types of the retina work in a harmonious concert to deliver light information to the brain. Light enters through the anterior portion of the eye, passing through the cornea, lens and iris all working to reduce scatter as the light makes its way through the vitreal cavity to the posterior eye so the photons may be detected by the photoreceptors (rods and cones) located in the outer nuclear layer. The photoreceptors

then convert the light into electric signals which are passed to the ganglion cell layer by a series of interneurons: horizontal, bipolar and amacrine cells. The specific combinations of these transmission connections provide the electrical signals with some initial processing and shaping of the visual image. This image is relayed to the visual cortex in the brain by the long axons of the ganglion cells. These axons exit the back of the eye through the optic nerve via the optic disc. Due to the delicate process of signal transmission, any disruptions in the development and formation of the retina produces serious consequences to the visual process.

The retina is a great model system for cell biology and developmental questions. The amount of cell diversity and complexity within such a small tissue makes the retina an ideal organ to study for questions of development, progenitors, and cell differentiation.

Formation and Maintenance of the Retina

Specification of the Eye Field

The retina is formed from a protuberance of the embryonic diencephalon which begins after neural plate formation. Cells in the neural plate undergo molecular changes that distinguish them from neuroepithelial cells, these molecular changes are known as eye field specification. Located in the medial anterior neural plate, the eye field contains progenitors of the neural derived eye tissue (Heavner and Pevny, 2012). The eye field is specified through the overlapping expression of a distinct set of transcription factors called eye field transcription factors (EFTFs) (Fig. 2A)((Zuber et al., 2003). Not all EFTFs are the same in their requirements amongst vertebrate models (Martinez-Morales, 2016). However, there seems to be a conserved set of EFTFs that are necessary in most models tested: *Rx*, *Pax6*, *Six3, Otx2* (Sinn and Wittbrodt, 2013). Additionally, *Lhx2* is an essential transcription factor for eye development in mammals. Studies have shown that this LIM- homeodomain transcription factor is necessary for eye

development. In LHX2-null mice eye development is halted at the optic vesicle stage, conditional knock-outs at different stages of development demonstrated that *Lhx2* is necessary for optic identity (Porter et al., 1997; Roy et al., 2013; Tétreault et al., 2009; Yun et al., 2009). During the early stages of patterning the identity of individual presumptive tissue domains remain dynamic due to the continued signaling needed to maintain tissue identity through the expression of domain specific transcription factors. Regions in the eye field stage are not defined by rigid tissue borders. Rather the cells in each region are 'primed' for their future tissue identities, but these regions remain dynamic at the eye field stage as transfers of precursor cells between regions have been observed (Martinez-Morales, 2016; Picker et al., 2009). Simultaneously, as intricate molecular signaling of specification and regionalization is happening in the anterior neural plate, the eye field is growing laterally towards the overlying surface ectoderm (Fig. 2). Once folding of the ocular compartment is completed the identity of the tissue becomes stabilized through established precursor populations (Fig. 2C). Stable cell populations arise through reciprocal repression at the transcript level, creating boundaries that divide the prospective eye into different tissues: optic stalk (OS), neural retina (NR), and retinal pigmented epithelium (RPE) (Martinez-Morales, 2016).

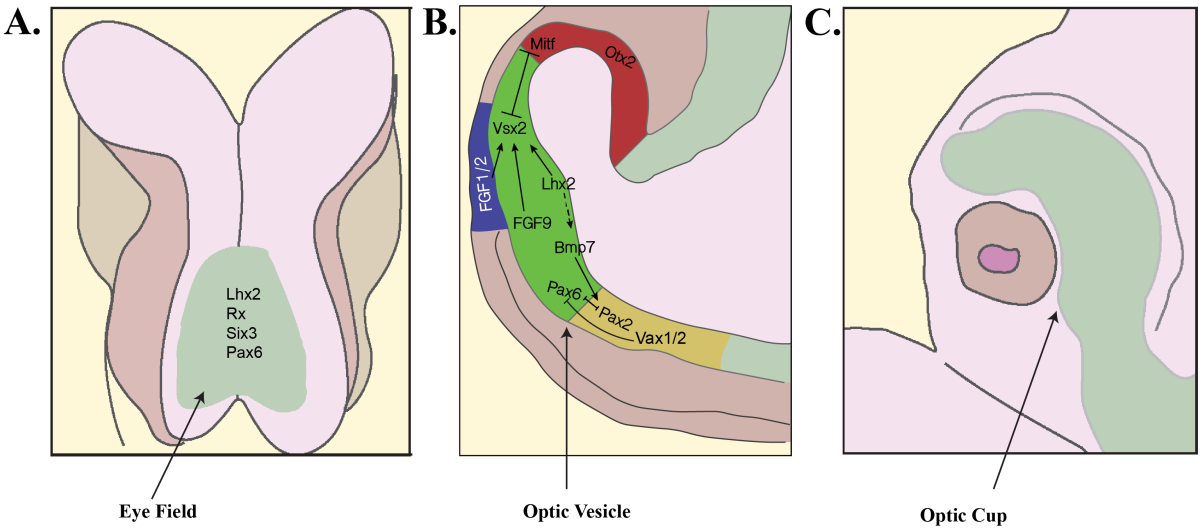

Figure 2. Early Eye Development. A) panel showing the structure of the forebrain and expression of the eye field and associated EFTFs. B) panel showing expression domains within the late optic vesicle C) panel showing the early optic cup.

Optic Vesicle Formation and Patterning

As the eye field expands laterally, it begins to bifurcate at the midline enabling the formation of two separate eyes (Fig. 2A). This evagination of the eye field forms two optic vesicles on either side of the head region (Fig. 2B) (Adler and Canto-Soler, 2007). The process of evagination begins with two grooves (optic sulci) that appear on either side of the expanded eye field, and by the time the optic vesicles are formed the neural tube has closed (Chow and Lang, 2001). During optic vesicle formation cells take on a new shape; changing from cuboidal, to columnar and then to a narrowed wedge shape at an apical point along the extended surface of the neuroepithelium as it takes shape into an optic vesicle (Svoboda and O'Shea, 1987).

The optic vesicle becomes filled with undefined precursor/progenitor cells known as optic neuroepithelial cells. These cells will give rise to mature eye structures: optic stalk, neural retina and RPE. In mice, this stage takes place at ~E9.5 (Heavner and Pevny, 2012). Through

patterning of the optic vesicle mostly along the dorsal-ventral axis the optic neuroepithelial cells within it start to take on different characteristics.

Lhx2 is a LIM homeobox gene and its expression is initiated by EFTFs in the optic neuroepithelium (Heavner and Pevny, 2012). *Lhx2* helps to connect inductive signals with regional and axial determinants. Yun et al. (2009) showed that regionalization is nonexistent in *Lhx2* null mice and dorso-ventral patterning is not completed providing strong evidence that *Lhx2* is necessary for mediating these patterning events in the OV. *Lhx2* is thought to regulate regionalization and patterning of the optic vesicle through regulation of BMP signaling, either through regulation of ligand expression or somewhere in the pathway itself (Yun et al., 2009). *Lhx2* is also thought to be necessary for the expression of *Tbx5*, *Vsx2* and *Mitf.* When BMP treatment was applied to *Lhx2*-null head cultures none of the above were expressed (Yun et al., 2009). Retinal and RPE identity are closely tied to *Lhx2* expression as both *Vsx2* and *Mitf* are likely direct transcriptional targets of *Lhx2* (Sigulinsky et al., 2015; Yun et al., 2009).

Sonic Hedgehog (Shh) signaling at the optic vesicle stage has the highest impact on the ventral patterning, facilitating the expression of *Pax2*, *Vax1* and *Vax2* (Cardozo et al., 2020). Homeobox genes such as *Pax2*, *Vax1* and *Vax2* are expressed strictly in the ventral region of the optic vesicle (Mui et al., 2005; Ohsaki et al., 1999; Take-uchi et al., 2003). Initially, *Pax6* is expressed throughout the optic vesicle, but over time its expression becomes restricted to the dorsal optic vesicle (Bäumer et al., 2003; Schwarz et al., 2000; Walther et al., 1991)*Pax2* and *Pax6* are initially co-expressed throughout the optic vesicle, but due to their mutual transcriptional repression they become expressed in opposite regions along the dorso-ventral axis (Bäumer et al., 2003; Schwarz et al., 2000). *Pax6* is repressed by *Vax1* and *Vax2* (Mui et al., 2005) which helps distinguish the boundary between the retina and optic stalk.

The most distal point of the optic vesicle is patterned to become the neural retina (NR). While the proximal-ventral region becomes the optic stalk (OS), the dorsal region of the vesicle

that link the two together is patterned to become the RPE (Fig. 2B). The NR is marked by the expression of *Vsx2,* the OS is marked by the expression of the transcription factor Pax2, while the future RPE is distinguished by *Mitf* expression (Fuhrmann, 2010; Kim and Kim, 2012; Martinez-Morales, 2016). By the late optic vesicle stage two different coordinated processes are happening simultaneously: the optic vesicle is patterned for the future tissues it will generate, and cells are changing shape and moving into new positions which allows for the formation of the optic cup (Fig. 2B).

Formation of the Optic cup

After the late optic vesicle stage, the optic neuroepithelium shape shifts again in a coordinated morphogenetic movement to form the optic cup. Usually, this occurs when the distal most region of the optic vesicle encounters the overlying surface ectoderm. This contact point between the surface ectoderm and the underlying optic vesicle forms the lens placode which is the precursor to the lens. At this point, a coordinated set of cellular movements and signaling causes the most distal point of the optic vesicle (presumptive NR) to invaginate forming the inner most surface of the optic cup. The inner most layer begins to thicken from cells elongating, packing, and proliferating (Graw, 2010) (Fig. 2C). The outer surface of the optic cup is formed by the naïve progenitors of the RPE, which begin to take on the columnar shape of the mature monolayer. The optic stalk remains connected to the emerging cup and serves as the foundation for the formation of the optic nerve.

Wnt signaling begins to be important once the optic cup is clearly specified and further divisions in peripheral versus central retinal character must be made. The peripheral optic cup is the region of the retina where the hinge domain forms, which is important for optic cup folding at the margins (Martinez-Morales et al., 2017). The peripheral optic cup is also the region where the ciliary marginal zone forms (CMZ) giving rise to the ciliary body and the iris. These two

events rely heavily on Wnt signaling (Cardozo et al., 2020). (Carpenter et al., 2015) showed that genetic inactivation of *Wntless* resulting in lack of Wnt secretion caused abnormalities in optic cup folding. A Wnt signaling component, *ß-catenin*, has been shown to be necessary for peripheral retina identity (Liu et al., 2007). Conversely, if canonical Wnt signaling is activated in the central retina the result is peripheral characteristics (Cho and Cepko, 2006).

BMPS are highly expressed in the dorsal region of the tissue. Experiments in chick have shown that *Bmp4* expression is restricted to the dorsal optic cup by Shh signaling, the interaction between BMP and Shh is thought to be responsible for the creation of dorsal and ventral compartments in the optic cup (Zhang and Yang, 2001). *Bmp4* facilitates expression of T-box family members and specifically *Tbx5* which help to define the dorso-ventral boundary in the mouse optic cup (Behesti et al., 2006). BMP signaling has also been shown to be necessary for retinal development in mice. Huang et al. 2015 showed that *Bmp4* null embryos lack a neural retina, while other studies showed homozygous inactivation of BMP receptors: 1a and 1b eliminates retinal formation, and heterozygous expression results in a retina with more ventral characteristics (Cardozo et al., 2020; Murali et al., 2005).

Establishment and maintenance of Retinal identity

Although, a retinal domain is first established in the optic vesicle around E8.5 in mice, (Heavner and Pevny, 2012) signaling, patterning and the consistent expression of various transcription factors to play a role in creating retinal identity. The lens placode, which orginiates from the surface ectoderm, acts as a signaling center for the retina. Studies in chick have shown that the lens placode is such an important signaling hub for *FGFs*; 1, 2, and 8; that if the overlying surface ectoderm is removed from the optic vesicle the neural retina is never specified (Hyer et al., 1998). However, this phenotype can be rescued by implantation of FGF-soaked beads or viral expression of Fgf (Hyer et al., 1998). These signals activate Ras-dependent

MAPK signal in the distal portion of the optic vesicle, which in turn leads to establishment of the neural retina domain of mouse (Zhao et al., 2001). FGF signaling is important for neural retina specification due to its activation of *Vsx2* (Fig. 2B). FGFs secreted from the surface ectoderm are responsible for activation of *Vsx2,* which demarcates the neural retina domain (Gamm et al., 2019; Horsford et al., 2005; Nguyen and Arnheiter, 2000). Subsequently, *Vsx2* expression represses the RPE determinant, *Mitf*, from being expressed in the retina (Horsford et al., 2005). Early inactivation of *Shp2*, involved in the activation of FGF signaling permitted the expansion of *Mitf*, in turn expanding the RPE at the expense of the retina (Cai et al., 2010). In the absence of FGF signals, the neuroretina domain is converted into an epithelial pigmented monolayer (Nguyen and Arnheiter, 2000).

There is contrary evidence from chick showing at the optic vesicle stage only BMP signaling from the lens ectoderm induces retinal identity, with no effect at all from FGFs (Pandit et al., 2015). Another study in mice confirms that *Bmp4* from the distal optic vesicle specifies the retina in the optic cup of mouse embryos (Huang et al., 2015a). In a subsequent study, (Huang et al., 2015b), showed that inhibition of BMP signaling in the lens ectoderm disrupts BMP signaling in the optic cup via upregulated BMP ligands in the lens placode. The result was inhibited lens and optic vesicle development through the disruption of the BMP gradient in the optic vesicle (Huang et al., 2015b).

Establishment of retinal identity requires a unique combination of FGF and BMP signaling at the intersection of the surface ectoderm and the optic vesicle at the distal tip of the optic vesicle. Maintenance of retinal identity requires correct formation of the optic vesicle and morphogenesis into an optic cup. From the optic vesicle stage, the retinal domain becomes clear by the expression of *Vsx2*, and this expression is maintained within retinal progenitors until progenitors begin to divide and differentiate into mature cell types, apart from bipolar cells

which continue to express *Vsx2*. *Vsx2* expression is maintained in the retinal domain of the optic cup through *Lhx2* and FGF signaling (Nguyen and Arnheiter, 2000; Yun et al., 2009).

Retinal progenitors

RPC Proliferation and cell-cycle dynamics

Proliferation is what drives the growth of a tissue during development. Simply put, proliferation is all about the increase in cell number of a tissue which is driven by the cell cycle and controlled via gene expression. Within a tissue, progenitors have the responsibility to balance cell division with maintenance of the progenitor pool to ensure that the correct number of cells are created over time without depleting the progenitor pool before the tissue is fully formed.

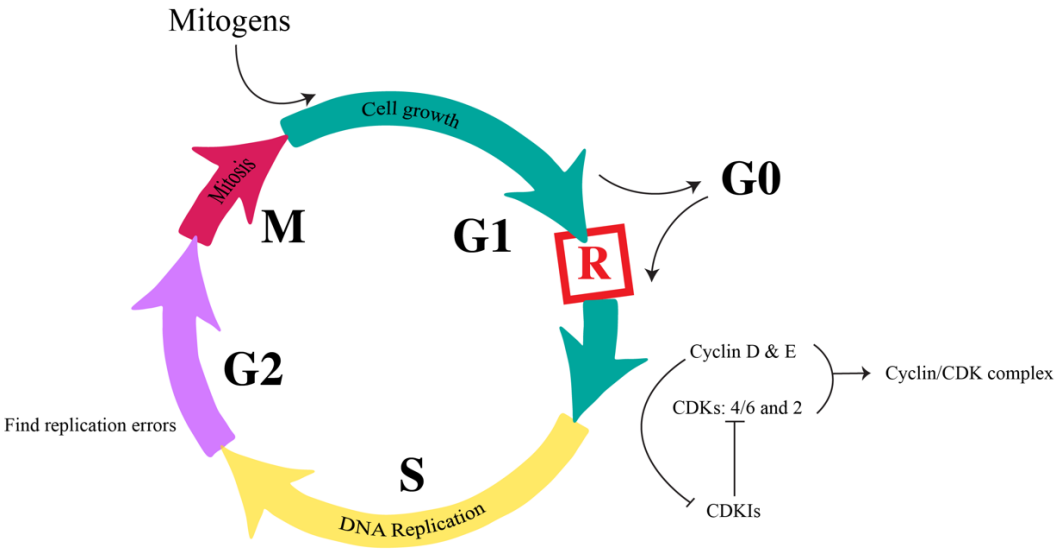

Figure 3. Cell Cycle diagram. Figure showing each phase of the cell cycle, arrows indicate sequence of phases. Cyclin and Cdk activation indicates activity necessary for G1 to S phase progression.

Retinal progenitors are subject to the somatic cell cycle (Fig. 3). Each phase is regulated in a tissue dependent manner. Each somatic cell cycle during development is moving the proliferating progenitor cell between S and M phase to achieve tissue growth and maturity. S phase is the replication phase where the cell genome is replicated. M phase is the mitotic phase of the cell cycle where the proliferating cell divides into two daughter cells through the process of mitosis. In between these are two gap phases: G1 and G2. The G2 phase exists so the cell may discover any DNA replication errors before heading into mitosis. G1 phase is for the growth of the cell, but this is the phase where signals have the largest impact on whether the progenitor exits or continues the cell cycle. G1 is divided into early G1 and late G1. In early G1, progenitors are proliferation-competent cells that require growth-promoting signals to continue through the cell cycle. In late G1, cells have already past the restriction point and no longer depend on growth-promoting mitogen signaling to make it through mitosis (Hardwick et al., 2014; Planas-Silva and Weinberg, 1997).

Early G1 requires input from growth-promoting mitogens, but the cell cycle itself is driven by cyclin-dependent kinases (CDKs) (Levine and Green, 2004). Through distinct expression phases, CDKs help to guide a cell through the cell cycle (Fig. 3). CDKs are regulated by phosphorylation at specific sites by other protein kinases. The phosphorylated CDK then binds its cyclin counterpart to form a functional cyclin-CDK complex. Once the CDK binds the appropriate cyclin, the complex is then targeted to the nucleus where cell-cycle dependent targets are activated (Schafer, 1998). A cell may not enter the next cell cycle phase until the previous cyclin has been degraded and the next phase of cyclins are expressed.

Ultimately, proliferation of the retina or any tissue is regulated at the level of the cell cycle, specifically the decision for a progenitor to reenter the cell cycle. This important decision is made during the G1 phase at a highly regulated restriction point (Giacinti and Giordano, 2006; Levine and Green, 2004; Lundberg and Weinberg, 1999). If cells do not pass the restriction

point, they are pushed into G0 and they exit the cell cycle. Not only are CDKs crucial for progression through G1, but inhibition of CDK-inhibitors (KIP and INK families) is also necessary for cell cycle progression from G1 to S phase. G1 CDKs require the binding of cyclins: D and E for activation, while simultaneously open to inhibition by cyclin-dependent kinase inhibitors (CDKIs). Mitogens promote growth in G1 by upregulating D-cyclins which does two things: 1) activates Cdk4 and or Cdk6, and 2) represses KIP-mediated inhibition of Cdk2: CyclinE complex. Mitogens are cell extrinsic factors that act as messages received by proliferating cells during G1 before the restriction point (Levine and Green, 2004). If cells are not exposed to mitogens in early G1 then cell cycle progression stops, and cells exit the cell cycle (Planas-Silva and Weinberg, 1997). Mitogen exposure after the restriction point is not necessary for further cell cycle progression.

Mitogens are tissue dependent. In the retina, Cyclin D1 expression is driven by: Shh (Jensen and Wallace, 1997; Sakagami et al., 2009; Wang et al., 2005), TGF alpha (Anchan et al., 1991; Lillien and Cepko, 1992) TGF beta-3 (Anchan and Reh, 1995), FGF1 and FGF2 (Lillien and Cepko, 1992), EGF (Anchan et al., 1991; Lillien and Cepko, 1992), VEGF (Hashimoto et al., 2006), NT3/Trk C signaling (Das et al., 2000), and Wnt signaling (Kubo et al., 2003; Kubo et al., 2005; Raay et al., 2005; Sánchez-Sánchez et al., 2010). It is through the initiation and completion of the cell cycle that allows a tissue to grow in cell number. Proliferation serves to make sure that the developing retina amasses enough cells prior to differentiation to ensure that the correct complement of cells exists within the retina. RPC proliferation drives retinal growth, which is important when the retina experiences a 400-fold increase in cells (Alexiades and Cepko, 1996).

Initiating neurogenesis

Neurogenesis in the retina is the process of cell differentiation that generates the cell diversity of the mature retina: six different types of neurons and one type of glia are created during this process. The first postmitotic cells arise in the center of the retina near the optic stalk at the apical edge of the retinal epithelium due to progenitor cell division (Hu and Easter, 1999; Laessing and Stuermer, 1996; Masai et al., 2000; McCabe et al., 1999). The newly born postmitotic ganglion cells migrate to the basal edge of the epithelium (Amini et al., 2018; Morest, 1970). The described pattern of differentiation is known as the wave of neurogenesis (Hu and Easter, 1999; Hufnagel et al., 2010). During their migration to the basal edge the newly postmitotic cells lose their progenitor morphology.

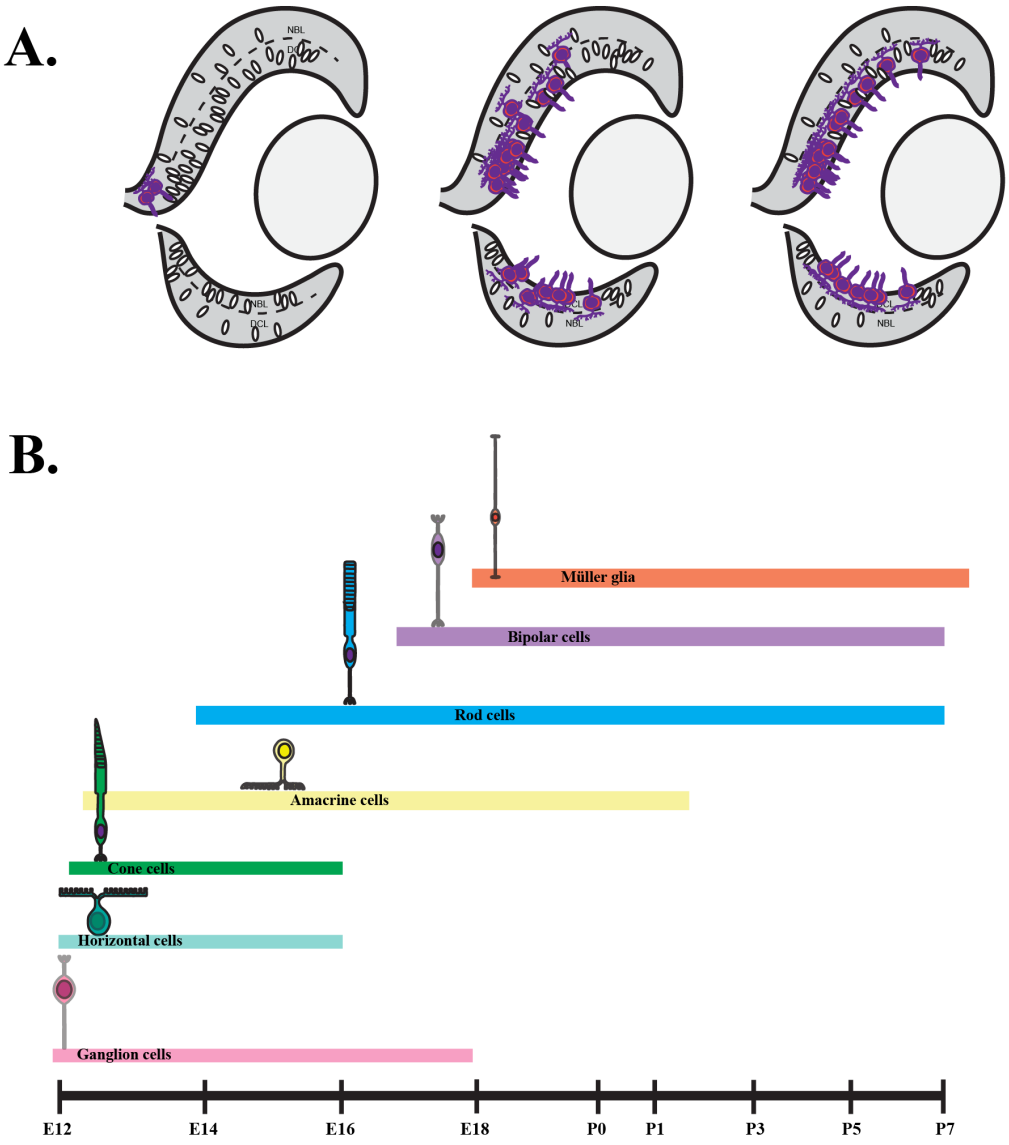

Figure 4. Neurogenesis in the developing retina. A) Illustration showing the location and position of the initiation of neurogenesis and the pattern through which it spreads throughout the retina. B) shows the overlapping consensus sequence of cell types generated throughout the process over the developmental period.

Depending on the time of cell cycle exit a precursor is fated to become a specific neuronal type or glia. The conserved sequence of cell type generation has been heavily studied. The generation of cell types happens in two waves; early born cell types: ganglion cells, cone photoreceptors, horizontal cells and amacrine cells, followed by late born cells: rod photoreceptors, bipolar cells and Müller glia (Bassett and Wallace, 2012; Georgi and Reh, 2010;

Heavner and Pevny, 2012; Rapaport et al., 2004). Not only does retinal neurogenesis produce cell types in a conserved overlapping sequence, but spatial orientation of where this process begins is also conserved within vertebrate organisms: chick, zebrafish, mouse, and xenopus (Hu and Easter, 1999; McCabe et al., 1999; Stiemke and Hollyfield, 1995; Young, 1985). The exact mechanism that initiates neurogenesis in mouse is not fully understood. Hints from chick and zebrafish have suggested that FGFs are the trigger that induce neurogenesis in the central retina (Martinez-Morales et al., 2005), however the closest recapitulation in mouse was inactivation of a downstream FGF signaling target that caused loss of retinal identity (Cai et al., 2010). Evidence suggests there may be other factors at work in initiating neurogenesis. Combinations of bHLH and homeodomain factors are key to cell type specification during neurogenesis (Hatakeyama and Kageyama, 2004; Ohsawa and Kageyama, 2008). Basic helix loop helix genes: *Ngn2* and *Atoh7* are expressed early prior to neurogenesis and their expression mimics that of the wave-like pattern seen during the progression of neurogenesis across the retina (Hufnagel et al., 2010) . Studies have shown that the initial activation of *Atoh7* is facilitated by FGF signaling, *Ngn2* and *Pax6* expression (Hufnagel et al., 2010; Skowronska-Krawczyk et al., 2004; Willardsen et al., 2009). FGF signaling likely regulates expression of *Atoh7* through downstream, FGF- dependent ETS transcription factors (McCabe et al., 2006; Willardsen et al., 2009). NGN2 has been shown to regulate expression of *Atoh7* through direct binding of *Atoh7* regulatory elements (Hutcheson et al., 2005; Skowronska-Krawczyk et al., 2009). Although *Ngn2* expression occurs prior to *Atoh7*, and *Ngn2* is partially responsible for *Atoh7* expression, loss of *Ngn2* does not prevent the expression of *Atoh7*. Loss of *Ngn2* delays both *Atoh7* expression and retinal neurogenesis but does not prevent or grossly change either(Hufnagel et al., 2010) . *Atoh7* is also required by postmitotic precursors for ganglion cell differentiation, and is regulated by *Pax6*, RPBJ*,* FGF and Shh signaling (Marquardt et al., 2001; Miesfeld et al., 2018; Riesenberg et al., 2009a; Willardsen et al., 2009). This demonstrates that many signals, intrinsic

and extrinsic, regulate the birth of the first postmitotic retinal cells and ganglion cell differentiation. The coincidence of signals and timing makes it difficult to parse out the essential factors for initiation of neurogenesis.

A recent study in zebrafish investigated cell division patterns in neurogenic RPCs one cell cycle prior to the generation of post-mitotic neurons (Nerli et al., 2020). They found that neurogenic RPCs arise from asymmetric cell divisions, and that they are distinct from nonneurogenic early RPCs, indicating neurogenic RPCs are an intermediate cell type. There is a clear possibility that cell cycle regulators and progenitor maintenance factors may also play a large role in the initiation of neurogenesis.

Progenitor Maintenance

Progenitor maintenance occurs during neurogenesis as RPC daughter cells remain in the cell cycle for another round of proliferation. Another option available to daughter cells is exit the cell cycle and become a postmitotic precursor, soon to be fated for one of the seven retinal cell types. The option to remain as a progenitor gives the cell full proliferative capacity.

The cell cycle factor, Cyclin D1 has been shown to be an important regulator of progenitor maintenance. Cyclin D1 is expressed in all RPCs throughout neurogenesis (Das et al., 2009). Studies investigating Cyclin D1 knockout mice have shown that not only do RPCs cycle at a slower rate, but they also exhibit early cell cycle exit and differentiation, which carries throughout neurogenesis as postmitotic cells are heavily skewed towards early born cell types (Das et al., 2009; Das et al., 2012). Cyclin D1 may also regulate progenitor maintenance through its transcriptional regulation activity. One of its transcriptional targets, Notch 1, is a key regulator of progenitor maintenance (Bienvenu et al., 2010).

The Notch signaling pathway is known for progenitor cell maintenance in many tissues: gut, CNS, and other tissues (Demitrack and Samuelson, 2016; Henrique et al., 1997; Moore and

Alexandre, 2020). Transient inhibition of Notch signaling with a pharmaceutical inhibitor, DAPT, led to increased cell differentiation at the expense of progenitor maintenance (Nelson et al., 2007). This was seen through decreased cell proliferation most likely due to lowered activity of cell cycle regulators like Cyclin D1 (Nelson et al., 2007). Further investigation into the Notch signaling pathway revealed that inactivation of RbpJ, an essential transcriptional effector, also causes increased cellular differentiation at the expense of maintaining the retinal progenitor pool (Zheng et al., 2009). Other downstream effectors of Notch, *Hes1* and *Hes5*, also play a role in progenitor maintenance. *Hes1* is not only a downstream effector of the Notch pathway but it is also regulated by Sonic Hedgehog (Shh) signaling, an important mitogen for RPCs (Jensen and Wallace, 1997; Levine et al., 1997; Wall et al., 2009). The convergence of both Notch and Shh signaling pathways on *Hes1* is only one example of shared regulation between two signaling pathways. Shh itself also regulates the cell cycle in part through *Cyclin D1* (Locker et al., 2006).

Delineation of signals important for progenitor maintenance and neurogenesis is complicated by the convergence of signaling pathways. It is possible that progenitor maintenance signals and mitogenic signals are not separate in progenitor cells. Both *Hes1* and *Hes5* may act as nodes between signaling pathways that promote progenitor maintenance and neurogensis (Murata et al., 2005; Ohtsuka et al., 1999).

Progenitor maintenance in the retina is also strongly tied to the retinal transcription factors *Lhx2* and *Vsx2*. *Lhx2* is expressed in all RPCs and has a definitive role in progenitor maintenance. Gordon et al. 2012, showed that early inactivation of *Lhx2* encouraged cell cycle exit at the expense of progenitor maintenance leading to a drastic decrease in RPCs. As previously mentioned, studies suggest that *Lhx2* directly regulates the essential retinal identity factor *Vsx2* (Gordon et al., 2013; Sigulinsky et al., 2015). *Vsx2* is thought to have a role in regulating RPC maintenance although, this is contrasted with the observation that RPCs in the Vsx2^{orJ} mouse mutant persist into adulthood (Dhomen et al., 2006; Kokkinopoulos et al., 2008).

These dynamics illustrate a factor important for RPC identity and possibly even progenitor maintenance, as it is down regulated upon cell cycle exit.

The role of Vsx2 in Retinal Development

Vsx2 is a paired-like CVC homeobox gene

Vsx2 is an acronym that stands for visual system homeobox 2. Although this is what it is best known as today, it was originally named *Chx10* when it was first described in mammals in 1994, due to its similarity to its *C. elegans* ortholog, ceh-10 (Levine et al., 1994; Liu et al., 1994). *Vsx2* has many defining characteristics: homeodomain, Q_{50} paired-like, OAR motif, octapeptide sequence and a CVC domain (Liang and Sandell, 2007) (Fig. 5). Each domain has its own defining characteristics. Its classification as a homeobox gene gives it some similarities to the rest of the homeodomain (HD) containing protein families in that it has a conserved helix-turn-helix DNA binding domain. The HD is a semi-conserved protein domain comprised of about 60 amino acids and has been observed in studied invertebrate and vertebrate models, homeodomain proteins have been categorized into different classes base on the variations in their sequence (Bürglin and Affolter, 2016). The Q_{50} paired-like classification puts *Vsx2* in a subclass of paired domain (PRD) genes due to the conserved homeodomain of the *Drosophila paired* gene, apart from a glutamine (Q) substitution at position 50 in the HD and the absence of a PRD domain (Galliot et al., 1999); Liu et al., 1994). The PRD-like subclass designates the homology of the homeodomain to that of PRD class homeodomain (Vorobyov and Horst, 2006). The octapeptide sequence is the smallest motif with only seven residues (Vorobyov and Horst, 2006). Studies have shown the octapeptide region functions through binding to the corepressor, Groucho (TLE family in mouse), to aid its repression (Fisher and Caudy, 1998; Muhr et al.,

2001). Structural studies show the octapeptide, commonly known as the EH1 motif, binds the WD repeat region of Groucho (Jennings et al., 2006). The presence of an octapeptide is very common in several classes of homeodomain proteins, but because *Vsx2* belongs to the paired-like class it contains a phenylalanine in its first position (Galliot et al. 1999; Liu et al. 1994; Ferda Percin et al. 2000). The OAR motif is found exclusively in the PD gene class and is so named from the homeodomain proteins where it was first identified: Otp, Aristaless and Rax (Galliot et al. 1999). The OAR motif is suggested to facilitate transcriptional activation (Vorobyov and Horst, 2006). The last defining peptide sequence in *Vsx2* is its CVC domain. The CVC domain is located between the homeodomain and the C terminus of the VSX2 protein and it is the defining domain of the CVC paired-like family (Galliot et al. 1999; Ferda Percin et al. 2000). The CVC domain was also named after the three homeodomain proteins where it was first identified: Ceh-10, Vsx1, and Chx10 (Burmeister et al., 1996).

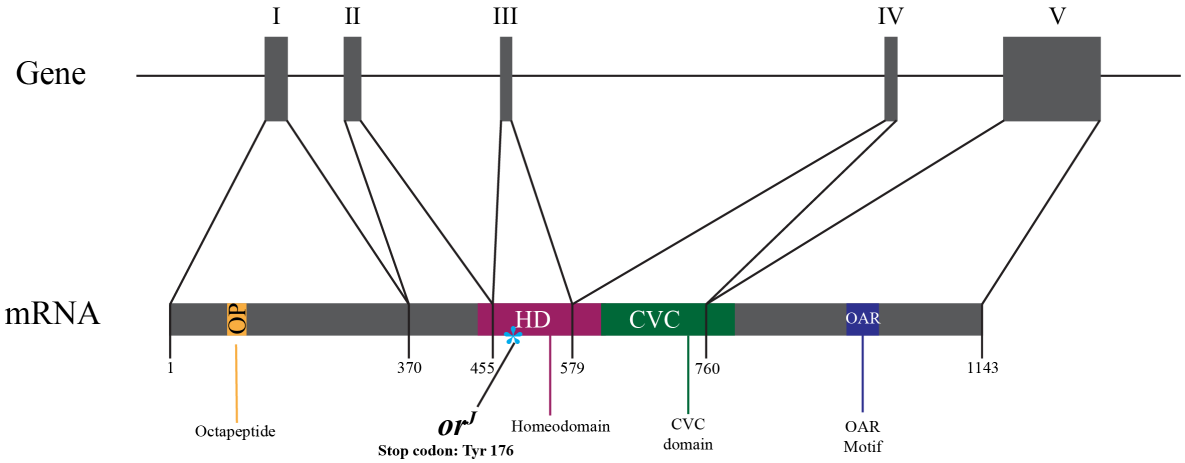

location. Asterisk denotes the location of the *orJ* mutation.

The CVC domain and homeodomain are the most strongly conserved domains amongst organisms with *Vsx2* orthologs: mouse, human, goldfish, and cavefish. The two domains are responsible for the transcriptional activity of VSX2. VSX2 mainly functions as a repressor with some weak activity for transcriptional activation (Dorval et al., 2005). Point mutations located in the homeodomain of *Vsx2* have shown that DNA binding efficacy significantly goes down when R_{200} and is mutated, providing evidence the homeodomain is necessary for DNA binding (Dorval et al., 2005; Ferda Percin et al., 2000; Zou and Levine, 2012). It has been demonstrated that the homeodomain is sufficient for DNA binding to occur (Dorval et al., 2005) but other studies have shown that the strength of the DNA binding relies on the CVC domain (Zou and Levine, 2012). Dorval et al. 2005, showed that another function of the CVC domain is to facilitate VSX2 repressor activity as deletion of the domain eliminated transcriptional repression even though DNA binding was only slightly weakened.

Vsx2 expression in the retina

Vsx2 expression first begins in the retina at ~E9.5 in the mouse, in the late optic vesicle stage. *Lhx2* is required but not sufficient for *Vsx2* expression; activation is achieved through signals coming from the overlying surface ectoderm (Nguyen and Arnheiter, 2000). Over the course of retinal development *Vsx2* becomes restricted to RPCs residing in the neural retina. Adjacent tissues, like the ciliary body only display weak expression of *Vsx2* (Rowan et al., 2004). RPCs manage to sustain high levels of *Vsx2* throughout retinal development, but upon cell cycle exit *Vsx2* is down regulated in all postmitotic cells except bipolar cells and Müller glia

(Burmeister et al., 1996; Rowan et al., 2004). The change in *Vsx2* expression pattern during development leaves its expression restricted to the outer region of the inner nuclear layer of the retina where these cells reside (Liu et al., 1994; (Belecky-Adams et al., 1997); Ferda Percin et al. 2000).

Mutations in *Vsx2* cause disruptions in retinal development

Identified mutations in *VSX2* are generally autosomal recessive and cause nonsyndromic congenital microphthalmia (small eye) in humans (Ferda Percin et al., 2000; (Bar-Yosef et al., 2004; Iseri et al., 2010; Smirnov et al., 2022; Wright et al., 2010). Other ocular anomalies like: coloboma, iris abnormalities, and cataracts have been observed in humans with mutations in *VSX2*. A new study screening patients with congenital stationary night blindness found three patients with missense mutations in *VSX2* (Smirnov et al., 2022). Many human patients with *VSX2* mutations do not have functional vision, at best few had any light perception at all (Reis et al., 2011). *VSX2* mutations identified in human patients likely affects VSX2 function by disrupting the homeodomain, CVC domain or by a truncation of the functional protein. The phenotypes of human patients carry over into mice. A couple spontaneously occurring *Vsx2* mutations exist in mouse: ocular retardation (*or*) and ocular retardation *J* (*orJ*). These mouse mutants also present with microphthalmia, cataracts, coloboma, deformities in retinal lamination plus optic nerve dysgenesis (Burmeister et al., 1996). Through the identification of the *orJ* mouse mutation, the field uncovered the phenotype is caused by a single point mutation (Burmeister et al., 1994). This single point mutation causes a premature stop codon in the homeodomain of VSX2, diminishing its DNA binding ability (Burmeister et al., 1996; Zou and Levine, 2012)

The *orJ* mutant

In the *orJ* mutant, there is a delay in the time to neurogenesis, reduced proliferation of RPCs and a complete absence of bipolar cells, and retinal identity issues (Horsford et al., 2005; Burmeister et al., 1996; Sigulinsky et al., 2015; Rowan et al., 2004). Studies have shown that while *Vsx2* is important for the maintenance of retinal identity, it is not necessary or sufficient for the initial specification of the retina (Horsford et al., 2005). Although, retinal development does occur it is disrupted: neurogenesis is temporally delayed, cells in the retina become pigmented, retinal lamination is severely affected, the retina is hypocellular and bipolar cells are completely absent (Burmeister et al., 1996; Rowan et al., 2004). Even though *Vsx2* is required for the specification and generation of bipolar cells; the absence of bipolar cells is not the primary cause of the hypocellularity seen in the mutant retina, it is the reduced RPC proliferation seen in the earlier developmental stages of the mouse retina (Green et al., 2003a). According to Green et al. 2003 this reduced proliferation stems from an increased accumulation of the cell cycle inhibitor *p27* in RPCs through a post-transcriptional mechanism involving CCND1 (cyclin D1). Previous studies have reported retinal size and RPC proliferation is restored after removal of the RPE determinant, *Mitf* (Horsford et al., 2005; Rowan et al., 2004).

The phenotypes of the ocular retardation mutant (*orJ*) are consistent with retinal expression of *Vsx2* and its role in retinal identity. Largely, *Vsx2* has been found to be important for retinal identity via suppression of other gene expression programs promoting specification of adjacent tissues and later born cell types. One of the major impedances to *orJ* retinal identity is expanded peripheral identities: ciliary epithelium and RPE (Rowan et al., 2004; Horsford et al., 2005; Sigulinsky et al., 2015). Several RPE-restricted genes, *Mitf, Tfec* and a few others, show inappropriate expression in the retinal domain of *orJ* mutants (Rowan et al., 2004; Horsford et al., 2005; Sigulinsky et al., 2015). The ectopic expression of these genes explains the hyperpigmentation seen in the periphery of *orJ* retinas (Rowan et al., 2004; Sigulinsky et al., 2015). *Mitf* overexpression leads to enhancement of the pigmentation program (Horsford et al.,

2005). The cell proliferation phenotype observed in the periphery of the *orJ* retina is reminiscent of ciliary epithelium and RPE as well (Sigulinsky et al., 2015; Rowan et al., 2004; Burmeister et al., 1996). Other homozygous ocular retardation mutants, such as $Vsx2^{R227W}$, show a significant increase in the RPE determinants, *Mitf* and *Otx* (Zou and Levine, 2012). However, studies have shown that when *Mitf* is reduced in *Vsx2* mutant backgrounds retinal development improves significantly (Horsford et al. 2005; (Konyukhov and Sazhina, 1966); Zou and Levine, 2012). These studies have led to the model that a major function of *Vsx2* is to control retinal identity, by defining the retinal domain through repression of non-retinal gene expression programs in addition to direct roles in promoting retinal gene expression programs, proliferation, and neurogenesis.

Unanswered Questions

Proper execution of the retinal development program requires a delicate balance of transcription factors, signaling pathway gradients and morphogenetic movements all connected in the correct sequence and executed at the right time. As a field, there is much left to investigate. Signaling events and transcription factors in the early retina remain largely understudied. *Vsx2* is expressed early in the retina and is an important transcription factor for eye and retinal development.

Many studies have reported that the *Vsx2* null retina has delayed neurogenesis, but how *Vsx2* provides temporal control of neurogenesis remains unknown. Does acquisition and maintenance of retinal identity play a role in the timing of neurogenesis? How is the identity of the retinal tissue firmly established in the early retina? What other factors interact with *Vsx2* for temporal control of neurogenesis? How does reducing *Mitf* in *Vsx2* mutants improve retinal development?

Another important question in the field that remains unanswered is what combination of transcription factors maintains RPCs? To date, there does not exist a single known gene that when inactivated causes a complete elimination of RPCs. This could be explained by a network of compensatory mechanisms in place, or simply that there is not a single factor responsible for progenitor maintenance. It is possible a population-wide regulatory mechanism exists and is not easily explained by a single factor, but rather a more complex mechanism based on the individual cells themselves and their relation to the rest of the cell population.

Explanation of Tools Used

Many of the questions spotlighted above are more approachable through a combination of new and old techniques. Mutated animal models have been the gold standard tool for understanding genetics and gene interaction since Mendel began crossing pea plants. When combined with new age RNA sequencing, many more complex questions can now be asked about mutants, and their phenotypes can now be dissected into distinct networks and pathways.

Epistasis and gene interactions

Epistasis can be defined as the dependence of the outcome of a mutation on the genetic background (Lehner, 2011; Miton et al., 2021). The readout is observed through phenotypic changes. A phenotype could be the growth rate (cell, tissue or organ), color (skin, fur or feather), disease symptoms or as finite as survival. When a mutation is identified through phenotypic effects, the addition of a second mutation may worsen, improve, or have no effect on the phenotype of the first mutation.

Epistasis is relevant from studies in evolution to causes of human disease (Lehner, 2011; Rauscher et al., 2021; Visser et al., 2011). Geneticists utilize epistasis to order mutations into a pathway through mapping out the connection between genotype and phenotype. This allows changes to a process or pathway to be easily identified when investigating whether genes interact. Utilizing a specific process like retinal development, that has many useful measurements, aids in the knowledge of how specific genes affect a process and how they interact. Both positive and negative forms of epistasis have been described.

Positive epistasis is described as an alleviation or suppression of the initial mutant phenotype (Fig. 6A), while the worsening or aggravation of an initial mutant phenotype is described as negative epistasis (Fig. 6B) (Lehner, 2011). In cases of no effect on the mutant phenotype several possibilities may explain this outcome. There may be no interaction between the genes and therefore no epistasis, there could be redundancy in the system or the genome, or translational buffering may be opposing the impact of altered mRNA levels on the proteome (Kusnadi et al., 2021).

Genomic buffering has best been described in quantitative studies of epistasis in yeast. One landmark study in yeast showed that growth rate in yeast lines with two mutations was higher than those with single mutations, indicating positive epistasis through buffering (Jasnos

and Korona, 2007). Buffering can result in positive epistasis or hide gene interactions all together (Jasnos and Korona, 2007; Visser et al., 2011).

Identifying and describing cases of epistasis is an informative step towards understanding the underlying interaction of the genetic variants, which enables the guidance of studies to identify the functional molecular mechanisms causing gene interactions.

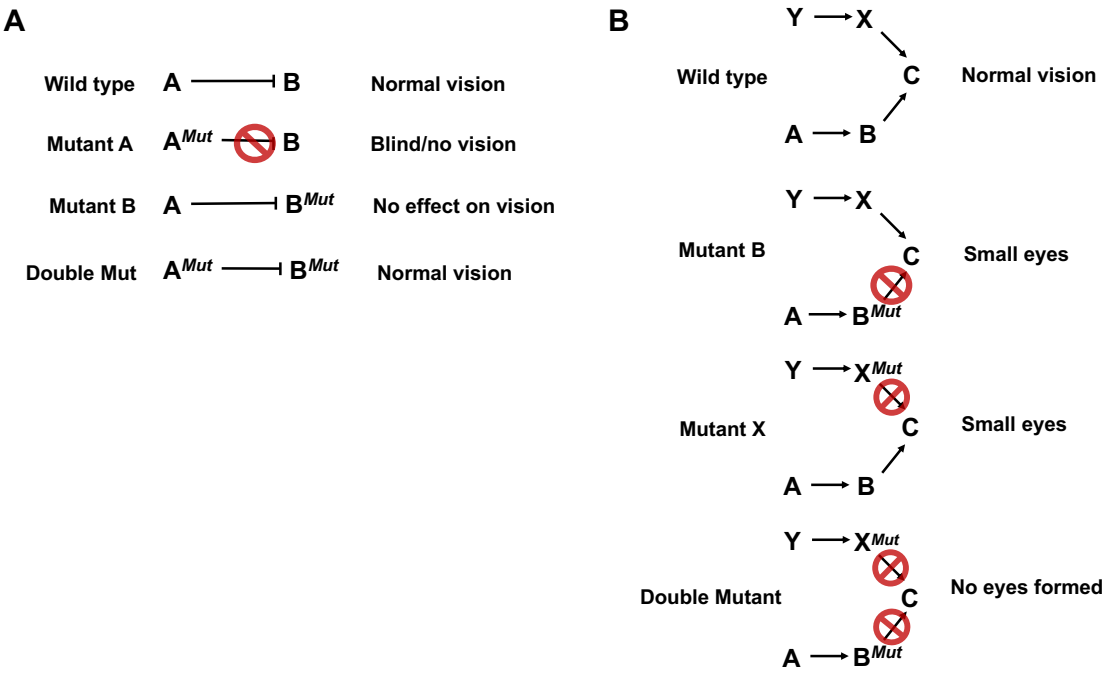

Figure 6. Positive and Negative epistasis. A.) Depicts very simple case of positive epistasis interaction where A suppresses B resulting in normal vision. Mutant allele of A can no longer suppress B resulting in a blind phenotype. In the case of mutant B, no effect is seen. However, positive epistasis occurs when the two mutants are combined, and the phenotype returns to normal vision. **B)** shows a simple case of convergent negative epistasis. A activates B and then B promotes the expression of C. In a parallel pathway, Y promotes X and X promotes the expression of C as well. Mutants of B and X produce similar phenotypes, but when they are combined in a double mutant the phenotype becomes worse.

RNA sequencing

RNA sequencing allows for transcriptome analysis, identification, and quantification to help answer many biological questions including differences in gene expression in mutant versus wild-type cells and during various developmental stages along with pharmacogenomic responses (Garg, 2021). RNA sequencing is a high throughput method that requires sample collection followed by preparation involving total RNA isolation and reverse transcription and conversion to cDNA, followed by construction of a sequencing library then sequencing on a massively parallel sequencing technology, Next Generation Sequencing (NGS), and finished by bioinformatic data analysis.

There are many different types of RNA that exist within the transcriptome. mRNA or messenger RNA is the most intensely studied and it functions as a transitory molecule and a template to be translated into proteins from DNA.

RNA sequencing is a high throughput method of measuring RNA molecules. Previous methods such as northern blotting and quantitative PCR are considered low throughput methods and are restricted to quantify a single transcript. Other methods such as hybridization-based microarray methods are also considered high throughput and cheaper methods for genome wide quantification of gene expression, but they are limited in accuracy and cross hybridization artifacts may appear during the analysis due to abundance of similar sequences (Shendure, 2008). NGS technology provides complete analysis of RNA aiding in the revolution of transcriptomics (Wang et al., 2009).

RNA Sequencing workflow

There is no optimal or straightforward pipeline for RNA sequencing due to the many applications of this technology (Conesa et al., 2016). However, the following section will summarize a general overview of a standard mRNA sequencing workflow (Fig. 6).

Experimental design is the first and most important step of any experiment. The experimental planning phase varies widely from experiment to experiment, meaning the exact parameters of each experimental design will vary. The appropriate library is chosen, along with sequencing depth and number of replicates needed. The samples are then depleted of ribosomal RNA.

The next step is quality control (QC) and read alignment. QC insures the sequencing quality of raw reads, GC content, adaptor presence and overrepresented k-mers, duplicated reads for detecting sequencing errors and eliminating PCR artifacts or contaminations. FastQC is a very common program that enables higher efficiency during the QC step. After QC, read alignment occurs. This includes mapping the sequencing reads to a reference genome; at this stage it is important to pay attention to the percentage of mapped reads as another quality control measure. The percentage of mapped reads will vary greatly with the organism, for example good, clean human samples should be mapped at 70-90% (Conesa, et al., 2016).

As part of quality control, the data is tested for reproducibility. Reproducibility testing includes looking for batch effects that exist between samples prepared on the same days when compared to other biologically equivalent samples. A great way to visualize this process and see batch effects clearly is to use a PCA plot. While evaluating these plots, biological and technical replicates should always cluster together.

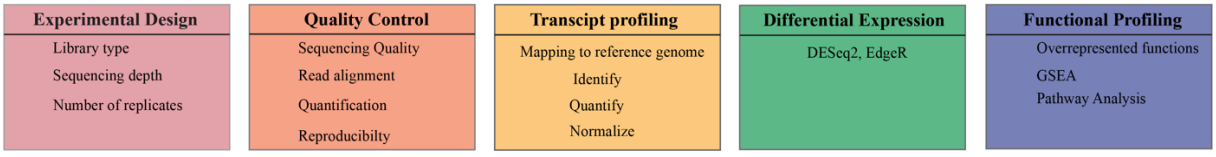

Figure 7. RNA sequencing workflow. Figure shows key steps in any RNA sequencing experiment.

Once reproducibility has been assessed specific transcripts can be identified. This involves mapping reads to a reference genome or transcriptome. At this stage, transcripts are both identified and quantified simultaneously or sequentially. The quantification of transcripts is the single most powerful part of the RNA sequencing process because it provides the ability to estimate gene and transcript expression. The raw transcript reads are normalized to a standard, for example: RPKM (reads per kilobase of exon model per million reads), FPKM (fragments per kilobase of exon model per million mapped reads), and TPM (transcripts per million). Once transcript quantification is completed differential gene expression may be assessed. Differential gene expression analysis is the comparison of gene expression values amongst samples. At this stage, batch effects may still exist even after sample-specific normalization, but experimental design is the best first line of defense against this problem. Some programs utilize raw read counts to perform normalization and differential expression. Newer programs like DESeq2 and EdgeR use a negative binomial as a reference distribution of reads to assess batch effects and normal distribution of raw reads. Studies have shown that the choice of differential gene expression analysis method can have a large impact on the outcome of analysis and no single method is likely to work for all datasets (Rapaport et al., 2013; Soneson and Delorenzi, 2013).

The last step in a standard RNA sequencing workflow is functional profiling. This step identifies molecular functions or pathways for differentially expressed genes (DEGs). There are a few main approaches for functional profiling: 1) comparing lists of DEGs against the rest of the genome for overrepresented functions, 2) gene set enrichment analysis (GSEA) which is based on ranking the transcriptome according to measurement of DE (differential expression), and 3) pathway analysis. Tools like Ingenuity Pathway Analysis (IPA), and GOseq have become available to aid in the last step of the analysis and estimate the bias effect of DE results. Resources like: Gene Ontology (GO), Bioconductor, DAVID, Babelomics and IPA enable

deeper analysis of RNA sequencing datasets due to their ability to offer functional annotation data on most model species.

Research presented

What began as a pursuit for genes that influence neurogenic timing in the *orJ* retina transformed into a search for genetic interactors of *Vsx2*. Due to the many eye and retinal phenotypes in *Vsx2* mutants, *Vsx2* is a critical regulator of eye development. Through the exploration of genes that influence the *orJ* phenotype, I have identified and investigated interactors of *Vsx2* utilizing a combination of phenotypic readouts, gene expression analysis and small molecule inhibitors creating a framework based on the logic of epistasis for identifying genetic interactors.

CHAPTER 2

A FRAMEWORK TO IDENTIFY FUNCTIONAL INTERACTORS THAT CONTRIBUTE TO THE DEFECTS OF EARLY RETINAL DEVELOPMENT IN *VSX2* MUTANT MICE

Amanda M. Leung[1], Mahesh Rao[2], Nathan Raju[2], Minh Chung[2], Alison Klinger[2], DiAnna Rowe[2], Xiaodong Li[2], Edward M. Levine[1,2,*]

[1]Department of Cell and Developmental Biology

Vanderbilt University, Nashville TN 37232

[2]Department of Ophthalmology and Visual Sciences

Vanderbilt University Medical Center, Nashville TN 37232

Abstract

A goal of developmental genetics is to identify functionally relevant gene interactions and assess their contributions to the phenotypic complexity and severity caused by specific genetic perturbations. We sought to identify potential interactors of the homeodomain transcription factor *Vsx2*, which when mutated, causes defective retinal development and microphthalmia. Our investigation was based on the principles of positive and negative epistasis and incorporated bulk RNA sequencing and categorical assignments of gene expression dependencies to *Vsx2* and its candidate interactors. This was first applied to an *in vivo* phenotypic comparison of combinatorial mutants of *Vsx2* and *Mitf*, a direct target of *Vsx2* repression, and then to *ex vivo* organotypic cultures of *Vsx2* mutant retinas treated with small molecule inhibitors of retinoid x receptors and gamma secretase, two candidate interactors of *Vsx2*. Whereas *Mitf* exhibited robust positive epistasis with *Vsx2*, its activity only partially accounts for the *Vsx2* mutant phenotype, suggesting other functional interactors. Small molecule inhibition of *Rxrg,* the highest ranked upregulated gene in the *Vsx2* mutant retina, yielded minimal evidence for functional interaction or epistasis with *Vsx2*. In contrast, inhibition of gamma secretase activity induced the expression of hundreds of *Vsx2*-dependent genes associated with proliferation to deviate further from wild type, providing evidence for functional interaction with *Vsx2* in a manner consistent with convergent negative epistasis. Combining *in vivo* and *ex vivo* testing with transcriptomic data analysis enabled the testing of candidate functional interactors in a streamlined manner that could be scaled up and applied to other complex development phenotypes.

Introduction

Vsx2 is an evolutionarily conserved homeodomain transcription factor that with *Vsx1*, defines the *Visual System Homeobox* (VSX; also referred to as Prd-L:CVC) subclass of homeobox genes(Bürglin and Affolter, 2016). Mutations in the human VSX2 gene cause bilateral congenital microphthalmia, disrupted retinal architecture, and lifelong blindness, abnormalities which are also present in *Vsx2* mutant mice (Burmeister et al., 1996; Reis et al., 2011; Truslove, 1962; Wright et al., 2010; Zou and Levine, 2012). A definitive marker of retinal domain specification during regionalization of the optic vesicle, *Vsx2* is expressed in retinal progenitor cells (RPCs) throughout development, ultimately resolving to cohorts of bipolar cells and Müller glia (Burmeister et al., 1996; Liu et al., 1994). As such, *Vsx2* has temporally shifting requirements through retinal development. During early retinal development, *Vsx2* regulates tissue identity (i.e. retinal), RPC proliferation, and the initiation of retinal neurogenesis (Bone-Larson et al., 2000; Burmeister et al., 1996; Dhomen et al., 2006; Green et al., 2003; Horsford et al., 2005; Sigulinsky et al., 2008). *Vsx2* also promotes optic cup morphogenesis in medaka and promotes multipotentiality in zebrafish RPCs (Gago-Rodrigues et al., 2015; Vitorino et al., 2009). The importance and conservation of VSX genes in visual system development is further exemplified by their roles in optic lobe formation in *Drosophila* and in *C. elegans,* where the VSX ortholog *Ceh-10* is a terminal selector gene for the AIY sensory interneuron, which is part of a light-responsive neural circuit in a related nematode species (Altun-Gultekin et al., 2001; Erclik et al., 2008).

The functional requirements of *Vsx2* in early retinal development are complex. Although retinal identity is compromised in *Vsx2* mutant mice, as revealed by ectopic expression of genes normally restricted to RPE or ciliary epithelium (Coles et al., 2006; Horsford et al., 2005; Rowan et al., 2004), the retinal domain is specified, optic cup morphogenesis occurs, and *Vsx2* mRNA

remains expressed (Bian et al., 2022; Burmeister et al., 1996; Capowski et al., 2016; Liu et al., 1994; Zou and Levine, 2012). Genetic analysis of two DNA-binding defective mutants (*Vsx2*^{R200Q}, *Vsx2*^{R227W}) suggest that *Vsx2* ensures lineage fidelity, allowing the retinal gene expression program to occur in the absence of extra-lineage or cryptic gene expression programs (Zou and Levine, 2012). Proliferation is greatly reduced in the *Vsx2* mutant retina, but RPCs still undergo cell cycle progression through retinal development and proliferation continues into the adult (Dhomen et al., 2006; Green et al., 2003). Except for mice homozygous for the *Vsx2*^{R227W} allele, neurogenesis occurs in the *Vsx2* mutant retina but with a delay of about two days, initiating at ~E13.5 (Bone-Larson et al., 2000; Burmeister et al., 1996; Sigulinsky et al., 2008; Sigulinsky et al., 2015; Zou and Levine, 2012). While this delay contributes to severely disrupted retina formation, these partial requirements highlight the complexity in how Vsx2 regulates RPC properties and early retinal development. Adding to this complexity, the disruptions in lineage fidelity, proliferation, and neurogenic timing temporally overlap. Analysis of *Vsx2* mutant - wt chimeric embryos suggest that lineage fidelity, proliferation, and neurogenic timing are under cell autonomous regulation by *Vsx2*, but proliferation also has a non-cell autonomous component that could act in parallel to *Vsx2* or converge onto *Vsx2*-regulated genes (Kindiakov and Koniukhov, 1986; Osipov and Vakhrusheva, 1984; Sigulinsky et al., 2015). To the extent that these phenotypes are interconnected, either hierarchically or at the level of gene regulation, is not clear.

Previously identified functional interactors of *Vsx2* in mice and human organoids include genes such as *Mitf*, *p27Kip1*, and *Prdm1*, and signaling pathways such as FGF, Sonic hedgehog, and Wnt (Brzezinski et al., 2010; Capowski et al., 2016; Gamm et al., 2019; Green et al., 2003; Katoh et al., 2010; Nguyen and Arnheiter, 2000; Sigulinsky et al., 2008; Zou and Levine, 2012). Identification of these interactors has been accomplished with genetics or pharmacological testing and it is likely that additional interactors can be identified through these approaches.

In this study, we suppress the activities of candidate functional interactors in the retina of the *Vsx2*-null mouse, *ocular retardation J* (*orJ)* (Burmeister et al., 1996; Zou and Levine, 2012). Beginning with *Mitf,* we assessed its genetic impact on the initiation of neurogenesis by immunohistology and an assessment of phenotypic traits with RNA sequencing data using a classification system of gene regulatory dependencies combined with gene set overrepresentation analysis (ORA). We then treated *orJ* retinal explants with small molecule inhibitors of two other candidate interactors, retinoid x receptor gamma (*Rxrg*) and gamma secretase, whose effects were also resolved by RNA sequencing and by applying the logic of *positive* and *negative* epistasis to the observed changes in gene expression. As defined by Lehner (Lehner, 2011), positive epistasis occurs when a second mutation decreases the phenotypic severity caused by the first mutation, and negative epistasis occurs when the phenotypic severity is increased. Positive epistasis has traditionally served as evidence for direct genetic interaction between two genes with one gene repressing the other as the simplest mechanism. Negative epistasis is more complicated because more severe phenotypes can arise through disruptions in separate mechanisms that are regulated independently by the genes under analysis, or through convergence onto common mechanisms (i.e. gene regulatory networks, signaling pathways). We show here that *Mitf* exhibits partial, but definitive positive epistasis*,* that *Rxrg* does not exhibit functional epistasis, and that gamma secretase activity exhibits convergent negative epistasis with *Vsx2*. This streamlined approach provides an enhanced level of resolution to test for factors that underlie the *orJ* phenotype and could be adapted to other mutations with complex phenotypes.

Results

Analogous to *Vsx2* for the retinal domain, *Mitf* marks the retinal pigmented epithelium (RPE) domain during optic vesicle regionalization and drives RPE differentiation (Bharti et al., 2006; Fuhrmann, 2010; Westenskow et al., 2009). *Mitf* is initially expressed throughout the optic vesicle and its subsequent downregulation in the nascent retinal domain is *Vsx2*-dependent, consistent with it being a direct target of Vsx2 repression (Arnheiter et al., 2006; Bora et al., 1998; Chow and Lang, 2001; Nguyen and Arnheiter, 2000; Yun et al., 2009; Zou and Levine, 2012). Loss of function mutations in *Mitf* suppress the mutant phenotypes of several *Vsx2* mutant alleles, and more severe phenotypes (hyperpigmentation, increased hypocellularity) occur when *Mitf* expression is enhanced (Horsford et al., 2005; Konyukhov and Sazhina, 1966; Rowan et al., 2004; Zou and Levine, 2012). *Mitf* is therefore an excellent candidate to be the major driver of the traits and underlying gene expression changes that define the early retinal development phenotype in *Vsx2* mutants. Addressing this first provides the context for placing other functional candidates into the highest level of the *Vsx2* interaction network.

The *mi* allele partially rescues the delay in neurogenesis in the *orJ* retina

The delayed onset of neurogenesis offered a straightforward measure to assess the impact of reducing *Mitf* activity, and the gap of 2 days between neurogenesis onset in wild type (E11.5) and *orJ* retinas (E13.5) provided a window to distinguish between full or partial restoration of timing. Neurogenesis initiates in the central retina and progresses toward the periphery over several days, thereby allowing evaluation of the pattern and progression. As previously documented, these features are easily tracked by the expression of Class III β-tubulin (Tubb3; **Figure 8A-F**,), which is activated in RPCs as they exit the cell cycle and transition to postmitotic, neuronal precursor states (Barton and Levine, 2008; Pacal and Bremner, 2014; Sharma and Netland, 2007).

The *Mitf* allele *mi* was used to generate combinatorial mutants (*orJ; mi*). The mutation is a three-nucleotide deletion that reduces DNA binding but dimerization with wild type Mitf protein and other interacting proteins still occur, conferring dominant-negative activity (Hemesath et al., 1994; Hodgkinson et al., 1993). For this reason, we used heterozygous mutants (mi^{het}), unless noted. As expected, neurogenesis initiated earlier in the *orJ;* mi^{het} retina compared to *orJ* (Fig. 8G-J; quantification in Fig. 8P). However, onset was still delayed by about 1 day compared to the wild type retina indicating a partial restoration in timing. This partial rescue could be due to the persistence of Mitf activity or related factors (see discussion). Indeed, more severe phenotypes are observed in *mi* homozygotes (mi^{homo}) or in combinatorial *Mitf* mutants (Hodgkinson et al., 1993; Steingrímsson et al., 1994; Steingrímsson et al., 2003). We therefore examined the *orJ;* mi^{homo} retina for further correction of the neurogenic delay (Fig. 8J-L). Neurogenesis appeared improved in some samples at E12.5, but the delay was still evident at E11.5 and in some retinas at E12.5 (Fig. 8J). Tubb3+ cells were found in the mi^{het} retina at E11.5, but precocious onset of neurogenesis was not likely (Fig. 8M-O).

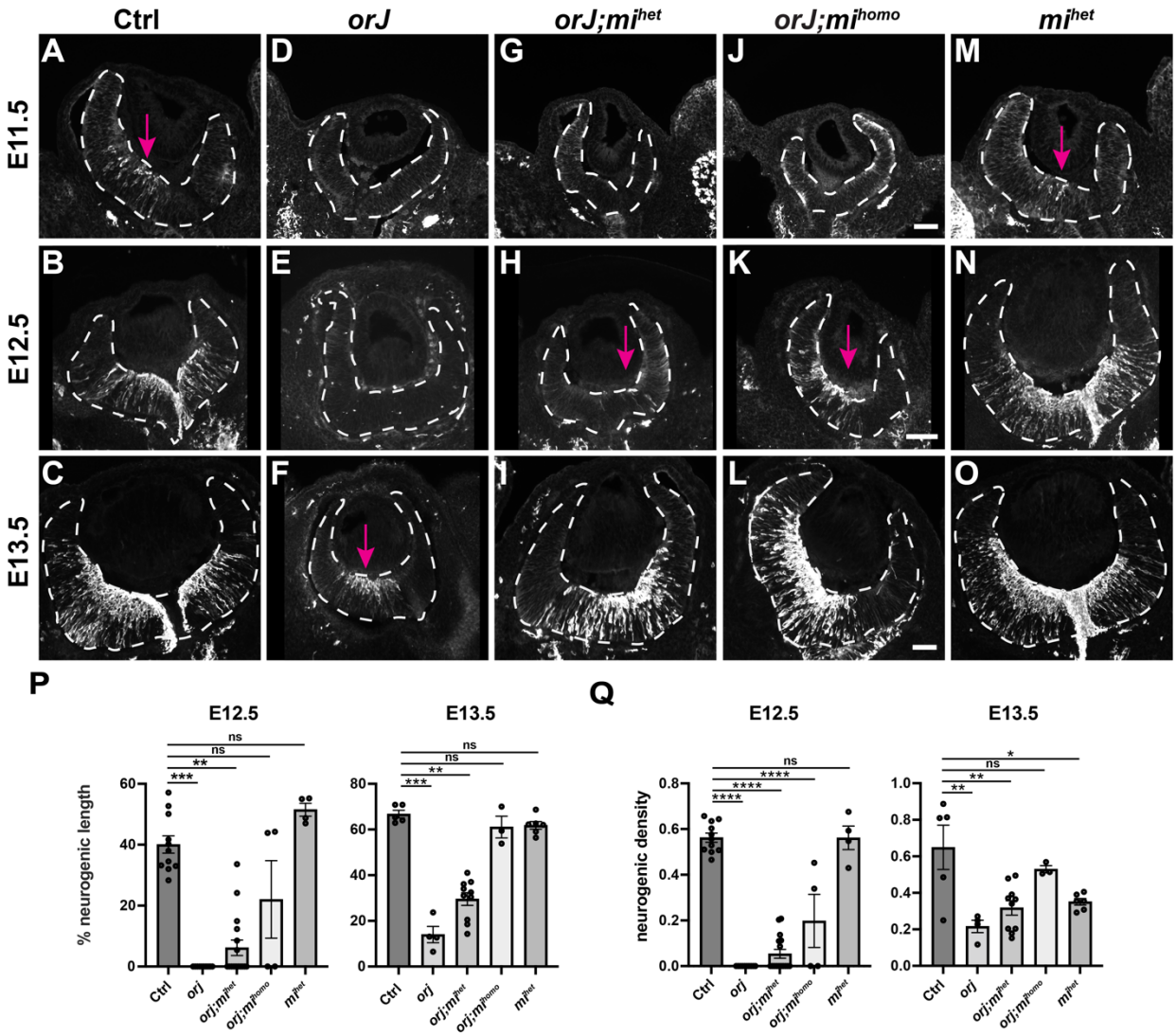

Figure 8. **Mitf contributes to the delayed onset of neurogenesis in the orJ retina.** (A-O) Tubb3 staining marks post-mitotic neuronal precursors from E11.5 – E13.5. Retinas are within dashed lines; magenta arrows point out the initial appearance of TUBB3 in each genotype by age. Scale bars are 50 µM for each age. (A-C) TUBB3+ cells are evident in the *orJ*^{het} (control) retina at E11.5, extending across the retina at E12.5 and E13.5. (D-F) In the *orJ* retina, TUBB3+ cells do not appear until E13.5. (G-I) TUBB3+ cells are detected in the *orJ; mi*^{het} retina at E12.5, with enhanced accumulation at E13.5. (J-L) TUBB3 expression is still not observed at E11.5 in the *orJ; mi*^{homo} retina but is improved by E12.5. (M-O) TUBB3+ cells are observed at all three ages in the *mi*^{het} retina. (P) Quantification of Tubb3 expression across the retina as a percentage of retinal length (neurogenic progression) at E12.5 and E13.5. (Q) Quantification of the Tubb3+ pixel ratio within neurogenic regions as a measure of neurogenic output at E12.5 and E13.5.

To quantify these observations, measurements were done for neurogenic progression and neurogenic output, the latter defined as the accumulation of neuronal precursors in the neurogenic region based on TUBB3 expression. Neurogenic progression was calculated as the percentage of the retina positive for TUBB3 staining along a line extending from the central retina to the peripheral edge, and neurogenic output was inferred from the ratio of TUBB3+ pixels to total pixels in the neurogenic region (see Methods). As expected, neurogenic progression lagged in the *orJ* retina but was improved in the combinatorial mutants, with the *orJ; mi*^{homo} retinas similar to wildtype at E13.5 (Fig. 8P; see Suppl File 1 for statistics). Neurogenic output was impaired in *mi*^{het} and *orJ* retinas relative to wild type, but the *orJ; mi*^{het} and *orJ; mi*^{homo} *mutants* showed improvements by E13.5 (Fig. 8R; see Suppl File 1 for statistics). These observations align with prior findings that the interaction between the *orJ* and *mi* alleles exhibits positive epistasis, but they also suggest that *Mitf*-independent factors contribute to the *orJ* phenotype.

Mitf partially accounts for the gene expression changes caused by the absence of *Vsx2*.

To gain a transcriptome-wide view of the changes caused by the *orJ* and *mi* mutations, we performed RNA sequencing on E12.5 retinas from *orJ*^{het} (control), *orJ*, and *orJ*; *mi*^{het} mice. This age captures the neurogenic delay in the *orJ* retina as well as improvements caused by the *mi* allele. *orJ*^{het} mice exhibit normal retinal development (Bone-Larson et al., 2000) and a pilot microarray experiment comparing *orJ*^{het} and wild type retinas revealed nearly identical gene expression profiles (unpublished observation). Library preparation and sequencing for all samples was done simultaneously, facilitating direct comparisons of gene expression across the 3 genotypes (Fig. 9A). Principal components analysis (PCA) revealed that most of the variance

between datasets correlated with genotype (Fig. 9B). The *orJ*; *mi*^{het} samples clustered between the control and *orJ* samples but were closer to *orJ* on the PC1 axis, indicating that reducing *Mitf* activity did not restore the transcriptome-wide expression profile to a wild type state but that the overall trend was towards restoration.

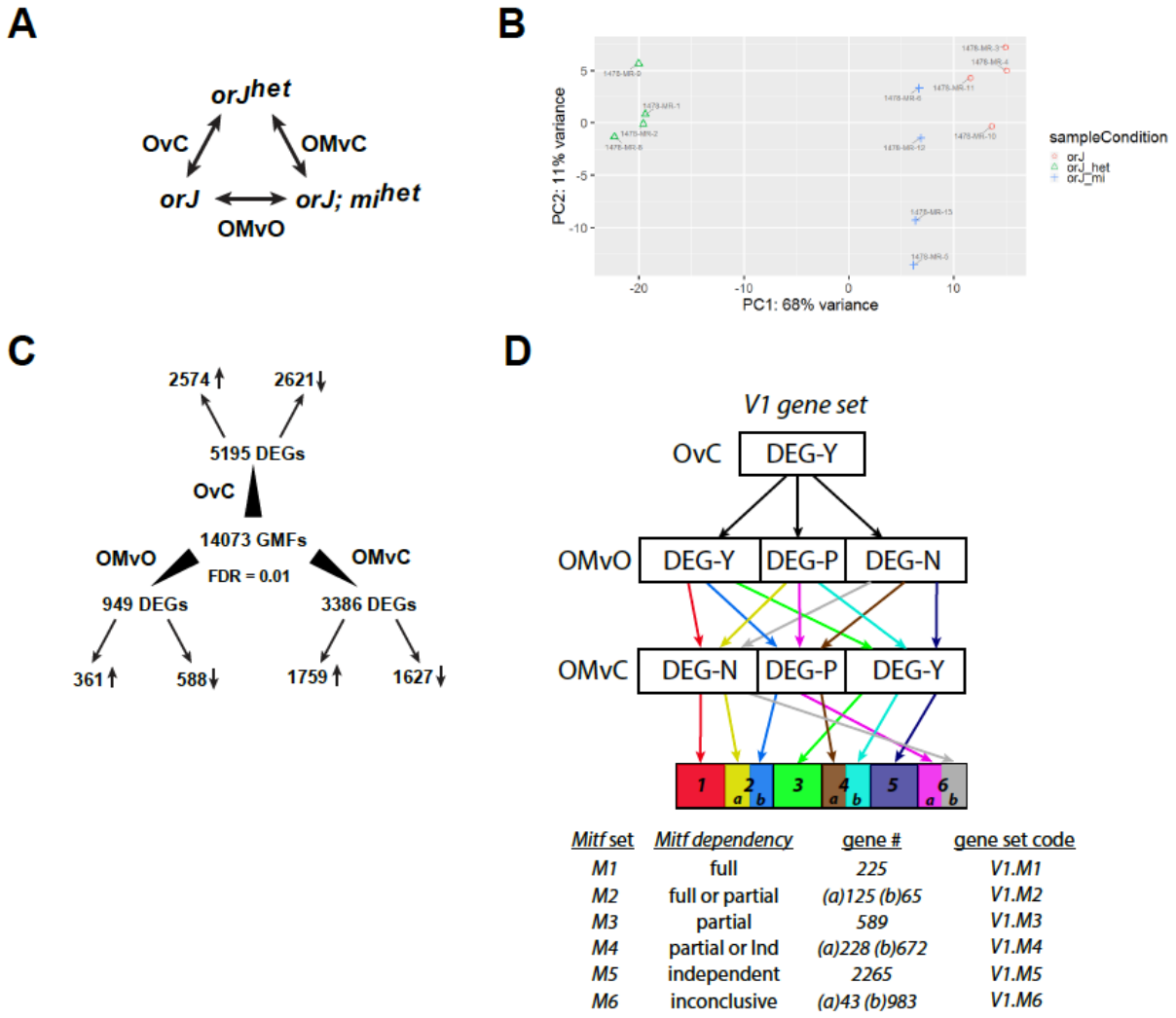

Mitf set	Mitf dependency	gene #	gene set code
M1	full	225	V1.M1
M2	full or partial	(a)125 (b)65	V1.M2
M3	partial	589	V1.M3
M4	partial or Ind	(a)228 (b)672	V1.M4
M5	independent	2265	V1.M5
M6	inconclusive	(a)43 (b)983	V1.M6

Figure 9. The *mi* mutation partially restores gene expression in the E12.5 *orJ* retina. (A) Tripartite design of differential gene expression analysis of RNA sequencing data across the 3 genotypes. Comparisons were made between *orJ*^{het} (C - control), orJ (O) and orJ; mi^{het} (OM) with 4 biological replicates per genotype. Genotype in first position was compared against the genotype in the second position for each comparison, thereby assigning the directions of expression changes to the first genotype. (B) PCA plot for the transcriptomes from each replicate. (C) Summary of differential expression analysis between the 3 genotypes. Genes were assigned as DEGs if they were within the 0.01 FDR cutoff. DEGs were then split by their directional change in expression (small arrows; see Supplemental File 1 for tabulated data). (D) Gene set classification of the Vsx2-dependent genes (V1 gene set; OvC, 0.01 FDR) based on Mitf-dependence (see text for details). Supplemental Figure 1 provides the initial categorizations of DEG classifications and first pass integration of V1 genes by their DEG classifications in the OMvO comparison.

DESeq2 was used to identify differentially expressed genes (DEGs) by pairwise comparisons across the three genotypes (Fig. 9C; Suppl. File 2). 14073 genome mapped features (GMFs) were identified and over 95% were protein-coding genes. Applying a false discovery rate (FDR) cutoff of ≤0.01 (equivalent to adjusted p-value), 5195 DEGs were identified in the *orJ* retina when compared to control (OvC), 949 DEGs were identified in the *orJ*; mi^{het} retina compared to *orJ* (OMvO), and 3380 DEGs were identified in the *orJ*; mi^{het} retina compared to control (OMvC). Like the PCA analysis, the varying degrees of differential gene expression between genotypes suggest that the *orJ*; mi^{het} retina is more like *orJ* than wild type.

Partitioning of genes based on *Vsx2* and *Mitf* dependence.

We generated a classification system based on a gene's probability of being differentially expressed in the *orJ* and *orJ; mi^{het} mutants* (Fig. 10; Fig. 9D). Two FDR cutoffs were applied resulting in three broad categories: Genes with a p_{adj} value of ≤0.01 were assigned a DEG status of '*yes'* (DEG-Y) indicating a DEG with high confidence, '*possible*' (DEG-P) with a p_{adj} value in the range of >0.01 and ≤0.05 indicating low confidence in the DEG designation, and *'no'* (DEG-N) with a p_{adj} value >0.05 (Fig. 10A; Suppl File 2). DEG status in the OvC comparison defined a gene's dependency on *Vsx2* and each gene was assigned to a *Vsx2* gene set: V1 for DEG-Y genes, V2 for DEG-P genes, and V3 for DEG-N genes. Except where noted, analyses were focused on the *Vsx2*-dependent genes (V1 gene set).

With *Vsx2*-dependencies defined, the impact of *Mitf* on gene expression was assessed. DEG status in the OMvO comparison defined a gene's dependency on *Mitf* (Fig. 10A; Suppl File 2) and applying this as a filter to the V1 gene set revealed simple regulatory relationships (Fig. 10B). DEG status in the OMvC comparison was not informative on its own with respect to *Vsx2* or *Mitf* regulation (Fig. 10A), but when applied as an additional filter, higher resolution was

achieved for predicting the extent of *Mitf* regulation (Fig. 9D; Suppl File 2). For V1.M1 genes, the changes in expression due to the lack of *Vsx2* are predicted to be fully dependent on *Mitf*, whereas V1.M3 genes are predicted to be partially *Mitf*-dependent, suggesting additional factors contribute to their differential expression. V1.M2 genes are also *Mitf*-dependent but distinguishing between full- or partial-dependence is less certain because of their DEG-P status in either the OMvO or OMvC comparisons. This is also true for V1.M4 genes but ambiguity lies in whether they are *Mitf*-dependent or -independent. V1.M5 genes are predicted to be *Mitf*-independent, and this gene set accounts for the largest cohort (44%) of *Vsx2*-dependent genes, in keeping with the partial restoration of the *orJ* phenotype by the *mi* mutation. The dependency of the V1.M6 genes on *Mitf* was deemed inconclusive because their DEG status in the two comparisons with the OM dataset resulted in low-confidence or ambiguous regulatory predictions (i.e., DEG-P in OMvO and OMvC or DEG-N in OMvO and OMvC).

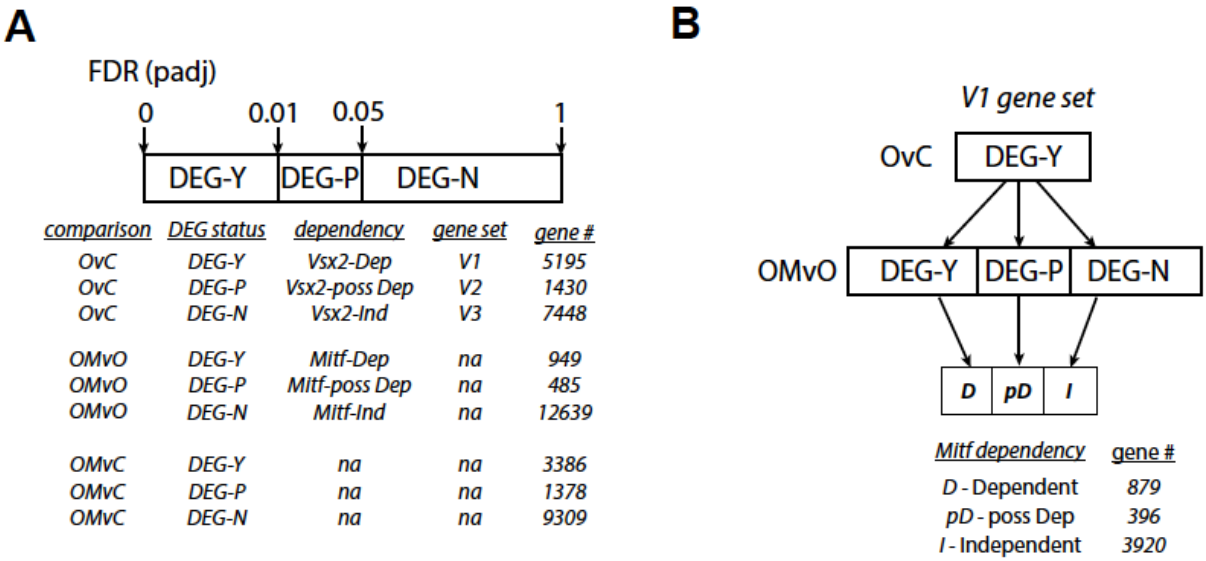

comparison	DEG status	dependency	gene set	gene #
OvC	DEG-Y	Vsx2-Dep	V1	5195
OvC	DEG-P	Vsx2-poss Dep	V2	1430
OvC	DEG-N	Vsx2-Ind	V3	7448
OMvO	DEG-Y	Mitf-Dep	na	949
OMvO	DEG-P	Mitf-poss Dep	na	485
OMvO	DEG-N	Mitf-Ind	na	12639
OMvC	DEG-Y	na	na	3386
OMvC	DEG-P	na	na	1378
OMvC	DEG-N	na	na	9309

Mitf dependency	gene #
D - Dependent	879
pD - poss Dep	396
I - Independent	3920

Figure 10. DEG classifications based on *Vsx2*- and *Mitf*-dependencies. (A) Two FDR cutoffs were used to assign all expressed genes to 3 categories based on their DEG status. The OvC comparison established regulatory dependencies on *Vsx2* and the OMvO comparison established regulatory dependencies on Mitf. The OMvO comparison was not informative at this level. Gene sets were defined based on *Vsx2* dependency. The number of genes in each DEG status group are shown. **(B)** DEG status of the V1 genes (DEG-Y in OvC comparison) in the OMvO comparison identified three categories of *Mitf* dependency.

Focusing on the cohort of *Mitf*-dependent genes (V1.M1 – V1.M3 gene sets), we predicted these genes would show improvements in their expression in the *orJ; mi*^{het} mutant, trending back towards control levels. Indeed, 993 of 1004 genes (98.9%) exhibited this behavior. Because this aligns well with positive epistasis at the genetic level, this can be considered evidence of positive epistasis at the level of gene expression. While this concordance is not unexpected, the minimal number of genes whose expression worsened (i.e., greater divergence from wild type expression in the *orJ; mi*^{het} retina compared to the *orJ* retina) suggests that the incomplete rescue was not due to aberrant effects of the *mi* mutation. Rather, it supports the hypothesis that additional factors contribute to the *orJ* phenotype.

It is also possible that *Mitf* may regulate the expression of genes that are not regulated by *Vsx2* (i.e., *Mitf*-dependent genes in the V3 gene set). This is an important consideration because *Mitf* is expressed in the embryonic retina (Bharti et al., 2008) and a role for *Mitf* in regulating retinal gene expression could complicate a phenotypic assessment of the epistatic interaction between *orJ* and *mi*. Of the 7448 V3 genes, only 35 exhibited *Mitf* dependency (V3.M1 gene set; Fig. 11; Suppl File 2), indicating that *Mitf* has a minor impact on the expression of *Vsx2*-independent genes. Despite this low number of genes, the *mi* mutation could promote a compensatory factor and one candidate is *Cyclin D2* (*Ccnd2*), a *Vsx2*-independent gene that is upregulated in the *orJ; mi*^{het} retina (Suppl File 2).

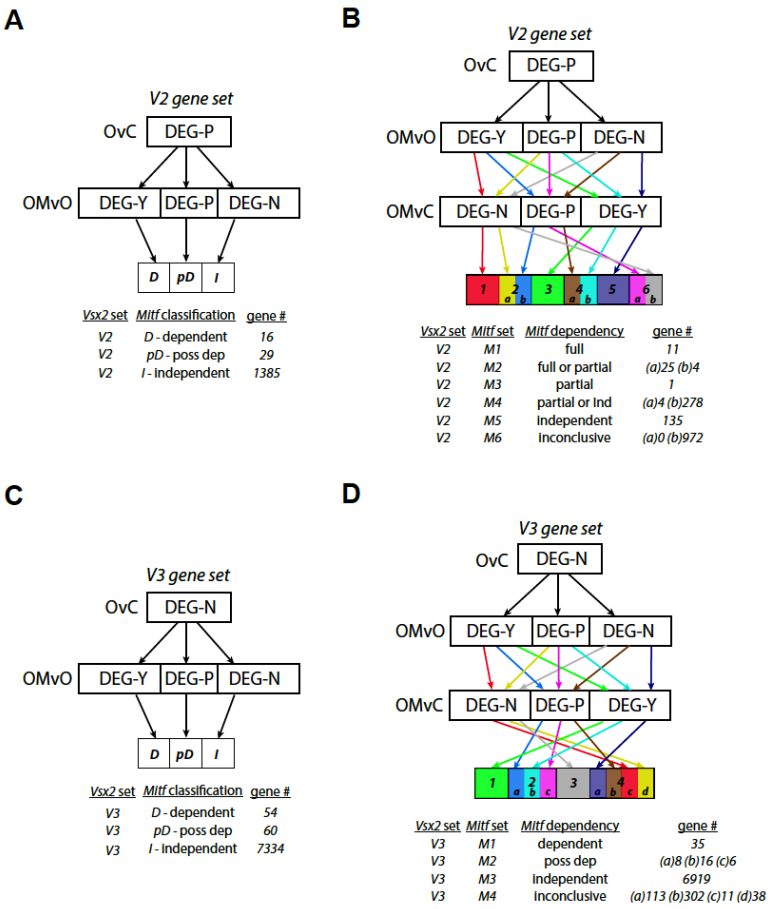

Figure 11. DEG classifications for the V2 and V3 gene sets. (A) DEG status of the V2 genes (DEG-P in OvC comparison) in the OMvO comparison identified 3 categories of *Mitf* dependency. **(B)** Similar to the V1 gene set, additional filtering of the V2 genes by DEG status in the OMvC comparison yielded 6 categories of *Mitf*-dependence. **(C)** DEG status of the V3 genes (DEG-N in OvC comparison) in the OMvO comparison identified three categories of *Mitf* dependency. **(D)** Additional filtering of the V3 genes by DEG status in the OMvC comparison yielded 4 categories of *Mitf*-dependence.

Designation of gene regulatory circuits for V1 genes based on *Mitf*-dependency

The high degree of positive epistasis at the level of gene expression allowed us to generate gene regulatory circuits (GRCs) for the *Vsx2*- and *Mitf*-dependent genes of the highest confidence, specifically those in the V1.M1, V1.M3, and V1.M5 gene sets. V1.M2 genes were not included in this analysis because of the uncertainty in predicting full or partial *Mitf*-dependence. Considering the directional changes in differential expression (ΔDE), 6 GRCs were identified (Fig. 12; Suppl File 2). In general, *Mitf*-dependent genes skewed toward GRCs based

on *Vsx2* inhibition (V1i.M1, V1i.M3) whereas a more balanced GRC distribution was observed for *Mitf*-independent genes (V1i.M5, V1p.M5). This is consistent with the idea that *Mitf* promotes expression of non-retinal genes to a greater extent than repressing expression of retinal genes. Since differentially expressed transcription factors (DETFs) could be candidates for extending the *Vsx2*-interaction network, DETFs were identified for each GRC with the top 2 ranked DETFs listed (Fig. 12; Suppl File 2). In general, the number of DETFs increased with the size of the DEG pool except for the V1p.M5 GRC, which has a similar number as V1i.M3 and V1p.M3. This could reflect a more direct role for *Vsx2* in regulating genes in the V1p.M5 GRC. Interestingly, the top DETFs in the V1p GRCs have established roles in promoting retinal development, and neurogenesis in particular (Jin and Xiang, 2017; Shiau et al., 2021).

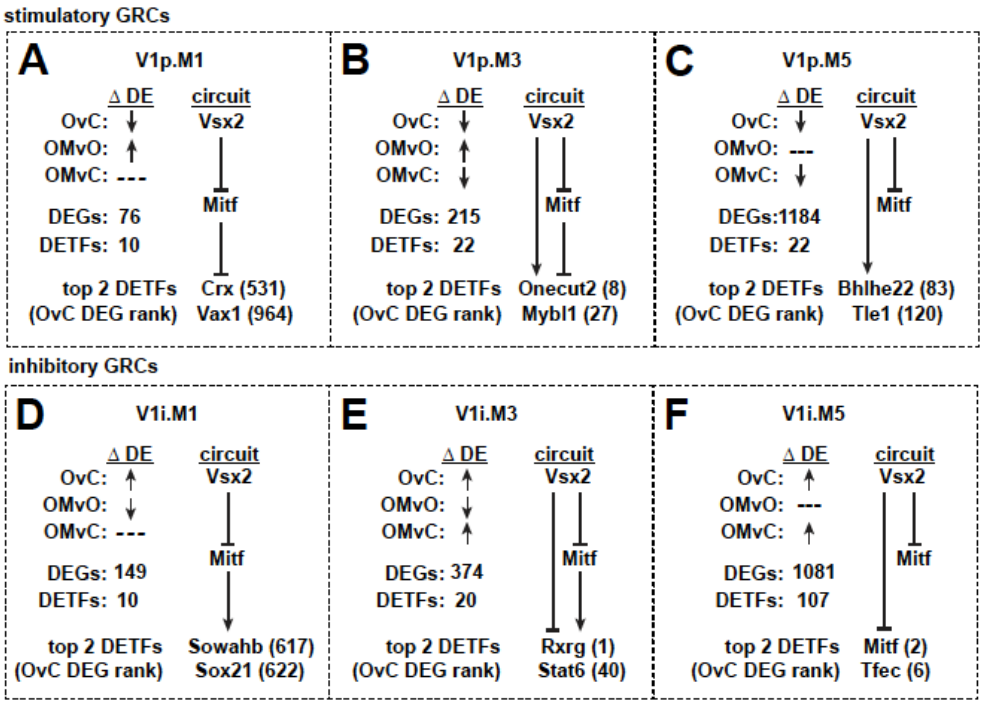

Figure 12. Classification of V1 genes into gene regulatory circuits (GRCs) based on *Mitf*-dependency and directional changes in gene expression. V1.M1, V1.M3, and V1.M5 genes were split into stimulatory and inhibitory GRCs based on their direction of expression change (ΔDE) in the OvC comparison with downregulated genes promoted by Vsx2 (stimulatory; V1p GRCs) and upregulated genes inhibited by Vsx2 (inhibitory; V1i GRCs). The ΔDE profiles in the OMvO and OMvC comparison further resolved circuit topology. The number of DEGs and DETFs are provided for each GRC and the top 2 DETFs by DEG rank (adj-p from OvC DESeq2 comparison) are shown.

Overrepresentation analysis reveals *Mitf*-dependent and -independent impacts on curated molecular pathways.

Functional annotation of DEGs was done with Ingenuity Pathway Analysis (IPA; Qiagen). We utilized the Canonical Pathways function which performs an overrepresentation analysis (CP-ORA) of curated collections of genes that are components of signaling, metabolic, and other defined molecular pathways (Krämer et al., 2014). The p-value for each pathway was calculated with the right-tailed Fisher's exact test and an alpha level of 0.05 was used to reject the null hypothesis – that overrepresentation of a pathway in the query data is due to random chance. The antilog of the p-value was used for visualization purposes and is referred to as the ORA score. An ORA score of 1.3 is equivalent to p = 0.05; larger ORA scores are equivalent to smaller p-values. IPA also calculates an activation z-score for pathways with known topology. Scores greater than 2 predict activated pathways and less than -2 predict inhibited pathways (Krämer et al., 2014).

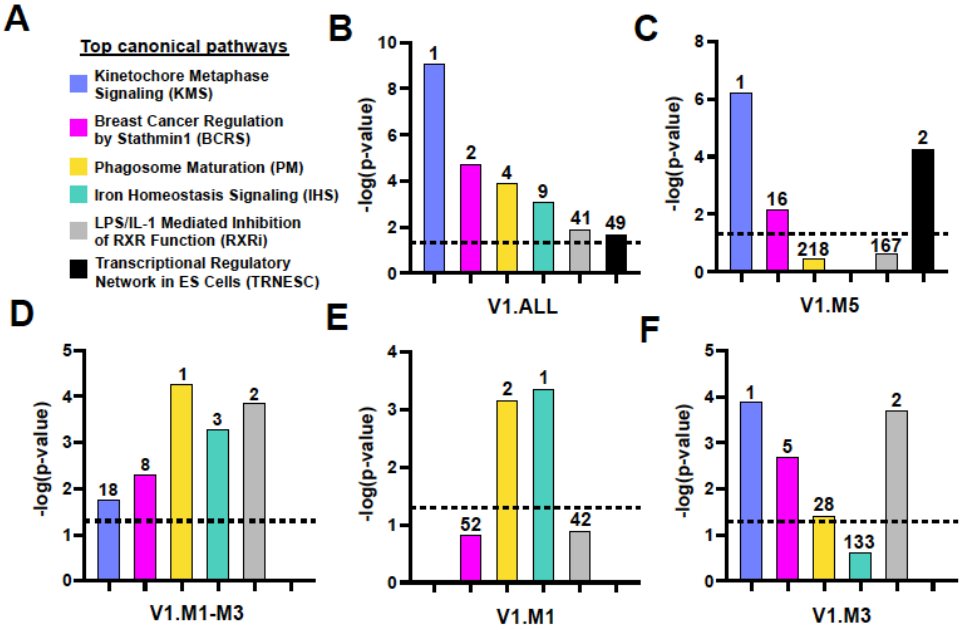

Figure 13. Comparison of overrepresented canonical pathways in V1 gene sets. CP-ORA was done for the full cohort of V1 genes (V1.ALL), for Mitf-dependent genes (V1.M1-M3; V1.M1; V1.M1) and Mitf-independent genes (V1.M5). The two top ranked pathways for each gene set based on ORA score (-log(p-value)) were identified in the other gene sets. (A) 6 canonical pathways were identified across the 5 gene sets. (B-E) Distribution of the 6 pathways by ORA score (y-axis) and rank (numbers above bars) for V1.ALL (B), V1.M5 (C), V1.M1-M3 (D), V1.M1 (E), and V1.M3 (F) gene sets. ORA scores ≥1.3 are considered significant.

CP-ORA was done for five DEG sets: V1.ALL, V1.M5, V1.M1-M3, V1.M1, and V1.M3 (tabulated results in Suppl File 3). As expected, the number of identified pathways increased with the number of genes in each DEG set (Suppl File 4). To compare pathways by their dependencies on *Vsx2* and *Mitf*, the two pathways with the highest ORA scores for each DEG set were identified and their ranks by ORA scores in the 5 DEG sets were assessed (Fig. 13; Suppl File 4). 6 pathways were identified (Fig. 13A) and all have significant ORA scores in the V1.ALL DEG set (Fig. 13B). The *Kinetochore Metaphase Signaling* (*KMS*) and *Breast Cancer Regulation by Stathmin1* (*BCRS*) pathways are associated with microtubule dynamics, mitosis, and cell cycle control, and are overrepresented in the V1.M3 and V1.M5 gene sets (Fig. 13C-F). Their activity Z-scores, indicative of an inhibited *KMS* pathway and activated *BCRS* pathway, are consistent with inhibited mitosis and cell cycle progression (Fig.14). The *Phagosome Maturation* (*PM*) and *Iron Homeostasis Signaling* (*IHS*) pathways are important for rod outer segment turnover and iron regulation in RPE (Chen et al., 2009; Wavre-Shapton et al., 2014), respectively, and both are overrepresented in the V1.M1 gene set, indicative of strong *Mitf*-dependency (Fig. 13C-F). The *LPS/IL-1 Meditated Inhibition of RXR Function* (*RXRi*) pathway was overrepresented in the V1.M3 gene set and its activity Z-score is consistent with inhibition (Fig. 13C-F; Fig. 14). Since *Rxrg* is a V1.M3 gene and the highest ranked upregulated DEG in the *orJ* retina, the presence of the *RXRi* pathway suggests elevated RXR activity. The *Transcriptional Regulatory Network in Embryonic Stem Cells* (*TRNESC)* was the only pathway to be specifically overrepresented in the V1.M5 set (Fig. 13C-F), and this is consistent with the high number of DETFs in this set (Fig.12C,F).

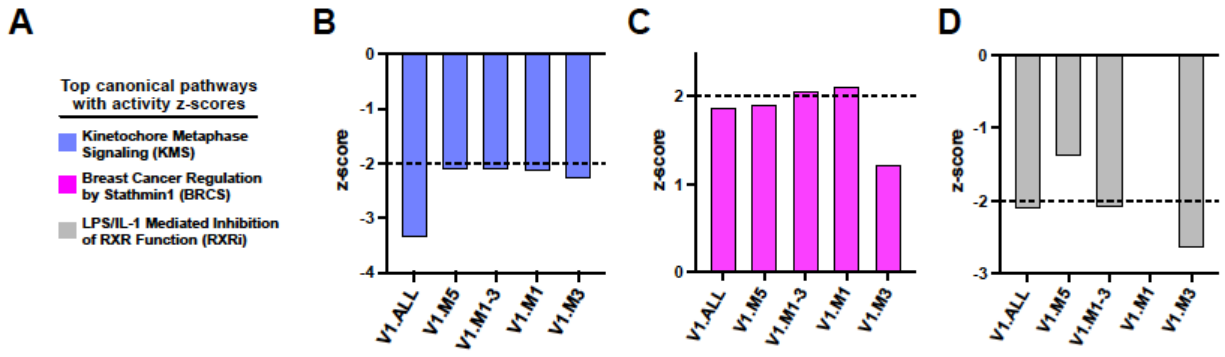

Figure 14. Canonical pathways with activity Z-scores. (A) Key for the 3 of 6 canonical pathways with activity Z-scores. **(B-D)** Z-score profiles by gene set for the KMS (B), BCRS (C), and RXRi (D) pathways. Positive scores predict activation; negative scores predict inhibition. Dashed lines indicate thresholds for significance.

Mitf partially accounts for lineage infidelity in the *orJ* retina.

Although IPA identified several gene ontology (GO) terms and disease categories corresponding to disrupted eye development and congenital CNS abnormalities (not shown), direct insight into potential effects on lineage fidelity were not obvious. This likely reflects a lack of contextual information in the Ingenuity Knowledge Base, an issue that could also apply to other broadly used knowledge databases. We predicted that ORA using lists comprised of genes specific to the nascent neural retina (NR) and RPE tissues would resolve this. We used the *My Lists* feature in IPA, which employs the same approach as CP for ORA, but for user-generated gene lists. To avoid subjectively selecting genes, we generated gene lists from RNA sequencing data produced from self-organizing mouse optic cup cultures that were treated for 5 days with FGF (bFGF) to generate neural retina-fated tissue (NR) or CHIR99201 (Wnt/b-catenin pathway agonist) to generate RPE-fated tissue (Andrabi 2015). We selected the most differentially expressed genes between them, aiming for approximately 100 genes in each list that were also present in our dataset (Fig. 15A; Suppl File 5**;** see methods).

ORA for the V1.ALL gene set revealed strong scores for the NR and RPE gene lists, suggesting that they provide good representation of both tissue states in the cohort of *Vsx2*-dependent genes (Fig. 15B, Suppl File 6). ORA for *Mitf*-dependent genes (V1.M1 - V1.M3) produced significant scores for the NR and RPE lists with a notably higher ORA score for RPE (Fig. 15B). Comparison of the ORA scores for the V1.M1, V1.M3, and V1.M5 gene sets revealed a trend away from *Mitf*-dependence for the NR genes and a trend toward *Mitf*-dependence for the RPE genes (Fig. 15C). Identifying the GRCs to which the NR and RPE genes belong confirmed these trends, but also revealed the majority of RPE genes are in the V1i GRCs whereas the NR genes are V1p GRCs (Fig. 15D,E). These observations support our earlier observation that *Mitf* negatively impacts lineage fidelity by promoting the expression of nonretinal genes to a greater extent than by repressing retinal genes.

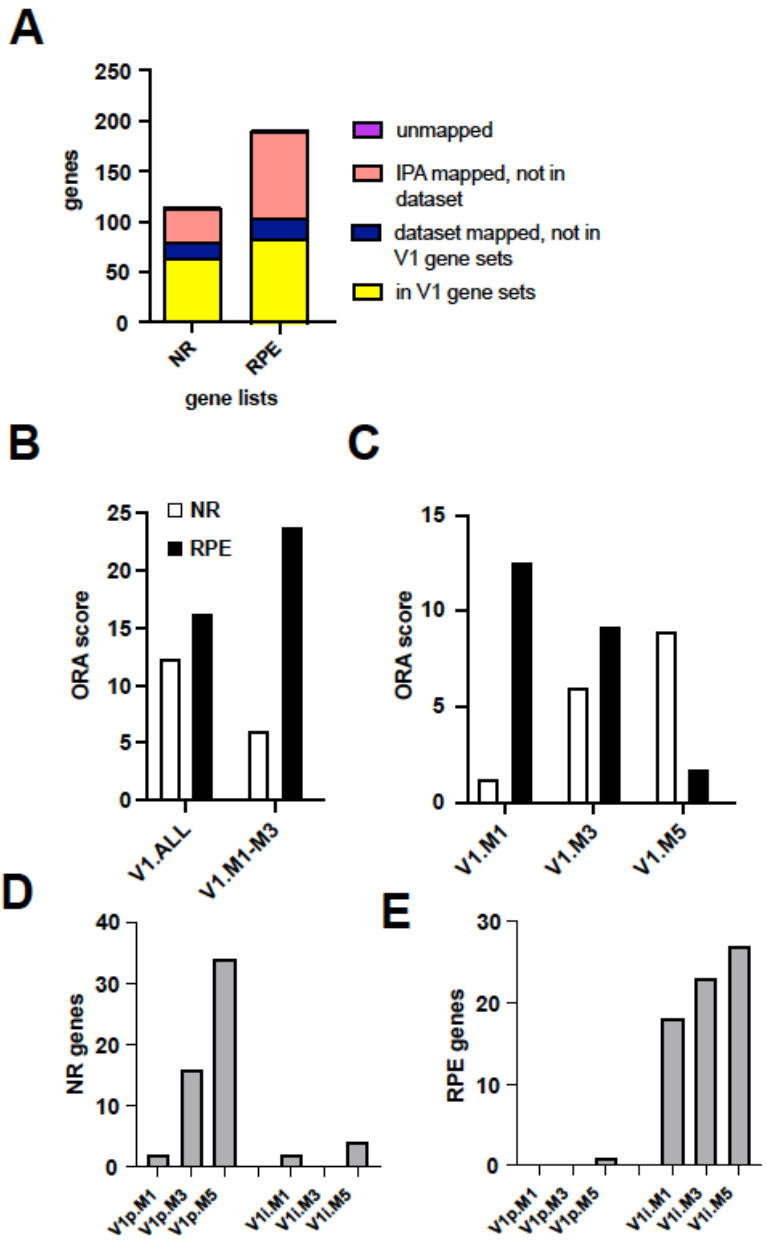

Figure 15. *Mitf* differentially impacts the expression of V1 genes associated with neural retina (NR) and RPE identity. ORA using differentially expressed genes culled from published RNA sequencing data of FGF- or Wnt-treated ESC-derived optic cup organoids to promote neural retina (NR) or RPE identities, respectively (Andrabe et al., 2015). (A) Distribution of NR and RPE genes in each list. Genes mapped to the RNA sequencing data of the three genotypes (blue and yellow bars) were used for ORA analysis. (B) ORA scores for the NR gene list (white bars) and RPE gene list (black bars) in the V1.ALL and V1.M1-M3 gene sets. (C) ORA scores for the NR and RPE gene lists in the V1.M1, V1.M3, and V1.M5 gene sets. (D) Distribution of genes from the NR gene list by GRC. (E) Distribution of genes from the RPE gene list by GRC.

Mitf activity is not a major factor in disrupting neurogenesis in the *orJ* retina

We applied similar logic to determine how genes associated with retinal neurogenesis and retinal cell types are affected in the *mutants*. Gene lists were generated through differential gene expression analysis of a single cell atlas of mouse retinal development (Clark et al., 2019). The analysis was limited to cells harvested at E11.5, E12.5, and E14.5 to generate gene lists for developmentally relevant cell types: early RPCs (eRPC), neurogenic RPCs (nRPC), RGCs, amacrine cells (Ama), horizontal cells (HC), cones (C), photoreceptor precursors (PhPr), and an aggregated non-retinal cell types grouping (RPE_M_O) that include RPE, ciliary margin (M), lens epithelium, and periocular mesenchyme (O); see methods; Suppl File 7). As with the NR and RPE lists, we aimed for approximately 100 genes from each list to be present in our dataset although this was not achieved for several lists (Fig. 16A; Suppl File 7). Rather than reduce stringency to include more genes, the Cones and Photoreceptor precursor gene lists were combined into a single list (C_PhPr) as were the amacrine and horizontal cell gene lists (A_HC) because of their high proportion of shared genes. Other genes that were found in more than one cell type were assigned to the cell type with strongest expression values (adj-p-val and % positive cells) or were excluded from all cell types (Suppl File 7).

ORA for the V1.ALL gene set produced significant scores for all cell types except the RPE_M_O list (Fig. 16B; Suppl File 8**)**. The ORA score for nRPC genes was highest, suggesting that *Vsx2* regulates many genes in nRPCs, or more generally, the nRPC state, which would be consistent with the delayed onset of neurogenesis. ORA was then done for the different V1 gene sets and the V1.M5 genes consistently produced the highest ORA scores for each cell type (Fig. 16C). *Mitf* is also likely to affect nRPC gene expression since the ORA scores were significant for the V1.M1-M3 and V1.M3 gene sets (Fig. 16C (nRPC graph)). Cone_PhPr genes were also overrepresented in the V1.M1-M3 set (Fig. 16C, Cone_PhPr graph). Gene distributions by GRC showed a skew toward V1p GRCs for nRPC and RGC genes and more even distributions

between V1p and V1i GRCs for eRPC, Cone_PhPr, and A_HC genes (Fig. 16D). The unexpected outcome of retinal cell type genes being inhibited by *Vsx2* could be because they are also expressed in RPE (i.e., *Crx*) or other non-retinal tissues, or are expressed prematurely in *orJ* RPCs (i.e., *Crx*, *Rxrg*). In sum, the gene lists used to represent each cell type correlate well the delay in neurogenesis and support the hypothesis that *Mitf* partially contributes to the delay in the onset of neurogenesis in the *orJ* retina.

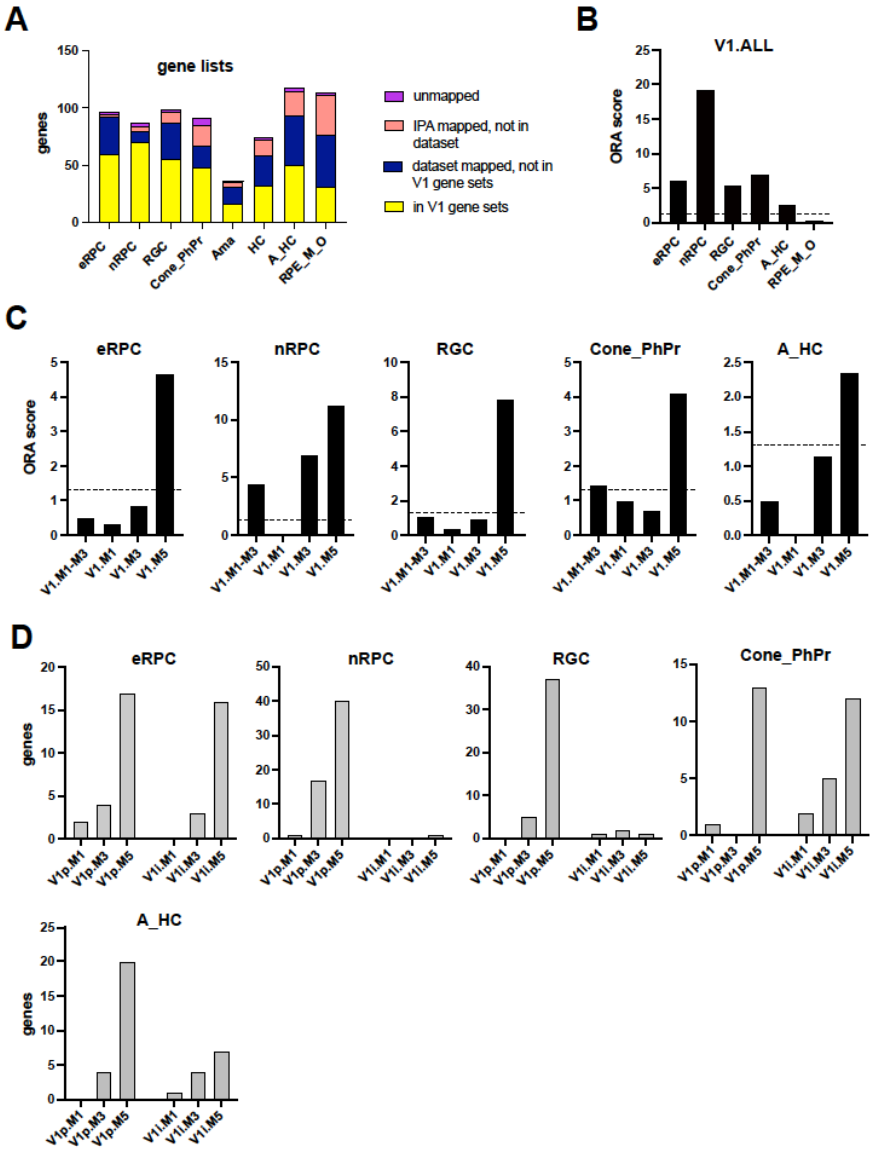

Figure 16. *Mitf* has a modest impact on the expression of V1 genes associated with retinal neurogenesis. ORA using differentially expressed genes by cell type from published scRNA-seq data of E11.5, E12.5, and E14.5 mouse retinas (Clarke, et al., 2019). (A) Distribution of cell type genes in each list. Genes mapped to the RNA sequencing data of the three genotypes (blue and yellow bars) were used for ORA analysis. The cone and photoreceptor precursor (PhPr) gene lists were combined (Cone_PhPr) because of high gene overlap and low numbers of dataset mapped genes. The same was done for amacrine (Ama) and horizontal cells (HC). RPE_M_O is not a true cell type but was assigned as a cell label in Clarke et al. (2019). (B) ORA scores for the cell type gene lists in the V1.ALL gene set. (C) ORA scores for each cell type gene lists from the V1.M1-M3, V1.M1, V1.M3, and V1.M5 gene sets. The RPE_M_O gene list was not included because of its low ORA score in the V1.ALL gene set and is not a true cell type. (D) Distribution of genes from the cell type gene lists by GRC.

Inhibition of RXR activity in *orJ* retinal explant culture reveals *Rxrg* to be a minor functional interactor with *Vsx2*.

That *Mitf* activity only partially accounts for the *orJ* phenotype reveals the pleiotropic nature of *Vsx2* interaction network at its highest level and suggests additional factors functionally could interact with the *orJ* allele to promote the mutant phenotype as well as to set the degree of phenotypic severity. The most direct approach to identify functional interactors is by genetic suppression of candidate factors *in vivo* as done for *Mitf*, but this is not easily done because of the limited availability of mutant alleles and the significant effort needed to generate combinatorial *mutants*. We therefore incorporated organotypic cultures of *orJ* retina with lens intact (retinal explants) and used small molecules to inhibit the activities of candidate interactors.

Our first focus was on *Rxrg*, the highest ranked DEG by adj-p-value in the OvC comparison (Suppl File 2). Antibody staining confirmed upregulation of *Rxrg* upregulation with a broad distribution across the E12.5 *orJ* retina (Fig. 17A). *Rxrg* is a nuclear receptor that binds to 9-cis retinoic acid and regulates transcription of target genes as a homodimer or in heterodimer combinations with other nuclear receptors that include the retinoic acid receptors (RAR) and thyroid hormone receptor (TR) (Cvekl and Wang, 2009). *Rxrg* is normally expressed in RGCs and cones (Buenaventura et al., 2019; Hoover et al., 1998; Lyu and Mu, 2021; Roberts et al., 2005), but the delay in neurogenesis suggests that its ectopic expression in *orJ* RPCs is not due to the differentiation of these cell types. *Rxrg* is also transiently expressed in the nascent RPE at E10.5 and at the peripheral border between the NR and RPE (Mori et al., 2001), suggesting that it could contribute to lineage infidelity in the *orJ* retina. Its pattern of ΔDE places it in the V1i.M3 GRC (Fig. 12E), suggesting that *Mitf* partially contributes to its upregulation. Based on these data, we hypothesized that *Rxrg* activity is an additional factor in causing the *orJ* phenotype and suppressing its activity will exhibit positive epistasis with the *orJ* allele.

E12.5 *orJ* retinal explants were treated for 24 hr with HX531, a highly selective small molecule inhibitor of RXR activity (IC_{50}: 18nM) (Nie et al., 2017). Contrary to our prediction, we did not observe changes in EdU incorporation or in the expression of Hes1, Neurogenin 2, or Tubb3, which mark proliferation, RPCs, nRPCs and postmitotic neuronal precursors, respectively (data not shown). The lack of effects suggests that RXR activity, and by inference, *Rxrg*, is not a strong interactor in promoting the *orJ* phenotype at E12.5, despite its misregulated expression. Another possibility was that HX531 lacked activity, but bulk RNA sequencing confirmed altered gene expression in HX531 treated *orJ* explants. Out of 19321 GMFs, 67 genes were identified as differentially expressed with an FDR cutoff of 0.05 (HX531 DEGs; Fig. 17C; Suppl File 9). Because of this low number, we performed qPCR on the top 3 DEGs and found that *Abca1* and *Scd2* were downregulated with HX531 treatment, but the downward trend in *Abcg1* was not significant (Fig. 17D), an issue that could be related to weak detectability with the qPCR probe used for this analysis. CP-ORA of the HX531 DEGs revealed that the most significantly overrepresented pathways are associated with RXR function (Fig. 17E, Suppl File 10), indicating that HX531 treatment had a predictable effect on gene expression. These pathways were also identified in the V1.ALL gene set with significant ORA scores for the LXR/RXR activation and RXRi pathways (Fig. 17F; Suppl File 3). ORA with the NR, RPE, and retinal cell type gene lists identified the NR gene list as overrepresented in the HX531 DEGs, but significance was reached with only 3 genes (Suppl File 11). ORA of the HX531 DEGs in the E12.5 retinal transcriptomes (O, OM, C) generated significant scores in the V1.All gene set and in gene sets with *Mitf*-dependence (Fig. 17G; Suppl File 12). These observations suggest that HX531 treatment had a measurable effect on genes related to RXR function with some dependent on *Vsx2* and *Mitf*, but the lack of overrepresentation with the gene lists associated with retinal identity and neurogenesis suggest that HX531 treatment, and by extension, RXR inhibition, did not have a measurable impact on the *orJ* phenotype.

We next determined the distribution of the 67 HX531 DEGs with respect to *Vsx2* regulation: 35 were *Vsx2*-dependent (V1 genes), 5 were possibly dependent (V2 genes), 12 were *Vsx2*-independent (V3 genes), and 15 were absent from the OvC dataset (Fig. 17H). Of the 40 HX531 DEGs with *Vsx2* dependence (V1 and V2 genes), 18 showed improved expression and 22 showed worsened expression (Suppl File 13**)**. Improved expression is consistent with positive epistasis and suggests that RXR activity contributed to their aberrant expression in the *orJ* retina. Worsened expression is consistent with negative epistasis and suggests that RXR activity prevented their expression from deviating further in the *orJ* retina, possibly through genetic compensation due to *Rxrg* upregulation. Worsened expression could also be due to a converging role for RXR activity and *Vsx2* in regulating these genes. Consistent with this, *Rxra* and *Rxrb* are abundantly expressed at E12.5 and remain expressed in the *orJ* retina (Suppl File 2). *Rxra* and *Rxrb* inhibition could also account for the differential expression of HX531 DEGs that are *Vsx2*-independent. *Abca1* and *Scd2* are examples of HX531 treatment affecting the expression of a *Vsx2*-dependent and -independent gene, respectively (Fig. 17I,J).

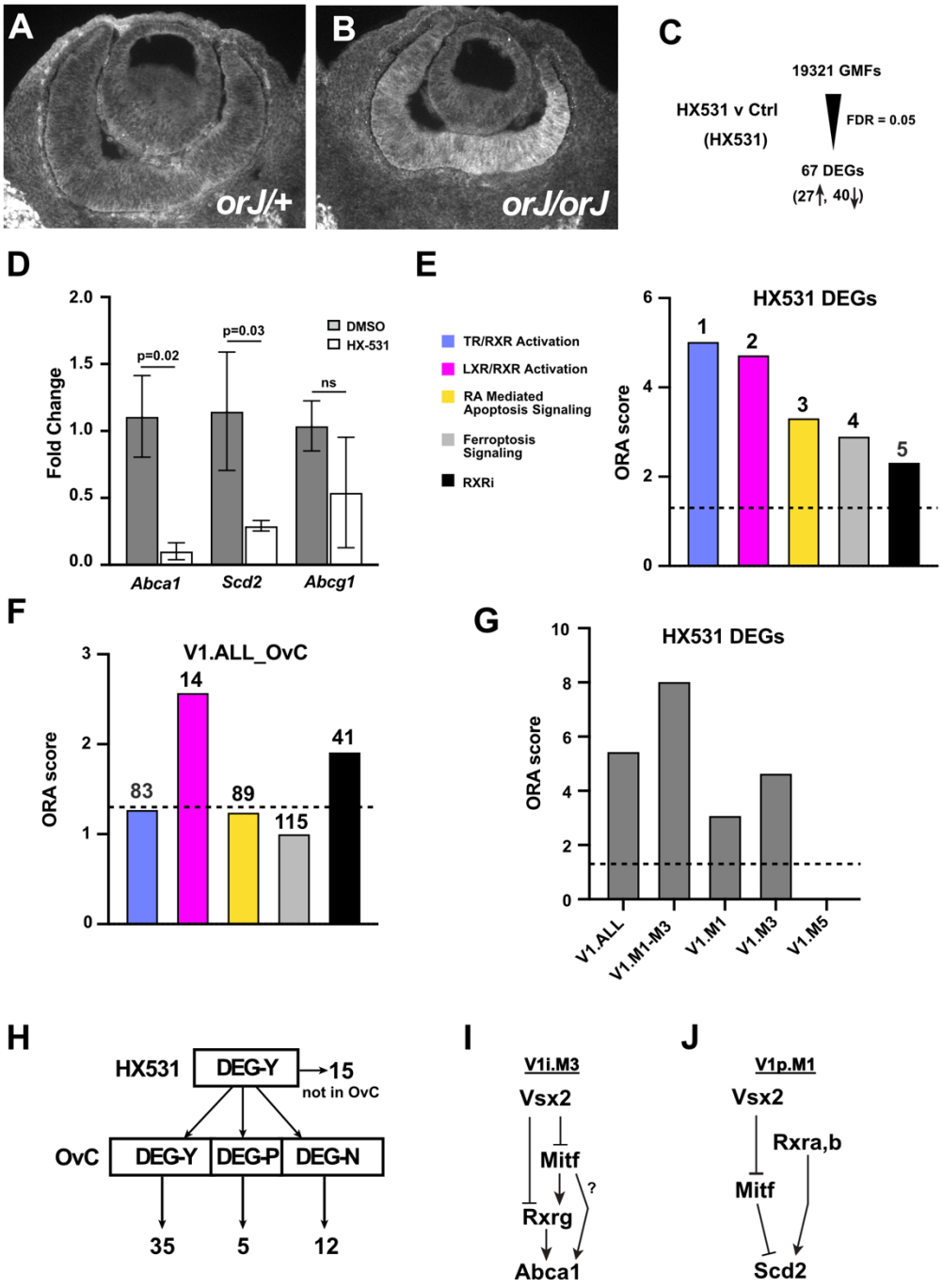

Figure 17. *Rxrg* is upregulated in the *orJ* retina but inhibition of RXR activity with HX531 has a small but measurable effect on gene expression. (A, B) Immunohistology for Rxrg expression in the E12.5 control (A) and orJ retina (B). (C) Bulk RNA sequencing of E12.5 orJ retinal tissues following HX531 treatment for 24 hr in explant culture. Pairwise comparison of the gene expression profiles from the HX531-treated and untreated (Ctrl) samples predicted 67 DEGs from 19321 GMFs with an FDR cutoff of 0.05. (D) qPCR of three DEGs, Abca1, Scd2, and Abcg1 support their reduced expression by HX531, but only Abca1 and Scd2 were statistically significant. (E) The top 5 overrepresented pathways identified by CP-ORA of the HX531 DEGs are related to RXR function. (F) Two of the pathways, LXR/RXR Activation and RXRi, had significant ORA scores from the CP-ORA analysis of the V1 gene set from the OvC comparison. (F) Predicted GRC for Abca1. Whether Rxrg fully accounts for the impact of Mitf on Abca1 expression is an open question. (G) Predicted GRC for Scd2. Whereas Mitf accounts for the upregulation in the orJ retina, HX531 treatment suggests RXR activity through Rxra or Rxrb could be promoting its normal retinal expression.

Inhibition of gamma secretase activity reveals convergent regulation of *Vsx2*-dependent genes associated with cell cycle progression and mitosis

We next focused on what could account for the delay in the onset of neurogenesis, and we reasoned that active Notch signaling could be a factor. Overexpression of the Notch1 intracellular domain (NICD) preserves the RPC state at the expense of neurogenesis (Dorsky et al., 1995; Jadhav et al., 2006; Mills and Goldman, 2017; Perron and Harris, 2000), and inhibiting Notch signaling promotes neurogenesis at the expense of RPCs (Jadhav et al., 2006; Kaufman et al., 2019; Nelson et al., 2007; Riesenberg et al., 2009b; Zheng et al., 2009). These effects are consistent with Notch signaling acting as a progenitor maintenance pathway and could account for the delayed neurogenesis in the *orJ* retina. Elevated Notch signaling could also account for the persistence of *orJ* RPCs through development despite their reduced rate of proliferation.

CP-ORA for the V1.ALL genes identified Notch signaling as an overrepresented pathway, but the activity Z-score was too low to predict a change in activation state (**Suppl File 3)** and is likely due to changes in expression of Notch pathway genes that are consistent with both activation and inhibition (**Suppl File 14**). For example, *Dll1* and *Dll4* are reduced in the *orJ* retina, but *Jag2* is upregulated. Expression of *Notch1* is reduced but *Notch2* is upregulated and *Notch3* expression is unaffected. The expression of *Hes5*, a functional readout of Notch signaling, is strongly reduced suggesting inhibited Notch signaling, but *Hes1* is unaffected, and *Hey2* is upregulated. Thus, although expression of Notch pathway genes is altered by the *orJ* mutation, predicting Notch signaling state by gene expression is ambiguous in this context.

A common pharmacological approach to block Notch signaling is with gamma-secretase inhibitors (GSIs) (Olsauskas-Kuprys et al., 2013; Strooper et al., 1999). Intracellular cleavage of Notch receptors by gamma secretase (GS) generates the NICD isoform which translocates to the nucleus to regulate target gene expression. Treatment of explants or organoids at the early stages

of retinal neurogenesis with GSI-IX (DAPT) caused RPCs to rapidly exit the cell cycle and transition into RGC and cone photoreceptor precursors, effects that align well with genetic models of abrogated Notch signaling (Jadhav et al., 2006; Kaufman et al., 2019; Nelson et al., 2007; Riesenberg et al., 2009b; Zheng et al., 2009). Since the components of the gamma secretase complex are expressed in the *orJ* retina (Suppl File 15**)**, we predicted that GSI treatment would inhibit proliferation and accelerate the onset of neurogenesis in the *orJ* retina.

We treated E12.5 control retinal explants with 1 μM dibenzazapine (DBZ), a potent GSI, for 24 hr. Retinal neurogenesis is underway by E12.5 and serves as a positive control since it overlaps with other studies incorporating DAPT treatment (Kaufman et al., 2019; Nelson et al., 2007). As expected, precocious neurogenesis was observed (Fig. 18A, left panels), demonstrating reproducibility with prior studies (5 μM DAPT gave similar results; not shown). We next treated E14.5 *orJ* retinal explants with 1 μM DBZ and neurogenesis was also observed, demonstrating that *orJ* RPCs exhibit similar responses to gamma secretase inhibition, although possibly less robustly, once neurogenesis begins (Fig. 18A, middle panels). However, we observed cytotoxicity with 1 μM DBZ (and 5 μM DAPT) in E12.5 *orJ* explants as indicated by pyknotic nuclei in the retina and lens (Fig. 18A, right panels). Lowering DBZ to 300 nM reduced pyknosis but precocious neurogenesis was not observed, even in E12.5 wild type retina (not shown). However, EdU incorporation was reduced in the E12.5 *orJ* retina and quantifications confirmed this with 300 nM DBZ and 1 μM DAPT (Fig. 18B). This suggests gamma secretase activity promotes proliferation in *orJ* RPCs, but the lower concentrations of DBZ and DAPT precluded an assessment of gamma secretase inhibition on accelerating neurogenesis onset in the *orJ* retina.

RNA sequencing and differential gene expression analysis was done for 300 nM DBZ- and vehicle-treated E12.5 *orJ* explants (Suppl File 16). Of the 19321 GMFs identified, 376 genes were differentially expressed based on an FDR cutoff of 0.01 (DBZ DEGs; Fig. 18C). This is

notably higher compared to HX531 treatment, where 67 DEGs were identified with a less stringent FDR cutoff (0.05). 317 of the 376 DBZ DEGs exhibited decreased expression, indicating that GS activity generally promotes gene expression in the *orJ* retina. 332 DBZ DEGs were *Vsx2*-dependent (DEG-Y; V1 genes), 13 were possibly dependent (DEG-P; V2 genes), 30 were *Vsx2*-independent (DEG-N; V3 genes), and 1 was not identified in the *mutants* dataset (Fig. 18D). Surprisingly, 337 DBZ DEGs with *Vsx2* dependence (V1 and V2 genes) exhibited worsened expression, with 47 showing increased and 290 decreased expression levels, respectively (Fig. 18E, underlined numbers; Suppl File 17). In contrast, only 8 DEGs exhibited improved expression (italicized numbers in Fig. 18E). These observations indicate that DBZ treatment altered the expression of a large cohort of *Vsx2*-dependent genes in the same direction as the *orJ* mutation, suggesting that *Vsx2* and gamma secretase activity regulate a common set of genes in a similar manner and is strong evidence for negative epistasis.

We next determined the extent to which the DBZ DEGs have regulatory input from *Mitf*. As expected, ORA of the DBZ DEGs in the V1 gene sets in the *mutants* dataset revealed strong scores in the V1.All gene set, but also in Mitf-dependent gene sets, with strong overrepresentation in the V1.M3 gene set, and DBZ DEGs were also overrepresented in the V1.M5 gene set, indicating distributions of DBZ DEGs among *Mitf*-dependent and -independent V1 genes (Fig. 18F). Most Mitf-dependent genes were found in the V1.M3 set and the distribution of the numbers of genes were similar between the V1.M3 and V1.M5 GRCs (Fig. 18G), and as expected from their ΔDE patterns (Fig. 18E), most genes are promoted by *Vsx2*.

CP-ORA was done for the DBZ DEGs and the overlap of the top 5 pathways was compared to the pathways identified in the V1.All gene set from the mutant analysis (upper graphs in Fig. 18H,I; Suppl File 18; Suppl File 3). All 5 pathways in the DBZ dataset were associated with cell cycle control and mitosis. Interestingly, all were enriched in the CP-ORA for the V1.All set with 4 pathways in the top 10 based on ORA scores. Of note, the *KMS* pathway

had the highest ORA score in both gene sets. The distribution of the activity Z-scores for the canonical pathways trended toward inhibition with significant Z-scores for the *KMS*, *Cell Cycle Control of Chromosomal Replication*, and *Mitotic Roles of Polo-like Kinase* pathways in both gene sets (lower graphs in Fig. 18H,I). The overlap in overrepresented canonical pathways and their predicted activation states further supports the idea that *Vsx2* and gamma secretase promote RPC proliferation by promoting the expression of a large cohort of genes in a convergent manner and that gamma secretase activity exhibits negative epistasis with *Vsx2*.

ORA analysis of the DBZ DEGs in the DBZ dataset with the NR, RPE, and the retinal cell type gene lists produced significant ORA scores for eRPC and nRPC genes with all identified genes reduced in expression (Fig. 18J; Suppl File 19). Since ORA scores for retinal cell types other than RPCs were not significant, it is unlikely that DBZ treatment drove RPCs toward neurogenesis. Rather, most of the genes identified in the eRPC and nRPC gene lists are associated with cell cycle control and metabolism with the nRPC genes *FoxN4* and *Notch1* being notable exceptions (Suppl File 19). *FoxN4* is a transcription factor required for generating amacrine and horizontal cell precursors and it promotes the expression of *Dll4* (Luo et al., 2012). Their reductions suggest that Notch signaling was inhibited in DBZ-treated explants and that neurogenic competence was suppressed, not enhanced, by gamma secretase inhibition.

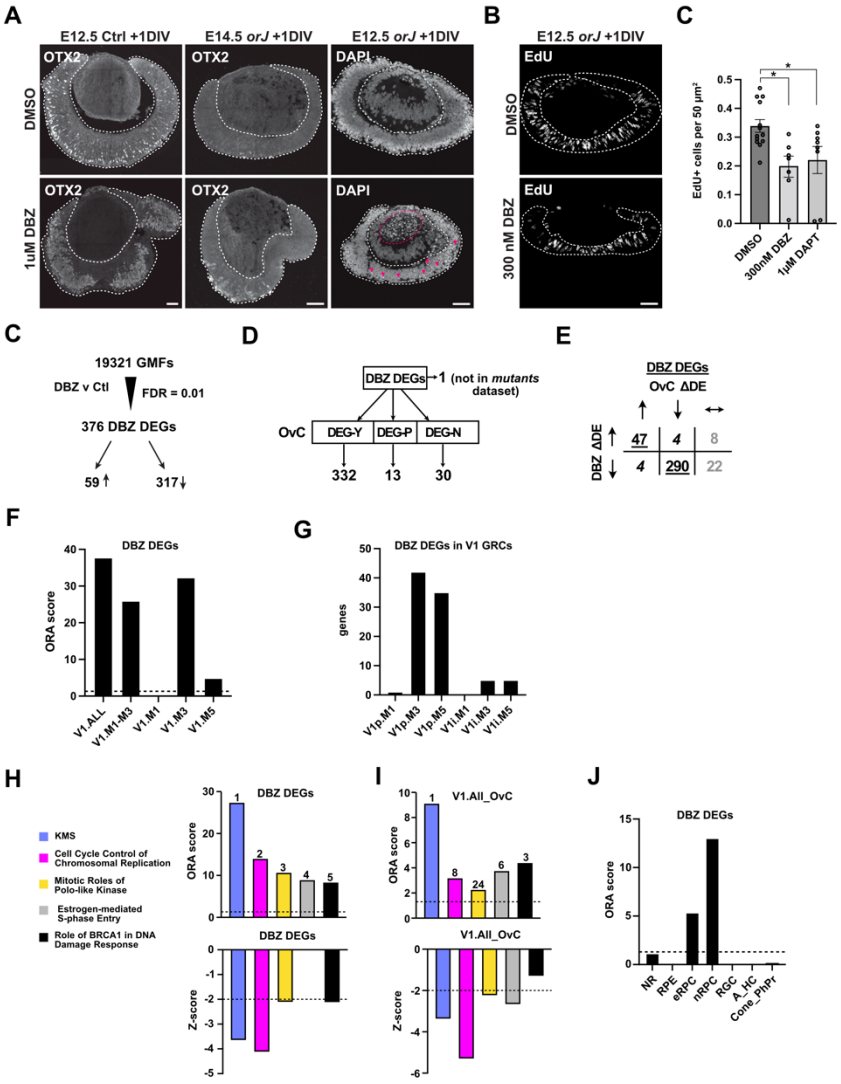

Figure 18. Gamma secretase inhibition negatively impacts the expression of V1 genes in the *orJ* retina. (A, B) Retinal explants were cultured for 24 hr (1DIV). Retinal tissue is contained within the yellow outlines. Scale bars: 50 µM (A) Expression of Otx2 and DAPI staining in retinal explants cultured in vehicle (0.1% DMSO) or 1µM DBZ. Left column shows E12.5 wild type retinas, middle column shows E14.5 orJ retinas, and right column shows E12.5 orJ retinas. Examples of pyknotic nuclei in the retina are indicated by arrows and in the lens with purple dashed oval in the DAPI stained E12.5 orJ retina treated with DBZ. (B) EdU incorporation in E12.5 orJ retinal explants cultured in vehicle or 300 nM DBZ. (C) Quantification of EdU+ cells. Error bars show S.E.M. Adjusted p-values were calculated with Tukey's multiple comparisons test following 1-way ANOVA. (D) Summary of RNA sequencing and differential gene expression from DBZ and vehicle (control) treated orJ explants. FDR cutoff of 0.01 was used to identify DEGs (DBZ DEGs). Up and down arrows indicate increased or decreased expression, respectively, in the DBZ treated retina compared to control. (D) Partitioning of DBZ DEGs by their Vsx2-dependence in the mutants dataset. 1 DBZ DEG was not identified in the mutants dataset. (F) ORA scores for DBZ DEGs in the indicated V1 gene sets within the mutants dataset. (G) Predicted GRCs for DBZ DEGs in the mutants dataset. (G) ORA for the DBZ DEGs with NR, RPE, and retinal cell type gene lists. (H) The top 5 pathways identified by CP-ORA with DBZ DEGs in the DBZ dataset. Upper graph shows ORA scores and lower graph shows Z-scores for pathway activity prediction. Negative Z-scores predict pathway inhibition and a value less than -2 (dashed line) is considered significant. (I) ORA scores and rank for the same 5 pathways in the V1.ALL gene set from the OvC comparison (upper graph). Lower graph shows Z-scores for pathway activity prediction. (J) ORA scores for the NR and retinal cell type gene lists from analysis of the DBZ DEGs in the DBZ dataset.

Discussion

We combined transcriptome profiling with *in vivo* and *ex vivo* interaction testing to characterize the contributions of candidate genes and molecular activities to the early retinal phenotype of the *orJ* mutant mouse. The triangular experimental design used for the genetic transcriptome analysis enabled a semi-quantitative assessment of the gene regulatory and phenotypic impacts of *Mitf*, a direct target of *Vsx2* transcriptional repression. Our finding that *Mitf* activity only partially contributes to the early *orJ* phenotype established the context for identifying additional interactors. This led to the identification of *Rxrg*, a top-ranked DEG in the *orJ* retina, but the weak effects of small molecule inhibition on RXR activity suggest that *Rxrg* has a minimal role in the phenotypic traits of the E12.5 *orJ* retina. RXR inhibition also identified *Rxra* and/or *Rxrb* as candidate regulators of a limited set of *Vsx2*-dependent and -independent genes. We also determined that gamma secretase activity supports RPC proliferation in the absence of *Vsx2* by sustaining expression of a large cohort of *Vsx2*-dependent genes in a manner consistent with convergent negative epistasis. This streamlined approach for interaction testing permitted straightforward assessments of candidate causal factors underlying a complex developmental phenotype.

That *Mitf* exhibits positive epistasis with *Vsx2* was expected and the nearly complete concordance of improved expression for *Vsx2*-dependent genes by introduction of the *mi* allele gave us confidence that epistasis can be assessed at the transcriptomic level. Whereas the impact of the *mi* allele on alleviating the ectopic expression of non-retinal genes was anticipated, the relatively minor impact on the expression of retinal genes was not. Since the RNA sequencing data was generated with the *mi* allele in the heterozygous state, it is possible that wild type Mitf protein was still active in the *orJ; mi*^{het} retina. However, this issue had to be balanced with the potential for non-cell autonomous effects on retinal development from disruptions in RPE

development caused by the *mi* allele in a homozygous state (Bumsted and Barnstable, 2000; García-Llorca et al., 2019; Wen et al., 2016). Genetic redundancy is also possible since *Tfeb*, a related bHLH-zip gene, was upregulated in the *orJ* retina. These issues are somewhat mitigated with the *mi* allele since the mutant protein functions in a dominant negative manner by heterodimerizing with wild type MITF and TFEB (Hemesath et al., 1994), and because a large cohort of *Mitf*-dependent genes were identified. Even with the possibility of residual *Mitf* and/or *Tfeb* activity, our data suggest that other factors contribute to the *orJ* phenotype. Despite its ectopic expression, *Rxrg* is an unlikely candidate, but other ectopically expressed DETFs identified in the V1i.M3 and V1.M5 GRCs remain viable candidates.

An important question is how much effort is needed to identify interactions or the lack thereof. While current sequencing-based technologies would offer higher resolution data than bulk RNA sequencing alone, they are resource intensive, and emergent candidates still need to be tested for functional interaction. For this study, we found that sufficient resolution was achieved with bulk RNA sequencing data that was then analyzed by categorical gene classification based on expression dependency and by ORA with canonical pathways and context-specific gene lists. The interaction tests for *Mitf* and gamma secretase activity clearly support this contention, but it is arguably the evidence for noninteraction between *Vsx2* and *Rxrg* that provides the strongest support. Although *Rxrg* is clearly repressed by *Vsx2* (directly or indirectly) and inhibiting RXR activity had a minimal effect on restoring gene expression, we could still assess functional interaction. Of the genes affected by HX531 treatment, they were not correlated with the phenotypic traits of tissue identity, proliferation, or neurogenesis as suggested by the lack of overrepresentation of genes in the context-specific gene lists. However, the affected genes were associated with RXR function, and their directional changes in expression and their degree of dependency on *Vsx2* provided initial evidence of gene regulation by *Rxra* and/or *Rxrb* in addition to *Rxrg*.

We note that our conclusion stating that *Rxrg* is not a strong interactor with *Vsx2* is only relevant for the specific conditions tested and phenotypic traits studied. Since the *LXR/RXR activation* and *RXRi* canonical pathways were overrepresented in the V1.ALL and HX-531DEGs, elevated RXR activity could cause changes in the *orJ* retina not revealed by our analyses, with possibilities being altered cholesterol transport and/or lipid metabolism due to the upregulation of the ATP-binding cassette genes *Abca1* and *Abcg1* and the Stearoyl-CoA-desaturase gene *Scd2* (Frambach et al., 2020; Storti et al., 2019; Sun et al., 2003). How this relates to *Vsx2* function is not known but could reflect a role for *Vsx2* in controlling the timing of *Rxrg*-dependent gene expression such that it is activated when RPCs transition into RGC and cone precursors (Buenaventura et al., 2019; Hoover et al., 1998; Lyu and Mu, 2021; Roberts et al., 2005).

Whereas *Rxrg* emerged as a candidate interactor from the RNA sequencing data of the *mutants*, our interest in gamma secretase activity arose from a prediction that inhibiting Notch signaling would accelerate the onset of neurogenesis in the *orJ* retina, a hypothesis based on prior knowledge of the function of Notch signaling and pharmacological gamma secretase inhibition in the embryonic retina. Although toxicity issues precluded us from testing this hypothesis, we found that gamma secretase inhibition with a low dose of DBZ further reduced RPC proliferation in *orJ* RPCs. This is not surprising since an established role for Notch signaling is to maintain stem/progenitor cells, but the extensive overlap and directional change in expression of gamma secretase-dependent genes with hundreds of *Vsx2*-dependent genes was unexpected. Importantly, it provides compelling evidence that the interaction of gamma secretase activity with *Vsx2* is one of negative epistasis where both support RPC proliferation by convergence onto a set of downstream genes or shared GRC. Convergent negative epistasis could also explain why RPCs persist and continue to proliferate (albeit slowly) in the *orJ* retina (Dhomen et al., 2006; Levine and Green, 2004).

A caveat with the above argument is the assumption that the impact of gamma secretase inhibition is due to reduced Notch signaling, but our data provides very limited evidence for this. Over 150 substrates of gamma secretase have been identified (Güner and Lichtenthaler, 2020) and many are present in the RNA sequencing data. It is possible, then, that the interaction between gamma secretase and VSX2 is independent of Notch signaling. Addressing this would require interaction testing that targets specific genes rather than gamma secretase activity or its component genes.

In sum, with the methods and analyses adopted here, we gained useful insights into functional interactions between candidate factors and *Vsx2* in early retinal development. We showed that the logic of positive and negative epistasis can be applied to genetic and non-genetic methods of suppression when combined with straightforward analysis of bulk RNA sequencing data. This approach should be scalable and could be applicable to other mutations that cause complex developmental phenotypes.

Materials and Methods

Mice

All procedures and experiments with mice are approved under protocol M1500036 by the Vanderbilt Institutional Animal Care and Use Committee and conform to the ARVO guidelines for the use of animals in vision research. 129S1 wild type mice (RRID:IMSR_JAX:002448) are used to maintain *Vsx2*^{orJ} mice. *Vsx2*^{orJ} mice (RRID:IMSR_JAX:000385) have been maintained in the lab for over 10 years with continual outcrossing to 129S1 wild type mice (RRID:IMSR_JAX:002448). *Mitf*^{mi} mice were obtained from the Jackson Laboratories (Jax) on a C57Bl6 background and is currently maintained at Jax with the *Mitf*$^{mi\text{-}wh}$ allele (RRID:IMSR_JAX:000158). The *mi* allele has been maintained for over 6 years in our laboratory and continually crossed to *Vsx2*^{orJ} mice.

Tissue collection

Single night mating was used to generate embryos. The day of the plug was considered embryonic day 0.5. Embryos were collected at the following time points: E11.5, E12.5, E13.5 and E14.5. Embryos were staged using fore and hindlimb staging (Wanek et al., 1989).

Retinal Explant Culture

Retinal explants (intact retina with lens) were collected and transferred into a 24-well plate, where each explant was bathed in 500 µL of standard DMEM/F12-based culture media. Control explants were treated with vehicle only (0.1% DMSO) and experimental explants were incubated with *Rxrγ* inhibitor (HX-531), GSIs (DAPT and DBZ). Retinal explants were cultured

for 24 hours at 37 degrees in a 5% CO_2 atmosphere. EdU (final concentration: 10 μM) was added to the media for 30 min prior to the end of the culture.

Compound	Target	Vehicle	Source/Cat #	Working concentration
HX-531	Rxra, Rxrb, Rxrg	DMSO 0.1 % v/v	Tocris/ 188844-34-0	100 nM
DAPT	Gamma Secretase	DMSO 0.1 % v/v	Sigma/ 208255-80-5	1 – 5 μM
DBZ	Gamma Secretase	DMSO 0.1 % v/v	Tocris/ 09984-56-5	300 nM – 1 μM

Table 1. Small Molecule Inhibitors

Tissue and Slide Preparation

Retinal explants and whole-head tissue were fixed in 4% PFA/PBS solution for 20 and 35 minutes, respectively. Following sucrose cryoprotection, samples were frozen in TissueTek OCT (Sakura Finetech) and stored at -80°C. 12 μm sections were adhered to Superfrost Plus slides (Fisher Scientific), dried on a warmer 37°C for 1-2 hr before storage at -20°C.

Immunohistochemistry

Slides were incubated in block solution (2% serum, 0.1% triton-x100, PBS pH 7.4) for 30-60 min at room temperature followed by primary antibody incubation overnight at 4°C overnight. After washing with PBS, sections were incubated with secondary antibodies in the dark for 2 hr at room temperature. DAPI (1:40000 in PBS) was added for 15 min. Slides were coverslipped with Fluoromount. EdU incorporation was detected with AlexaFluor 647 Click-iT Cell Reaction Kit (Invitrogen-Molecular Probes, Eugene, OR, USA).

Antibody	Species	Dilution	Manufacturer	Antigen Retrieval	Blocking buffer
Tubb3	Rabbit	1:10000	Biolegends	No	Goat/Donkey
Otx2	Rabbit	1:10000	Millipore	No	Goat/Donkey
Ngn2	Mouse	1:1000	R&D Systems	No	Goat/Donkey
Hes1	Rabbit	1:1000	Cell Signaling	No	Goat/Donkey
Atoh7	Rabbit	1:400	Novus Biologicals	No	Goat/Donkey
POU4F	Goat	1:500	Santa Cruz	No	Donkey

Table 2. Antibodies for Immunofluorescence

Microscopy

Images were captured on a LSM 710 confocal microscope using the 40x water objective. Z-stack and tile scan was performed on each section to get a single image. Tile scanning was stitched online using the online stitching function during acquisition of each image using the Zeiss Zen software, and a composite of the z-stack was created in ImageJ/Fiji (Schindelin et al., 2012) using Image>Stacks>Max Projection.

Quantifications and statistical tests of neurogenic length, Tubb3 expression, and EdU incorporation

ImageJ was used to obtain the retinal length using the freehand line tool to measure the inner edge of the retina (closest to the lens). The neurogenic region of the retina was defined by measuring the linear length of the tissue that TuJ1-positive cells occupied. % neurogenic length was calculated by dividing the neurogenic region by the retinal length and multiplying by 100. The Kruskal-Wallis test followed by Dunn's multiple comparisons test was used for statistical analysis (**Suppl File 1**).

Neurogenic density was defined by ratio of Tubb3-positive pixels as a proxy for cells within the neurogenic region. This was measured by outlining region positive for Tubb3 staining and clearing the outside of the ROI using Edit>Clear Outside in ImageJ. Neurogenic regions were made binary with *Threshold* tool and *Analyze>Histogram* was used to count the number of

positive (white) and negative (black) pixels. The These values were used to produce the density within the neurogenic region by calculating the ratio of positive pixels over total pixels. For samples that did not display any positive beta tubulin staining, the % neurogenic length and Tubb3+ pixel ratios were set to 0. One-way ANOVA, Browne-Forsythe test followed by Tukey's multiple comparisons test were used for statistical analysis (**Suppl File 1**).

EdU was manually counted in a blinded manner using the multi-point tool in ImageJ. Area was determined by ROI selection of calibrated images using the measure function in ImageJ. One Way ANOVA and Tukey's multiple comparisons test was used for statistical analysis (**Suppl File 1**).

RNA preparation, sequencing, and processing

For the *mutants* analysis, isolated retinal tissue was flash frozen in liquid N_2, and stored at -80°C. Upon thawing, samples were pooled (4 control, 6 *orJ,* 6 *orJ; mi*^{het}) and total RNA was isolated with the RNeasy mini-Kit (Qiagen). Each pool was an independent replicate and 4 replicates per genotype were sequenced. Libraries were prepared from RNA samples with a RIN of 7 or greater with the NEB Ultra II library kit.

For explant cultures, lens was dissected away from the retina at the end of the culture period, flash frozen in liquid N_2, and stored at -80°C. Samples were prepped individually for analysis with Trizol (Invitrogen). 4 replicates per condition were sequenced. Vehicle controls were paired with treatments (i.e., 4 vehicle replicates for HX531 treatments; 4 vehicle replicates for DBZ treatments). Libraries were prepared from RNA samples with a RIN of 7 or greater with the NEBNext® Single Cell/Low Input RNA Library Prep Kit.

150 bp paired end sequencing was done with the NovaSeq6000 S2 flow cell at the Vantage core facility (Vanderbilt University). Data processing was done by Creative Data Solutions (Vanderbilt University). Paired end raw FASTQ files were assessed for quality by

FastQC (https://www.bioinformatics.babraham.ac.uk/projects/fastqc/) and TrimGalore (https://www.bioinformatics.babraham.ac.uk/projects/trim_galore/) respectively. Reads were aligned to the reference mouse genome mm10 (GRCm38) using Spliced Transcripts Alignment to a Reference (STAR) version 2.6 (Dobin et al., 2013) using GENCODE comprehensive gene annotations (Release M14) as a reference. Approximately 70% of the raw reads were uniquely mapped to the reference genome. HTSeq was used for counting reads mapped to genomic features (Anders et al., 2015) and pairwise differential gene expression analysis was performed using DESeq2 (Love et al., 2014)

Bioinformatics Analyses

Preparation of the DESeq2 datasets in Supplemental Files:

Mutants dataset (Suppl File 2): Gene metadata, log2FC, adjusted p-values, the FDR rank based on the adjusted p-values, and the means of the normalized counts for each genotype were merged into a single file from each of the DESeq2 comparisons. Molecular function for each gene from IPA was also merged into the file. DEG designations for each gene in the pairwise comparisons were assigned based on two adj p-value cutoffs (red; see results). *Vsx2*- and *Mitf*-dependencies (orange) were assigned from the filtering method shown in Fig. 2 and Supplemental Figs. 1 and 2. Vsx2 and Mitf gene sets were assigned as well as GRCs (blue). Genes that didn't fall into a GRC are indicated by #N/A.

HX531 dataset (Suppl File 9): Gene metadata, log2FC, adjusted p-values, rank based on the adjusted p-values, means of the normalized counts for each treatment and the mean expression of both treatments combined were retained. DEG designations were based on a single adj-p value cutoff (FDR) of 0.05, resulting in DEG-Y and DEG-N classifications (red).

DBZ dataset (Suppl File 16): Gene metadata, log2FC, adjusted p-values, rank based on the adjusted p-values, means of the normalized counts for each treatment and the mean expression of both treatments combined were retained. DBZ DEG designation was based on two adj-p value cutoffs (FDR) resulting in DEG-Y, DEG-P and DEG-N classifications (red).

Ingenuity Pathway Analysis (IPA)

The DESeq2 pairwise comparison tables were uploaded onto the Ingenuity server and the Core Analysis package was used to perform CP-ORA and ORA. The reference genome for CP-ORA and ORA were the dataset themselves as opposed to the complete mouse genome. Statistics (Fishers exact test, Z-score algorithm) were done on specified subsets of genes from the datasets and referred to in IPA as *analysis ready molecules* (ARMs). ARMs based on *Vsx2*- and *Mitf*-dependencies were specified with a code that was interpretable to IPA and based on the *Vsx2* and *Mitf* gene set classifications (Data Note in prep; available upon request). In cases when HX531 DEGs or DBZ DEGs were analyzed by ORA in the *mutants* dataset, gene lists were generated for these DEG sets (see below). ARMs and gene expression data were still pulled from the *mutants* dataset and were based on the *Vsx2* and *Mitf* gene set classification code.

Generation of NR and RPE gene lists

Bulk RNA sequencing data was obtained from Supplementary Table 1 in Andrabi et al (Andrabi et al., 2015). We used the *Day15 +FGF / Day15 +Wnt* column under the header *Comparison of Gene Expression Levels* to identify NR genes. The inverse values for this column were generated and placed into a new column titled *Day15 +Wnt / Day15 +FGF*, which was then used to identify RPE genes. For each gene list, filtering was done to include only those genes with a gene expression ratio greater than 10 for each identity. This yielded 115 neural

retina and 192 RPE genes. These lists were loaded into IPA for ORA with results reported in the *My Lists* section of the Core analysis output. The expression data from Andrabi and colleagues and the gene lists can be found in Suppl File 5.

Generation of retinal cell type gene lists

Single-cell RNA-Seq data files were obtained from GEO accession: GSE118614 (Clark, et al., 2019). The GSE118614_barcodes, GSE118614_genes, and GSE118614_10x_aggregate.mtx files were read into R and merged to generate a SC-RNA object which included the barcodes, genes, gene counts, and the relevant age and cell type metadata. The object then underwent filtering. Any cell with the 'Doublets' cell type and a cell age greater than E14.5 were filtered out of the object.

The FindMarkers function from the Seurat V3 package was used to identify differentially expressed genes between the cell types of interest and the remaining cell population in the object. The logfc.threshold was set to 0.10 and a Wilcoxon rank sum test was used to assess differential expression. The comparison groups to generate the resulting gene lists were:

1. 'Neurogenic RPCs' vs. all others
2. 'Early RPCs' vs. all others
3. 'Amacrine Cells' vs. all others
4. 'Retinal Ganglion Cells' vs. all others
5. 'Cones' and 'Photoreceptor Precursors' vs. all others
    a. Cones and PhPrs were grouped into the same identity class.
6. 'Horizontal Cells' vs. all others
7. 'RPE/Margin/Periocular Mesenchyme/Lens Epithelial Cells" vs. all others

Filtering was done to restrict the number of differentially expressed genes to approximately 100 genes for each cell type. Filtering parameters included cutoffs for avg logFC, adj p-value and the ratio of the percentage of cells expressing each gene in the target cell type compared to all others. The resulting lists were then compared to identify shared genes, which were culled from all lists. *Ascl1* was the sole exception, which was assigned to the nRPC list based on its known function in RPCs. Culling negatively impacted the Amacrine (A) and Horizontal cell (HC) gene lists because of a dearth of cell type specific genes as well as a large overlap in shared genes between the two cell types. The gene lists were merged into a common A_HC gene list and the shared genes were retained. All gene lists were loaded into IPA and are provided in Supplemental File 7.

Generation of a HX531 gene list

57 genes were identified in the HX531 DESeq2 dataset with the following cutoffs: FDR ≤ 0.05 and mean normalized counts ≥ 100 for vehicle and HX531 treatments combined. This gene list was loaded into IPA and is available upon request.

Generation of a DBZ gene list

119 genes were identified in the DBZ DESeq2 dataset with the following cutoffs: FDR ≤ 0.001 and |log2FC| > 0.8. These genes constituted the DBZ DEG gene list and were loaded into IPA and is available upon request.

Quantitative reverse transcription PCR (qPCR)

Total RNA was isolated using TRIzol reagent (Thermo Fisher Scientific, Cat#15596026). cDNAs were synthesized using SuperScript IV VILO Master Mix (Thermo Fisher Scientific, Cat# 11766051). qPCR was done on QuantStudio 3 Real Time PCR Systems (Thermo Fisher

Scientific) with the TaqMan gene expression Master Mix (Thermo Fisher Scientific, Cat# 444557) and TaqMan gene probes for *Abca1, Abcg1, Scd2*, *Gapdh* (Assay ID: Abca1-Mm00442646_m1; Abcg1 - Mm00437390_m1; Scd2 – Mm01028542_m1).

Relative changes in gene expression were determined with the delta-delta-Ct method (DDCt). Gapdh was used as the endogenous control for the initial normalization (DCt values). DDCt values were generated by normalizing DCt values to the mean DCt value of the control samples (untreated). Data is presented in graphs as the fold change in gene expression ($RQ = 2^{-DDCt}$). Graphing and statistical tests were done with GraphPad Prism (version 9.0) and Microsoft Excel (version 16.43). Descriptive statistics for RQ values and test results are provided in Supplemental File 1. Hypothesis testing was done on DDCt values.

Supplemental Information

Supplemental File 1: Summary statistics for Fig. 1P and 1Q.

Supplemental File 2: DESeq2 results, DEG status, gene set classifications, and GRC designations for the E12.5 *orJ* (O), *orJ;mi*^{het} (OM), and *orJ*^{het} (C) retinal transcriptomes (*mutants* dataset).

Supplemental File 3: CP-ORA results for the V1 gene sets in the *mutants* dataset.

Supplemental File 4: Top canonical pathways for V1 gene sets in the *mutants* dataset.

Supplemental File 5: NR and RPE gene lists with filtering parameters, summary data, lists. Dataset used for gene list generation from Andrabe et al., 2015.

Supplemental File 6: ORA results for NR and RPE gene lists with the V1 gene sets in the *mutants* dataset.

Supplemental File 7: Retinal cell type gene lists with filtering parameters, summary data, and differential gene expression data for each cell type. Dataset used for gene list generation from Clark et al., 2019.

Supplemental File 8: ORA results for retinal cell type gene lists with the V1 gene sets in the *mutants* dataset.

Supplemental File 9: DESeq2 results and DEG status for E12.5 *orJ* retinal explants treated with HX531 or vehicle (HX531 dataset).

Supplemental File 10: CP-ORA results for the HX531 DEGs in the HX531 dataset.

Supplemental File 11: ORA results for NR, RPE, and retinal cell type gene lists with the HX531 DEG set in the HX531 dataset.

Supplemental File 12: ORA results for HX531 DEG list with the V1 genes sets in the *mutants* dataset.

Supplemental File 13: Comparison of directional changes in expression of HX531 DEGs in the HX531 and *mutants* datasets to assess epistasis correlation between *orJ* mutation and inhibition of RXR activity.

Supplemental File 14: Expression of Notch pathway genes from CP-ORA of the V1.All gene set in the *mutants* dataset.

Supplemental File 15: Expression of GS complex genes from *mutants* dataset.

Supplemental File 16: DESeq2 results and DEG status for E12.5 *orJ* retinal explants treated with DBZ or vehicle (DBZ dataset).

Supplemental File 17: Comparison of directional changes in expression of DBZ DEGs in the DBZ and *mutants* datasets to assess epistasis correlation between *orJ* mutation and inhibition of GS activity.

Supplemental File 18: CP-ORA results for the DBZ DEGs in the DBZ dataset.

Supplemental File 19: DESeq2 results of eRPC and nRPC genes found in DBZ DEGs in the DBZ dataset.

CHAPTER 3

DISCUSSION

Summary and Main points

Vsx2 remains a critical regulator of retinal development. Its roles have been well characterized: defining the early retinal domain, regulating neurogenic timing, driving bipolar cell type specification, and demarcating retinal progenitor cells throughout differentiation. Although *Vsx2* is of critical importance much was unknown about its interactions with other genes. This thesis uncovered the extent of known interactors like *Mitf* and discovery of potential new interactors like *Rxrg* and gamma secretase in the *orJ* mutant model of *Vsx2*.

Mitf was a known interactor of *Vsx2* (Zou and Levine, 2012; Horsford et al., 2005; (Capowski et al., 2014) but the extent of the interaction effects in the *orJ* retina was unknown. Through the creation of genetic mutants, a positive epistatic relationship between *Vsx2* and *Mitf* was confirmed. Through gene expression analyses in double mutants, the contribution *of Mitf* to the *orJ* phenotype was assessed, while simultaneously identifying additional contributing genes. Gene expression analysis clarified the partial contribution by *Mitf* and allowed for the discovery of *Mitf*-regulated genes in the *orJ* retina.

Differential expression analyses identified a novel target, RXRG, as a potential interactor of *Vsx2*. Further genetic analysis of *ex vivo* inhibition of RXR signaling revealed that RXRG is a minor interactor of *Vsx2* despite the large expression change seen in the OvC dataset.

Finally, gamma secretase was identified through *ex vivo* tissue inhibition as a *Vsx2* interactor with redundant functions to *Vsx2* in early retinal development. This established a novel convergent negative epistatic relationship between gamma secretase and *Vsx2* in cell proliferation during early retinal development.

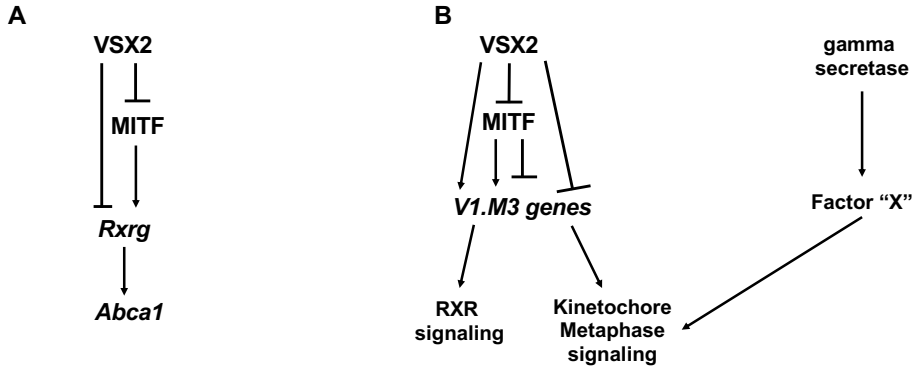

Figure 19. Pathway summary of VSX2 interactors. A) shows *Rxrg* regulation by VSX2 and MITF following mutant experiments and gene expression analyses. **B)** shows convergent negative epistasis on the Kinetochore Metaphase Signaling pathway between VSX2 and gamma secretase.

Major Contributions

This body of work has increased the knowledge of the retinal development field in several major ways. First, the identification of retinoid x receptor gamma as a genetic interactor of *Vsx2* in the developing retina is a novel interaction. Prior to these experiments Retinoid X Recptor signaling was not suspected to have a role in early retinal development or differentiation. The second major contribution was the identification of gamma secretase as a contributor to proliferation in the early retina. Lastly, the application of epistatic logic to gene expression studies to guide the identification of genetic interactors.

Retinoid x receptor gamma (RXRG) has a clearly defined role in photoreceptor differentiation during retinal neurogenesis (Hoover et al., 1998; Roberts et al., 2005), but earlier functions and expression data were limited and under investigated. Retinoic acid (RA) signaling is well documented in eye development with signaling beginning as early as the optic vesicle stage, around E8.5 in mouse, and drives the reciprocal interaction between the OV and the lens placode (Cvekl and Wang, 2009) and references within). The expression of aldehyde

dehydrogenase 1 family members A1/A2/A3 are responsible for the conversion of retinaldehyde to the retinoic acid receptor (RAR) ligand, all trans RA, sets up an RA signaling gradient in the developing retina such that the ventral retina is high in RA, the dorsal retina has low RA, and the transitional region is void of RA (Cvekl and Wang, 2009). Receptors for RA, retinoic acid receptors (RARs) and retinoid x receptors (RXRs) are expressed throughout eye development in different tissues (Cevkyl and Wang, 2009). Retinoid x receptor gamma (RXRG) and retinoic acid receptor alpha (RARA) proteins are expressed in the mouse neural retina beginning at E10.5 and become localized to cone photoreceptors and ganglion cells respectively (Cvekl and Wang, 2009; Mori et al., 2001). The RPE also expresses RARA and RXRG (Cvekl and Wang, 2009). RARA is expressed in the RPE from E10.5 to adult, while RXRG was only detected at E10.5 (Mori et al., 2001).

The studies covered in this thesis suggest novel roles for RXR signaling during early retinal development. One caveat to the experiments presented in this thesis is the use of nonspecific inhibition of RXRG. Small molecule inhibition of RXRG specifically was not available at the time of experimentation. The results conclude the effects of the pan-RXR inhibitor are driven primarily by RXRG due to its high expression level in the *orJ* mutant. The early time point of the study suggests that *Rxrg* may be an active component of the transition to neurogenesis in the absence of *Vsx2* in retinal progenitors.

The second major contribution to the field is the discovery of gamma secretase involvement in cell proliferation in the early retina. Many studies previously involving gamma secretase solely focused on its effects of manipulating the Notch signaling pathway. Through gene expression analysis the effects of gamma secretase were examined. It is a novelty that gamma secretase itself contributes to proliferation during retinal development.

The last major contribution involves utilizing the logic of epistasis to identify strong candidate genetic interactors. Recently, many developmental approaches in the retina focus on

specific networks or circuits that regulate cell type specification and differentiation over time. Here, I have described a classical biology approach to analyzing large datasets by focusing specifically on interactors of *Vsx2* during a critical time in retina development.

Epistasis has had many definitions since the word was first conceived by Bateson in the early 1900's (Sameith et al., 2015); and more refs within). However, biologists today utilize the term epistasis with regards to genetic interactions. Genetic interactions are defined by the phenotypic effect of perturbation in one gene is dependent upon the perturbation in another gene (Lee et al., 2010). While phenotypic and gene expression analyses herein have verified positive epistasis exists between *Vsx2* and *Mitf, Rxrg* emerged strictly through gene expression data and a phenotypic change has yet to be detected in the *orJ* context. The logic of epistasis facilitated the consideration of *Rxrg* as a candidate interactor of *Vsx2* due to its corrective gene expression across mutant datasets. Applying epistatic logic to gene expression data can be a powerful tool for identifying genetic interactors.

Future directions

Identifying genetic interactors and regulatory circuits of *Vsx2* through the mutant variant, *orJ*, has led to more questions about the candidates and pathways identified. Some outstanding questions are: 1) What is the specific interaction mechanism between *Vsx2* and *Mitf* during early retinal development? 2) During retinal development does VSX2 interact directly with *Rxrg*, or is the upregulation of *Rxrg* a compensatory mechanism occurring in the *orJ* mutant? 3) How do VSX2 and gamma secretase exert control of the RPC cell cycle? 4) What is the role of the Notch signaling pathway in the *orJ* retina? And 5) What are the temporal requirements of *Vsx2*

regarding maintenance of retinal identity and acquisition of neurogenic competence in retinal progenitor cells?

Identify the full scope of the interaction between *Vsx2* and *Mitf*

Through the exemplified and outlined framework demonstrated in Chapter 2, it is possible to identify many more interactors of *Vsx2*. However, there is already a substantial amount of data and evidence to support further investigation of the interaction between *Vsx2* and *Mitf*. It is known that VSX2 likely binds to the promoter of the *D-Mitf* isoform expressed in the *orJ* retina (Bharti et al., 2008; Zou and Levine, 2012). Clearly there is a repressive relationship between *Vsx2* and *Mitf* in the retina, but it is unclear what mechanism of epistatic interaction occurs between the *orJ* and *mi* alleles.

Some hints may be found in the datasets described in Chapter 2. The smallest subset of genes identified in the overlap of OMvO dataset describes 225 genes whose expression change was fully dependent on *Vsx2* and *Mitf* (V1.M1).

The *Mitf* locus is very complex, with nine different promoters (Bharti et al., 2008) and multiple different isoforms, it is a difficult interactor to characterize. While years of research on the *Mitf* locus has been conducted still there is more to learn. The positive epistasis confirmed here and throughout the field has not yet addressed the exact underlying mechanism of this interaction. One study from (Xu et al., 2007) showed that the sensory neuron miRNA cluster 96/182/183 was capable of binding to and inhibiting the activity of the *Mitf* locus. MiRNAs are abundant regulators of gene expression especially in developmental timing and cell differentiation (Chen et al., 2004; Wightman et al., 1993). DICER, an important enzyme in the production of miRNAs, is expressed in the retina has been shown to be important for the RPC switch from producing early born cell types to producing later born cell types in the developing mouse retina (Georgi and Reh, 2010). Other more recent studies have shown roles for miRNAs

in timing of photoreceptor cell fate specification (Xiang et al., 2022) and regulation of amacrine cell genesis by miR216b (Zhang et al.). It seems likely that miRNAs may play a role in the interaction between *Vsx2* and *Mitf* due to their early expression in opposing domains of the optic cup, miRNAs may aid in the lineage fidelity and maintenance functions of *Vsx2* in the retina and *Mitf* in the RPE.

Rxrg as an interactor of VSX2

RXR signaling came up continuously throughout the genetic analysis of the *orJ* mutant. However, there is a lack of previous evidence in the field to explain what type of RXR signaling is occurring and through what mechanism it is regulated. *Rxrg* is the most upregulated DEG in the OvC dataset and was categorized into the V1.M3 subset (meaning that *Rxrg* is partially *Mitf* dependent). The partial dependency on *Mitf* begs the question, is *Rxrg* expression part of the retinal development trajectory, or is this a compensatory effect of the *orJ* mutation?

Future efforts should focus on functional biological testing of RXRG and its potential role in retinal cell differentiation.

The results presented in Chapter 2 indicate this may be a compensatory effect of the *orJ* mutation. The partial dependency on *Mitf* expression indicates *Rxrg* is at least partially regulated by MITF, whose expression in the retina is dependent on the loss of VSX2 expression caused by the *orJ* mutation. To delineate compensation of *Rxrg* from epistasis in the *orJ* mutant, double mutant mice ($Vsx2^{orJ/orJ}$;$Rxrg^{-/-}$) should be examined. A worsening of eye and or retinal phenotype in $Vsx2^{orJ/orJ}$;$Rxrg^{-/-}$ would provide evidence of compensation in the *orJ* mutant, however an improvement in the eye and or retina phenotype would provide a case for positive epistasis, and no effect would provide evidence for a case of translational buffering ((Kusnadi et al., 2021).

In the event epistasis occurs between *Rxrg* and *Vsx2,* upregulated *Rxrg* may contribute to dysregulated lipid transport through its targeted upregulation of *Abca1* and *Abcg1*. How this may be connected to progenitor maturation and transition to neurogenesis is not known at this time. However, neurogenesis in the adult hippocampus is shown to be positively affected by the addition of omega 3 polyunsaturated fatty acids by promoting dendritic arborization and new spine formation (Crupi et al., 2013), and liver x receptor (LXR)/RXR activation has been shown to influence transcriptomic profiles of differentiated neurons (Simandi et al., 2018). Therefore, evidence of increased lipid presence has documented positive effects on neurogenesis in the CNS.

RXRG and its putative partner receptor RARA are reported to be expressed in the early retina and RPE starting at E10.5 (Mori et al., 2001). The presence of RXRG in the early neural retina lends the possibility that RXRG regulates the lipid metabolism of progenitor cells through its direct interaction with the promoters of *Abca1* and *Abcg1*, and this regulation must be altered to allow progenitors to modulate their cellular lipid metabolism to meet new metabolic requirements of neurogenesis. In this example, if progenitors do not have the ability to shift their lipid metabolism, they would be unable to proceed with differentiation due to lipid constraints which could delay their maturation and ultimately their time to neurogenesis.

Other lipid links to *Rxrg* in the retina point to Docosahexanoic acid (DHA). All RXR receptors have been found to be activated by DHA (Urquiza et al., 2000). DHA was found to promote photoreceptor differentiation and rescue photoreceptors from apoptosis (Rotstein et al., 1998). The link between RXRG and DHA is likely when considering the role of *Rxrg* in promoting cone photoreceptor differentiation (Roberts et al., 2005) Cvkeyl and Wang, 2009; and references therein), combined with the finding that DHA also promotes photoreceptor differentiation during retinal development (Rotstein et al., 1998). In the context of the *orJ* mutant, DHA levels could be elevated causing the elevation of *Rxrg* and downstream genes,

Abca1 and *Abcg1*. Lowering DHA levels in culture may lower RXRG protein levels thereby lowering expression of *Abca1* and *Abcg1,* and this may aid in some restoration of the *orJ* phenotype. To find the connection between *Rxrg*, *Abca1*, *Abcg1* and *Vsx2* more investigation is needed.

Gamma Secretase and VSX2 in the RPC cell cycle and proliferation

Findings from expression analyses led to the conclusion that both gamma secretase and *Vsx2* contribute to cell cycle and proliferation mechanics in early RPCs. However, it is not known if both *Vsx2* and gamma secretase play the same roles in wild-type conditions.

Gamma secretase is an intramembrane heterotetrameric protease complex whose substrates vary greatly across systems and cell types. Out of the four subunits that make up the complex, presenilin is the only active protease (Güner and Lichtenthaler, 2020). The most well-known substrates of gamma secretase are members of the Notch signaling pathway, and the Aβ proteins well characterized in Alzheimer's disease (Bolduc et al., 2016; Shih and Wang, 2007). Notch signaling inhibition is one of the most common uses for gamma secretase inhibitors (GSIs) in part because of its activity in developmental biology and roles in regulating cancer (Shih and Wang, 2007). To date, substrates of gamma secretase are not well characterized in the cell cycle or proliferation.

More recently gamma secretase has demonstrated the ability to cleave receptor tyrosine kinases (RTKs), creating a new signaling pathway for RTKs (Merilahti and Elenius, 2019). Gamma secretase is not capable of cleaving all RTKs, but notably fibroblast growth factor receptor (FGFR) 3/4 are a couple of its RTK substrates (Güner and Lichtenthaler, 2020; (Merilahti et al., 2017). FGFR3 and FGFR4 have known roles in cell proliferation and have been demonstrated to be expressed in the retina (Cinaroglu et al., 2005; Fuhrmann et al., 1999) The connection between *Vsx2*, gamma secretase and cell proliferation becomes distinct when

you consider that FGF signaling from the surface ectoderm of the optic cup is necessary for the expression of *Vsx2* in the neural retina (Nguyen and Arnheiter, 2000). It is not difficult to imagine a scenario where gamma secretase cleaves FGFR1 and FGFR2 to initiate direct nuclear translocation and as a result affects cell cycle dynamics and proliferation. A case for FGFR1 direct cleavage by the protease Granzyme B has been demonstrated in breast cancer cells (Chioni and Grose, 2012). A similar mechanism could tie *Vsx2* and gamma secretase together in retinal progenitor cells.

However, it is more likely that *Vsx2* and gamma secretase are not part of the same linear pathway. Expression data published in this thesis does not support a single linear pathway for both *Vsx2* and gamma secretase. Perhaps they are each linearly affecting the cell cycle and proliferation in parallel pathways, both involving different FGF signaling or Notch signaling. The data in Chapter 2 indicates that *Vsx2* and gamma secretase interact through convergent negative epistasis on shared targets of cell cycle and proliferation pathways.

Investigating the Notch Pathway in the early *orJ* retina

Abrogating Notch signaling to encourage cell differentiation and affect cell type outcomes is well documented in the retina (Jadhav et al., 2006; Nelson et al., 2006). The initial goal of applying GSI to *orJ* retinal explant cultures was to inhibit Notch signaling. Based on previous findings in the field, the initial hypothesis was that inhibiting Notch signaling in the *orJ* retina would aid in the amelioration of the delayed neurogenesis phenotype. Due to unforeseen tissue toxicity at levels high enough to cause precocious neurogenesis, this question could not be adequately addressed. However, the observation of reduced proliferation at lower doses of DBZ and DAPT suggested that gamma secretase was still having an effect.

However, it is possible Notch signaling was interrupted in the *orJ* retina based on the gene expression analyses from GSI-treated *orJ* explants. It is likely that gamma secretase effects are

symptoms of at least partial Notch signaling inhibition. The IPA analysis of Notch pathway activation in *orJ* mutants was unclear. However, it was clear that the Notch pathway was affected in the *orJ* retina but detecting inactivation or deactivation was not possible. Sequencing data from GSI-treated explants did show the Notch target gene *Foxn4* decreased in expression after inhibititon of gamma secretase, providing some evidence that Notch signaling was at least partially affected by DBZ treatment. It is possible that 1) Notch signaling is not carried out through the canonical pathway or 2) the Notch signaling pathway is not functional in *orJ* RPCs. Reports of non-canonical Notch signaling are present in the literature (Andersen et al., 2012; Steinbuck and Winandy, 2018). Non-canonical signaling is described as CSL-independent and ligand-indepdent Notch activity. Experiments in fly and mouse show that non-canonical Notch signaling involves antagonizing Wnt/ß-catenin signaling (Andersen et al., 2012). Many published observations surrounding non-canonical Notch signaling is described in progenitor cell populations capable of expansion and or differentiation (Andersen et al., 2012).

The data presented in this thesis indicates neurogenic RPCs gene regulation is a target of GSI. If GSI is a proxy for inhibited Notch signaling, a case could be made for the role of Notch in regulating activities of both early RPCs and neurogenic RPCs. Could non-canonical Notch signaling be active in the early retina and early RPCs before switching to canonical Notch signaling in nRPCs during cell differentiation?

To properly examine the effects of Notch signaling in the *orJ* retina other inhibitors of Notch signaling could be used. A novel inhibitor of RBPJ, RIN1, blocks the functional interaction of RBPJ thereby inhibiting the transcriptional activation of Notch signaling (Hurtado et al., 2019). For a genetic approach, Notch conditional alleles would allow precise inactivation of *Notch1* in the *orJ* mutant. *In vivo* manipulations should result in more robust gene expression changes and a stronger, more stable phenotypic readout.

Uncovering temporal requirements for *Vsx2* in retinal identity maintenance and acquisition of neurogenic competence

Gene expression analyses of the *orJ* retina provided evidence to support the idea that *Vsx2* regulates the neurogenic state of RPCs. Tissue-wide gene expression in the pre-neurogenic (E12.5) *orJ* retina showed a significant overrepresentation score for the neurogenic RPC gene list, indicating that in the absence of VSX2 protein genes highly expressed in neurogenic RPCs were significantly impacted. Further expression analyses with the *mi* allele solidified this observation. When investigating expression changes in the double mutants, it appeared that inhibiting *Mitf* activity in the *orJ* retina had a minor impact on restoring nRPC gene expression, meaning other factors, not *Mitf*, are important for nRPC expression.

Expression of *Vsx2* begins in the mouse optic cup around E9.5 (Liu et al., 1994) and continues to be expressed into the mature retina in bipolar cell neurons and a subset of Müller glia (Burmeister et al., 1996; Rowan et al., 2004; (Hatakeyama et al., 2001). Clearly *Vsx2* is important for proper retinal development, but its function and mechanism of action during early retinal development is still unclear. I have demonstrated and reported here its importance in neurogenic timing, retinal identity and its role in progenitor cell proliferation. However, substantiated evidence for its role in progenitor acquisition of neurogenic competence and its temporal requirements for retinal identity maintenance remain under investigated.

One way to clarify these roles is through *Vsx2* conditional knockouts. A conditional *Vsx2* allele to will not only allow for the assessment of *Vsx2* contribution to eRPC expression and nRPC expression, but also test the temporal requirements of retinal identity maintenance.

Early inactivation of *Vsx2* at the late optic cup stage (E10.5) followed by gene expression analysis and performing overrepresentation analysis on codified gene lists would allow for a deeper understanding of the role of *Vsx2* in early retinal identity as well as early retinal

progenitors. Phenotypic analysis of these conditional inactivation mutants would allow us to assess effects on neurogenesis and formation of the mature retina.

Later inactivation of *Vsx2* at the early retina stage (E12.5) would also allow for analysis of retinal identity maintenance, and the role of *Vsx2* in the acquisition of neurogenic competence in RPCs. How does timing of *Vsx2* inactivation affect the retinal development trajectory? Also, is *Vsx2* continuously required throughout RPC proliferation and differentiation into postmitotic cells, or is it only required to begin the process of neurogenesis? Will bipolar cells and all subsets of Müller glia be generated if *Vsx2* is inactivated at the early retina stage? Utilizing a conditional allele of *Vsx2* would help to solidify and clarify the roles and requirements of *Vsx2* during retinal development.

APPENDIX

INTERACTION ANALYSIS OF PAX6^{SEY} AND VSX2^{ORJ} IN RELATION TO TEMPORAL REGULATION OF RETINAL NEUROGENESIS.

Summary

As part of the initial goal to find genetic interactors of *Vsx2* in early retinal development, the transcription factor PAX6 arose as a good candidate. To find a positive interaction between *Vsx2* and *Pax6* in the early retina, the $Pax6^{Sey}$ allele was bred into the $Vsx2^{orJ}$ mice. The resulting embryos were assessed for improvements to the *orJ* phenotype, focusing on the onset of neurogenesis. The results indicated that in regard to the onset of neurogenesis, the *sey* allele further delayed the onset in double mutants, establishing a negative epistatic relationship between the *orJ* and *sey* alleles in the early retina.

Introduction

Pax6 is a well-known and critical transcription factor for eye development. Its functions are well conserved across species. Studies in fly, fish, and mice confirm its importance for the proper development and function of the eye. Experiments in fly first showed that ectopic expression of Pax6 can trigger the development of a de novo eye structure (Halder et al., 1995).

Prior studies indicate that Pax6 can influence neurogenic competence and early neurogenesis. Pax6 in combination with Sox2 was shown to set the boundary between the non-neural peripheral and neural compartments of the retina (Matsushima et al., 2011). In this context, a higher relative ratio of *Sox2* to *Pax6* favored the neural fate (Matsushima et al. 2011). *Pax6* has been found to promote either neural retina or RPE by acting as a proretinogenic or antiretinogenic factor depending on the context (Bharti et al., 2012). Bharti et al., 2012 found that when PAX6 was expressed with FGF and DKK3 the retinal fate was promoted, while its expression with MITF/TFEC promoted the RPE fate.

In another study, precocious, although sporadic, neurogenesis was observed in *Pax6*$^{-/-}$ mutants (Philips et al., 2005). It is important to note that Philips et al., 2005 did find that precocious neurons were produced in the E10.5 *Pax6*$^{-/-}$ optic vesicle structure, the traditional retinal neuron components were not all expressed. Pan-neuronal marker, TUBB3, was expressed along with a couple of other ganglion cell proteins, but without *Pax6* none could adopt specific retinal fates. Our lab produced data consistent with these findings, Sox2 mRNA and protein levels are lower in the Vsx2 *orJ* mutant compared to control and *Pax6* levels are not significantly different between the Vsx2 *orJ* mutant and control (data not shown). It is possible then, that the delay in neurogenesis and more peripheral character of the Vsx2 *orJ* retina (Rowan et al., 2004) is due to an imbalance in the ratio of Sox2 to Pax6. To test this, we asked whether genetically reducing *Pax6* activity was sufficient to restore the delay in neurogenic timing due to *Vsx2* loss of function.

Methods

Mice

The Pax6^{sey} allele was gifted by the Pevny lab in 2014. The mice originally came from Dr. A LaMantia at George Washington University. These mice were then bred into the 129s background. Vsx2$^{orJ/orJ}$ on the 129s background were crossed with Pax6$^{Sey/+}$ mice for 3 generations before developmental studies began on the F2 generation. Mice were staged for developmental equivalency and images were taken of the entire embryo before any further tissue processing.

Immunohistochemistry

Slides were stained over a 48 hr period. Staining procedures followed same protocol described in the data chapter.

Antibody	Species	Dilution	Manufacturer	Antigen Retrieval	Blocking buffer
Tubb3	Rabbit	1:10000	Biolegends	No	Goat/Donkey
Sox2	Rabbit	1:400	Millipore	No	Goat/Donkey
Pax6	Mouse	1:50	Santa Cruz	No	Goat/Donkey

Table 3. Immunostaining Antibodies

Quantification

Quantifying captured images for progression and density of neurogenesis was performed as part of the same analysis in the Data Chapter of this document. TUBB3 positive staining indicated if a sample was positive for neurogenesis. The percentage of samples with TUBB3 positive staining was also used to show the difference between *orJ* samples and *orJ;sey* samples.

Results

Phenotypic differences detected in double mutants.

As early as E12.5 differences can be detected between *orJ* and *orJ;sey/+* mutants. *orJ* embryos show a clear sign of microphthalmia at this stage along with obviously increased pigmentation (Fig.A1_E). The developing *orJ;sey/+* eye appears to develop a separate phenotype when compared to control and *orJ* at E12.5 (Fig. A1_D-F). Differences between E13.5 *orJ* and *orJ;sey/+* are not apparent at this stage. However, it appears at E14.5 that differences between *orJ* and double mutant embryos (*orJ;sey/+*) begin to arise (Fig. A1_J-L). Pigmentation appears to increase from E12.5 to E13.5 in the double mutant making it look more like the *orJ* mutant than control embryos. The triangular shape that the developing RPE takes on in the double mutant is very distinct and specific to the double mutants that were sampled.

By E14.5 the double mutant embyros appear to have more severe microphthalmia more than their single mutant littermates (Fig. A1_J-L). The developing eye has looks more recessed

into the developing head and less eye is visible from the epidermal surface. Single mutant eyes appear larger than their double mutant counterpart in the samples collected. However, both mutants exhibit severe microphthalmia when compared to control.

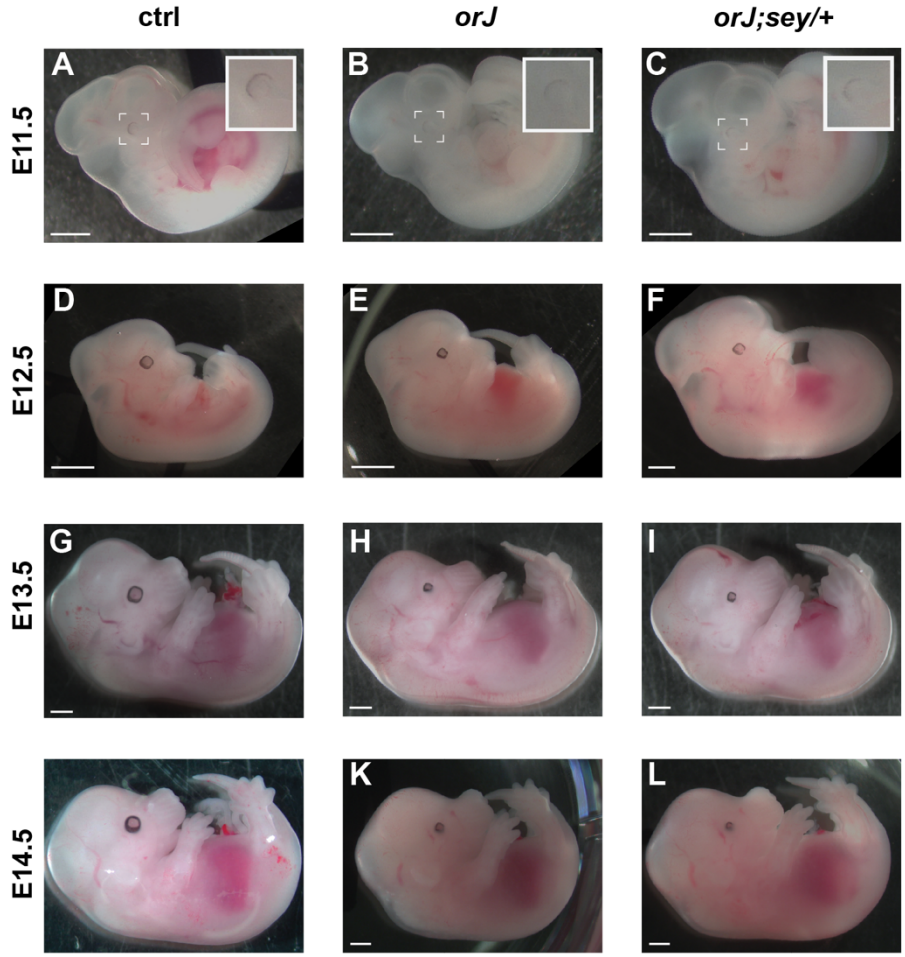

Figure A1. *orJ*, and *orJ;sey* embryos

Suspected yet unverified difference in *Pax6* and *Sox2* levels

The neurogenic focus of these experiments led to a concentration on the E12.5 time point because of its relevance. E12.5 has emerged as a neurogenically relevant time point due to the observation that control retinas have already begun neurogenesis while single mutants (Vsx2$^{orJ/orJ}$) will not begin until a full embryonic day after E12.5. A preliminary staining of

PAX6 and SOX2 proteins at E12.5 (Fig. A2) showed that PAX6 was elevated in the single mutant under identical capture conditions compared to double mutants but it was unclear if SOX2 expression was changed between the two mutant conditions. It was expected that PAX6 protein was diminished in the double mutant due to the mutant *Pax6* allele (*sey*), but the hypothesis was that SOX2 protein levels would increase due to PAX6 decrease. However, the change in SOX2 is less clear. Neither mutant at this stage has shown any signs of neurogenesis when stained for beta-tubulin (Fig. A3). This is an important distinction because phenotypic divergence from control embryos is detected at this stage and have different expression levels of common retinogenic genes.

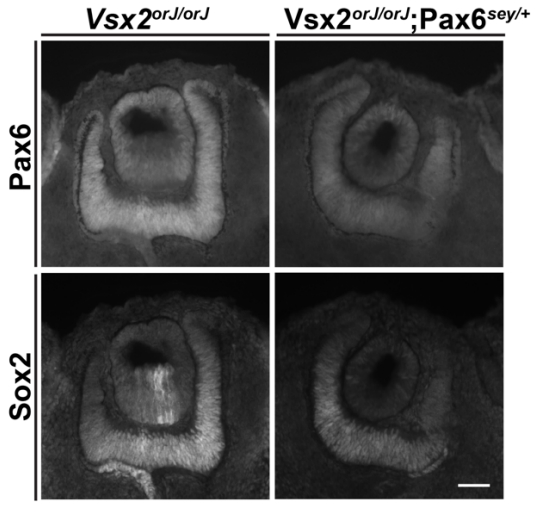

Figure A2. E12.5 expression of PAX6 and SOX2 in *orJ* and *orJ;sey/+*mutants

Onset of neurogenesis is worsened when Pax6^{Sey} and Vsx2^{orJ} are combined.

In an attempt to restore the balance *Sox2* and *Pax6* expression in the developing *orJ* retina, using the *sey* allele, we assayed the *orJ;sey/+* double mutants for neurogenesis using TUBB3 positive expression. However, after quantifying the neurogenic progression through density and spread of TUBB3+ staining we found that in all measured parameters the neurogenic

trajectory was worsened. Beginning with the stained images the double mutants did not reliably begin neurogenesis at E13.5. Only about half the samples (8/15) showed TUBB3+ staining, whereas the single *orJ* mutant all samples (3/3) contained TUBB3+ cells by E13.5 (Fig A3_A). The spread of the neurogenic wave was significantly smaller in the double mutant than in *orJ* (Fig. A3_B). The density of the TUBB3 positive cells in the double mutants was also much less than that of the *orJ* retinas (Fig. A3_C). Once all this data had been collected and quantified it became apparent that the *sey* allele further delayed neurogenesis, and possibly changed the neurogenic trajectory in a novel way.

Conclusion and Recommendations

Negative epistatic relationship between sey and orJ on neurogenic timing

The quantification of TUBB3 positive samples showed a distinct delay in *orJ;sey/+* double mutants in comparison to *orJ* single mutants. When considering the onset of neurogenesis as a phenotype, a negative epistatic relationship between the *orJ* and *sey* allele has been identified in the neurogenic retina. What interaction exists between the *sey* and *orJ* allele that is having a worsening effect on the timing of neurogenesis?

Pax6 and *Vsx2* are known to have roles in proliferation of RPCs in the early retina (Green et al., 2003; Hsieh and Yang, 2009; Philips et al., 2005; Sigulinsky et al., 2008). It is possible that the mutant alleles are each impacting different proliferation and/or cell cycle targets.

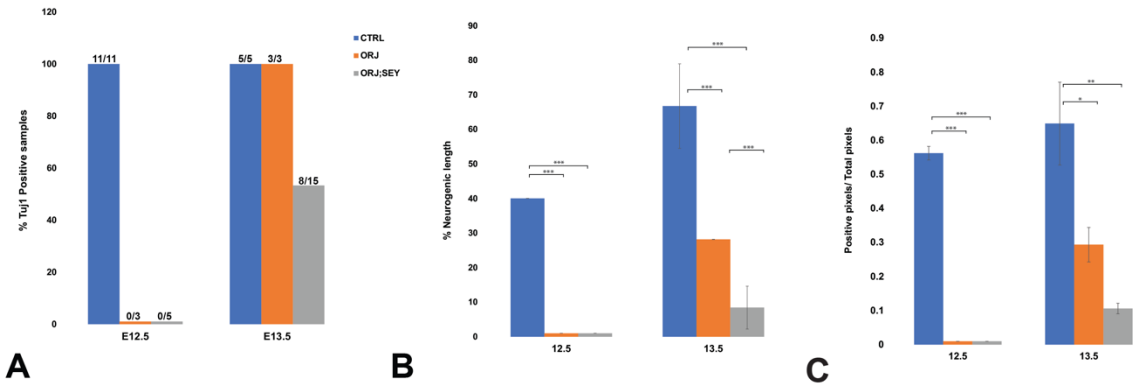

Figure A3. Beginning Neurogenesis *orJ* versus *orJ;sey/+*

Dosage effects of Pax6 in developing retina

An observation by Philips et al. 2005 showed evidence of retarded neurogenesis in mouse $Pax6^{+/-}$ optic vesicles. Like the above-described findings, this was also a surprising result. The main finding of Philips et al. 2005, was that the absence of *Pax6* resulted in precocious neurogenesis. The publication reports retinal neurons were detected a full day earlier in $Pax6^{-/-}$ retinas, along with a decrease in progenitor proliferation. This paper does provide evidence that *Pax6* regulates the timing of retinal neurogenesis. One potential cause of further delayed neurogenesis in *orJ;sey/+* mutants is decreased expression of proliferation factors driven by the decrease in *Pax6* expression.

Potential interaction between Vsx2 and Pax6, and Mitf

RPCs express both *Vsx2* and *Pax6* early on in retinal development. Absence of either or both factors disrupt retinal development and neurogenic timing. However, retinal and eye development are much more sensitive to the expression levels of *Pax6*. Phenotypic differences are seen in development even when one copy of *Pax6* is still intact, whereas $Vsx2^{orJ/+}$ animals are

indistinguishable from wild-type mice. However, in the absence of *Vsx2*, *Vsx2*$^{orJ/orJ}$ retinal and eye development is completely disturbed.

To understand the full extent of the *sey* allele on the timing of neurogenesis in the Vsx2$^{orJ/orJ}$ mutant and how gene expression changes, RNA sequencing should be completed. Special attention should be paid to cell proliferation factors and promoters of neurogenesis.

REFERENCES

Adler, R. and Canto-Soler, M. (2007). Molecular mechanisms of optic vesicle development: complexities, ambiguities and controversies. *Developmental biology* 305, 1–13.

Alexiades, M. R. and Cepko, C. (1996). Quantitative analysis of proliferation and cell cycle length during development of the rat retina. *Developmental dynamics : an official publication of the American Association of Anatomists* 205, 293–307.

Altun-Gultekin, Z., Andachi, Y., Tsalik, E. L., Pilgrim, D., Kohara, Y. and Hobert, O. (2001). A regulatory cascade of three homeobox genes, ceh-10 , ttx-3 and ceh-23 , controls cell fate specification of a defined interneuron class in C. elegans. *Development* 128, 1951–1969.

Amini, R., Rocha-Martins, M. and Norden, C. (2018). Neuronal Migration and Lamination in the Vertebrate Retina. *Front Neurosci-switz* 11, 742.

Anchan, R. M. and Reh, T. A. (1995). Transforming growth factor-β-3 is mitogenic for rat retinal progenitor cells in vitro. *J Neurobiol* 28, 133–145.

Anchan, R. M., Reh, T. A., Angello, J., Balliet, A. and Walker, M. (1991). EGF and TGF-α stimulate retinal neuroepithelial cell proliferation in vitro. *Neuron* 6, 923–936.

Anders, S., Pyl, P. T. and Huber, W. (2015). HTSeq—a Python framework to work with high-throughput sequencing data. *Bioinformatics* 31, 166–169.

Andersen, P., Uosaki, H., Shenje, L. T. and Kwon, C. (2012). Non-canonical Notch signaling: emerging role and mechanism. *Trends Cell Biol* 22, 257–265.

Andrabi, M., Kuraku, S., Takata, N., Sasai, Y. and Love, N. R. (2015). Comparative, transcriptome analysis of self-organizing optic tissues. *Sci Data* 2, 150030.

Arnheiter, H., Hou, L., Nguyen, M.-T. T., Bismuth, K., Csermely, T., Murakami, H., Skuntz, S., Liu, W. and Bharti, K. (2006). MITF. *springer* 27–49.

Barton, K. M. and Levine, E. M. (2008). Expression patterns and cell cycle profiles of PCNA, MCM6, cyclin D1, cyclin A2, cyclin B1, and phosphorylated histone H3 in the developing mouse retina. *Developmental dynamics : an official publication of the American Association of Anatomists* 237, 672–82.

Bar-Yosef, U., Abuelaish, I., Harel, T., Hendler, N., Ofir, R. and Birk, O. S. (2004). CHX10 mutations cause non-syndromic microphthalmia/anophthalmia in Arab and Jewish kindreds. *Hum Genet* 115, 302–309.

Bassett, E. A. and Wallace, V. A. (2012). Cell fate determination in the vertebrate retina. *Trends in neurosciences* 35, 565–73.

Bäumer, N., Marquardt, T., Stoykova, A., Spieler, D., Treichel, D., Ashery-Padan, R. and Gruss, P. (2003). Retinal pigmented epithelium determination requires the redundant activities of Pax2 and Pax6. *Development* 130, 2903–2915.

Behesti, H., Holt, J. K. and Sowden, J. C. (2006). The level of BMP4 signaling is critical for the regulation of distinct T-box gene expression domains and growth along the dorso-ventral axis of the optic cup. *BMC Developmental Biology* 6, 1–22.

Belecky-Adams, T., Tomarev, S., Li, H. S., Ploder, L., McInnes, R. R., Sundin, O. and Adler, R. (1997). Pax-6, Prox 1, and Chx10 homeobox gene expression correlates with phenotypic fate of retinal precursor cells. *Invest Ophth Vis Sci* 38, 1293–303.

Bharti, K., Nguyen, M. T., Skuntz, S., Bertuzzi, S. and Arnheiter, H. (2006). The other pigment cell: specification and development of the pigmented epithelium of the vertebrate eye. *Pigment Cell Research* 19, 380–394.

Bharti, K., Liu, W., Csermely, T., Bertuzzi, S. and Arnheiter, H. (2008). Alternative promoter use in eye development: the complex role and regulation of the transcription factor MITF. *Development* 135, 1169–1178.

Bharti, K., Gasper, M., Ou, J., Brucato, M., Clore-Gronenborn, K., Pickel, J. and Arnheiter, H. (2012). A Regulatory Loop Involving PAX6, MITF, and WNT Signaling Controls Retinal Pigment Epithelium Development. *PLoS Genetics* 8, e1002757.

Bian, F., Daghsni, M., Lu, F., Liu, S., Gross, J. M. and Aldiri, I. (2022). Functional analysis of Vsx2 super-enhancer uncovers distinct cis-regulatory circuits controlling Vsx2 expression during retinogenesis. *Development* 149,.

Bienvenu, F., Jirawatnotai, S., Elias, J. E., Meyer, C. A., Mizeracka, K., Marson, A., Frampton, G. M., Cole, M. F., Odom, D. T., Odajima, J., et al. (2010). Transcriptional role of cyclin D1 in development revealed by a genetic–proteomic screen. *Nature* 463, 374–378.

Bolduc, D. M., Montagna, D. R., Seghers, M. C., Wolfe, M. S. and Selkoe, D. J. (2016). The amyloid-beta forming tripeptide cleavage mechanism of γ-secretase. *Elife* 5, e17578.

Bone-Larson, C., Basu, S., Radel, J. D., Liang, M., Perozek, T., Kapousta-Bruneau, N., Green, D. G., Burmeister, M. and Hankin, M. H. (2000). Partial rescue of the ocular retardation phenotype by genetic modifiers. *J Neurobiol* 42, 232–247.

Bora, N., Conway, S. J., Liang, H. and Smith, S. B. (1998). Transient overexpression of the Microphthalmia gene in the eyes of Microphthalmia vitiligo mutant mice. *Dev Dynam* 213, 283–292.

Brzezinski, J. A., Lamba, D. A. and Reh, T. A. (2010). Blimp1 controls photoreceptor versus bipolar cell fate choice during retinal development. *Development* 137, 619–629.

Buenaventura, D. F., Corseri, A. and Emerson, M. M. (2019). Identification of Genes With Enriched Expression in Early Developing Mouse Cone Photoreceptors. *Invest Ophth Vis Sci* 60, 2787–2799.

Bumsted, K. and Barnstable, C. (2000). Dorsal retinal pigment epithelium differentiates as neural retina in the microphthalmia (mi/mi) mouse. *Investigative ophthalmology & visual science* 41, 903–8.

Bürglin, T. R. and Affolter, M. (2016). Homeodomain proteins: an update. *Chromosoma* 125, 497–521.

Burmeister, M., Novak, J., Liang, M.-Y., Basu, S., Ploder, L., Hawes, N. L., Vidgen, D., Hoover, F., Goldman, D., Kalnins, V. I., et al. (1996a). Ocular retardation mouse caused by Chx10 homeobox null allele: impaired retinal progenitor proliferation and bipolar cell differentiation. *Nature Genetics* 12, 376–384.

Cai, Z., Feng, G.-S. and Zhang, X. (2010). Temporal Requirement of the Protein TyrosinePhosphatase Shp2 in Establishing the Neuronal Fatein Early Retinal Development. *The Journal of Neuroscience* 30,.

Capowski, E. E., Simonett, J. M., Clark, E. M., Wright, L. S., Howden, S. E., Wallace, K. A., Petelinsek, A. M., Pinilla, I., Phillips, M. J., Meyer, J. S., et al. (2014). Loss of MITF expression during human embryonic stem cell differentiation disrupts retinal pigment epithelium development and optic vesicle cell proliferation. *Hum Mol Genet* 23, 6332–6344.

Capowski, E. E., Wright, L. S., Liang, K., Phillips, M. J., Wallace, K., Petelinsek, A., Hagstrom, A., Pinilla, I., Borys, K., Lien, J., et al. (2016). Regulation of WNT Signaling by VSX2 During Optic Vesicle Patterning in Human Induced Pluripotent Stem Cells. *STEM CELLS* 34, 2625–2634.

Cardozo, M. J., Almuedo-Castillo, M. and Bovolenta, P. (2020). Patterning the Vertebrate Retina with Morphogenetic Signaling Pathways. *Neurosci* 26, 185–196.

Carpenter, A. C., Smith, A. N., Wagner, H., Cohen-Tayar, Y., Rao, S., Wallace, V., Ashery-Padan, R. and Lang, R. A. (2015). Wnt ligands from the embryonic surface ectoderm regulate 'bimetallic strip' optic cup morphogenesis in mouse. *Development* 142, 972–982.

Chen, C.-M. A. and Cepko, C. L. (2000). Expression of Chx10 and Chx10-1 in the developing chicken retina. *Mech Develop* 90, 293–297.

Chen, C.-Z., Li, L., Lodish, H. F. and Bartel, D. P. (2004). MicroRNAs Modulate Hematopoietic Lineage Differentiation. *Science* 303, 83–86.

Chen, H., Lukas, T. J., Du, N., Suyeoka, G. and Neufeld, A. H. (2009). Dysfunction of the Retinal Pigment Epithelium with Age: Increased Iron Decreases Phagocytosis and Lysosomal Activity. *Investigative Opthalmology Vis Sci* 50, 1895.

Chioni, A.-M. and Grose, R. (2012). FGFR1 cleavage and nuclear translocation regulates breast cancer cell behavior. *J Cell Biol* 197, 801–817.

Cho, S. and Cepko, C. (2006). Wnt2b/β-catenin-mediated canonical Wnt signaling determines the peripheral fates of the chick eye.

Chow, R. L. and Lang, R. A. (2001). Early eye development in vertebrates. *Annual review of cell and developmental biology* 17, 255–96.

Cinaroglu, A., Ozmen, Y., Ozdemir, A., Ozcan, F., Ergorul, C., Cayirlioglu, P., Hicks, D. and Bugra, K. (2005). Expression and possible function of fibroblast growth factor 9 (FGF9) and its cognate receptors FGFR2 and FGFR3 in postnatal and adult retina. *J. Neurosci. Res.* 79, 329–339.

Clark, B. S., Stein-O'Brien, G. L., Shiau, F., Cannon, G. H., Davis-Marcisak, E., Sherman, T., Santiago, C. P., Hoang, T. V., Rajaii, F., James-Esposito, R. E., et al. (2019). Single-Cell RNA-Seq Analysis of Retinal Development Identifies NFI Factors as Regulating Mitotic Exit and Late-Born Cell Specification. *Neuron* 102, 1111-1126.e5.

Coles, B. L., Horsford, J. D., McInnes, R. R. and Kooy, D. (2006). Loss of retinal progenitor cells leads to an increase in the retinal stem cell population in vivo. *European Journal of Neuroscience* 23, 75–82.

Conesa, A., Madrigal, P., Tarazona, S., Gomez-Cabrero, D., Cervera, A., McPherson, A., Szcześniak, M., Gaffney, D. J., Elo, L. L., Zhang, X., et al. (2016). A survey of best practices for RNA-seq data analysis. *Genome Biology* 17,.

Crupi, R., Marino, A. and Cuzzocrea, S. (2013). n-3 fatty acids: role in neurogenesis and neuroplasticity. *Curr Med Chem* 20, 2953–63.

Cvekl, A. and Wang, W.-L. (2009). Retinoic acid signaling in mammalian eye development. *Experimental Eye Research* 89, 280–291.

Das, I., Sparrow, J. R., Lin, M. I., Shih, E., Mikawa, T. and Hempstead, B. L. (2000). Trk C Signaling Is Required for Retinal Progenitor Cell Proliferation. *J Neurosci* 20, 2887–2895.

Das, G., Choi, Y., Sicinski, P. and Levine, E. M. (2009). Cyclin D1 fine-tunes the neurogenic output of embryonic retinal progenitor cells. *Neural Development* 4, 15.

Das, G., Clark, A. M. and Levine, E. M. (2012). Cyclin D1 inactivation extends proliferation and alters histogenesis in the postnatal mouse retina. *Developmental dynamics : an official publication of the American Association of Anatomists* 241, 941–52.

Demitrack, E. S. and Samuelson, L. C. (2016). Notch regulation of gastrointestinal stem cells. *J Physiology* 594, 4791–4803.

Dhomen, N. S., Balaggan, K. S., Pearson, R. A., Bainbridge, J. W., Levine, E. M., Ali, R. R. and Sowden, J. C. (2006). Absence of chx10 causes neural progenitors to persist in the adult retina. *Investigative ophthalmology & visual science* 47, 386–96.

Dobin, A., Davis, C. A., Schlesinger, F., Drenkow, J., Zaleski, C., Jha, S., Batut, P., Chaisson, M. and Gingeras, T. R. (2013). STAR: ultrafast universal RNA-seq aligner. *Bioinformatics* 29, 15–21.

Dorsky, R. I., Rapaport, D. H. and Harris, W. A. (1995). Xotch inhibits cell differentiation in the Xenopus retina. *Neuron* 14, 487 496.

Dorval, K. M., Bobechko, B. P., Ahmad, F. K. and Bremner, R. (2005). Transcriptional Activity of the Paired-like Homeodomain Proteins CHX10 and VSX1. *Journal of Biological Chemistry* 280, 10100–10108.

Erclik, T., Hartenstein, V., Lipshitz, H. D. and McInnes, R. R. (2008). Conserved Role of the Vsx Genes Supports a Monophyletic Origin for Bilaterian Visual Systems. *Curr Biol* 18, 1278–1287.

Fisher, A. L. and Caudy, M. (1998). Groucho proteins: transcriptional corepressors for specific subsets of DNA-binding transcription factors in vertebrates and invertebrates. *Gene Dev* 12, 1931–1940.

Frambach, S. J. C. M., Haas, R. de, Smeitink, J. A. M., Rongen, G. A., Russel, F. G. M. and Schirris, T. J. J. (2020). Brothers in Arms: ABCA1- and ABCG1-Mediated Cholesterol Efflux as Promising Targets in Cardiovascular Disease Treatment. *Pharmacol Rev* 72, 152–190.

Fuhrmann, S. (2010). Eye morphogenesis and patterning of the optic vesicle. *Current topics in developmental biology* 93, 61–84.

Fuhrmann, V., Kinkl, N., Leveillard, T., Sahel, J. and Hicks, D. (1999). Fibroblast growth factor receptor 4 (FGFR4) is expressed in adult rat and human retinal photoreceptors and neurons. *J Mol Neurosci* 13, 187–197.

Gago-Rodrigues, I., Fernández-Miñán, A., Letelier, J., Naranjo, S., Tena, J. J., Gómez-Skarmeta, J. L. L. and Martinez-Morales, J. R. (2015). Analysis of opo cis-regulatory landscape uncovers Vsx2 requirement in early eye morphogenesis. *Nature communications* 6, 7054.

Galliot, B., Vargas, C. de and Miller, D. (1999). Evolution of homeobox genes: Q50 Paired-like genes founded the Paired class. *Dev Genes Evol* 209, 186–197.

Gamm, D. M., Clark, E., Capowski, E. E. and Singh, R. (2019). The Role of Fgf9 In The Production of Neural Retina And Rpe In A Pluripotent Stem Cell Model of Early Human Retinal Development. *Am J Ophthalmol*.

García-Llorca, A., Aspelund, S. G., Ogmundsdottir, M. H., Steingrimsson, E. and Eysteinsson, T. (2019). The microphthalmia-associated transcription factor (Mitf) gene and its role in regulating eye function. *Sci Rep-uk* 9, 15386.

Garg, M. (2021). Advances in Animal Genomics. 61–73.

Georgi, S. A. and Reh, T. A. (2010). Dicer Is Required for the Transition from Early to Late Progenitor State in the Developing Mouse Retina. *The Journal of Neuroscience* 30,.

Giacinti, C. and Giordano, A. (2006). RB and cell cycle progression. *Oncogene* 25, 5220–5227.

Gordon, P. J., Yun, S., Clark, A. M., Monuki, E. S., Murtaugh, L. C. and Levine, E. M. (2013). Lhx2 balances progenitor maintenance with neurogenic output and promotes competence state progression in the developing retina. *The Journal of neuroscience : the official journal of the Society for Neuroscience* 33, 12197–207.

Graw, J. (2010). Chapter Ten Eye Development. *Curr Top Dev Biol* 90, 343–386.

Green, E. S., Stubbs, J. L. and Levine, E. M. (2003). Genetic rescue of cell number in a mouse model of microphthalmia: interactions between Chx10 and G1-phase cell cycle regulators. *Development* 130, 539–552.

Güner, G. and Lichtenthaler, S. F. (2020). The substrate repertoire of γ-secretase/presenilin. *Semin Cell Dev Biol* 105, 27–42.

Halder, G., Callaerts, P. and Gehring, W. J. (1995). Induction of Ectopic Eyes by Targeted Expression of the eyeless Gene in Drosophila. *Science* 267, 1788–1792.

Hardwick, L. J., Ali, F. R., Azzarelli, R. and Philpott, A. (2014). Cell cycle regulation of proliferation versus differentiation in the central nervous system. *Cell and Tissue Research*.

Hashimoto, T., Zhang, X.-M. M., Chen, B. Y. and Yang, X.-J. J. (2006). VEGF activates divergent intracellular signaling components to regulate retinal progenitor cell proliferation and neuronal differentiation. *Development (Cambridge, England)* 133, 2201–10.

Hatakeyama, J. and Kageyama, R. (2004). Retinal cell fate determination and bHLH factors. *Seminars in cell & developmental biology* 15, 83–9.

Hatakeyama, J., Tomita, K., Inoue, T. and Kageyama, R. (2001). Roles of homeobox and bHLH genes in specification of a retinal cell type. *Development* 128, 1313–1322.

Heavner, W. and Pevny, L. (2012). Eye Development and Retinogenesis. *Cold Spring Harbor Perspectives in Biology* 4, a008391.

Hemesath, T., Steingrimsson, E., McGill, G., Hansen, M., Vaught, J., Hodgkinson, C., Arnheiter, H., Copeland, N., Jenkins, N. and Fisher, D. (1994). microphthalmia, a critical factor in melanocyte development, defines a discrete transcription factor family. *Genes & Development* 8, 2770–2780.

Henrique, D., Hirsinger, E., Adam, J., Roux, I. L., Pourquié, O., Ish-Horowicz, D. and Lewis, J. (1997). Maintenance of neuroepithelial progenitor cells by Delta–Notch signalling in the embryonic chick retina. *Curr Biol* 7, 661–670.

Hodgkinson, C. A., Moore, K. J., Nakayama, A., Steingrímsson, E., Copeland, N. G., Jenkins, N. A. and Arnheiter, H. (1993). Mutations at the mouse microphthalmia locus are associated with defects in a gene encoding a novel basic-helix-loop-helix-zipper protein. *Cell* 74, 395–404.

Hoover, F., Seleiro, E. A., Kielland, A., Brickell, P. M. and Glover, J. C. (1998). Retinoid X receptor gamma gene transcripts are expressed by a subset of early generated retinal cells and eventually restricted to photoreceptors. *J Comp Neurology* 391, 204–13.

Horsford, D. J., Nguyen, M.-T. T., Sellar, G. C., Kothary, R., Arnheiter, H. and McInnes, R. R. (2005). Chx10 repression of Mitf is required for the maintenance of mammalian neuroretinal identity. *Development (Cambridge, England)* 132, 177–87.

Hsieh, Y.-W. W. and Yang, X.-J. J. (2009). Dynamic Pax6 expression during the neurogenic cell cycle influences proliferation and cell fate choices of retinal progenitors. *Neural development* 4, 32.

Hu, M. and Easter, S. S. (1999). Retinal Neurogenesis: The Formation of the Initial Central Patch of Postmitotic Cells. *Dev Biol* 207, 309–321.

Huang, J., Liu, Y., Oltean, A. and Beebe, D. C. (2015a). Bmp4 from the optic vesicle specifies murine retina formation. *Developmental Biology* 402, 119–126.

Huang, J., Liu, Y., Filas, B., Gunhaga, L. and Beebe, D. C. (2015b). Negative and positive auto-regulation of BMP expression in early eye development. *Developmental Biology* 407, 256–264.

Hufnagel, R. B., Le, T. T., Riesenberg, A. L. and Brown, N. L. (2010). Neurog2 controls the leading edge of neurogenesis in the mammalian retina. *Developmental biology* 340, 490–503.

Hurtado, C., Safarova, A., Smith, M., Chung, R., Bruyneel, A. A. N., Gomez-Galeno, J., Oswald, F., Larson, C. J., Cashman, J. R., Ruiz-Lozano, P., et al. (2019). Disruption of NOTCH signaling by a small molecule inhibitor of the transcription factor RBPJ. *Sci Rep-uk* 9, 10811.

Hutcheson, D. A., Hanson, M. I., Moore, K. B., Le, T. T., Brown, N. L. and Vetter, M. L. (2005). bHLH-dependent and -independent modes of Ath5 gene regulation during retinal development. *Development* 132, 829–839.

Hyer, J., Mima, T. and Mikawa, T. (1998). FGF1 patterns the optic vesicle by directing the placement of the neural retina domain. *Development (Cambridge, England)* 125, 869–77.

Iseri, S. U., Wyatt, A. W., Nürnberg, G., Kluck, C., Nürnberg, P., Holder, G. E., Blair, E., Salt, A. and Ragge, N. K. (2010). Use of genome-wide SNP homozygosity mapping in small pedigrees to identify new mutations in VSX2 causing recessive microphthalmia and a semidominant inner retinal dystrophy. *Hum Genet* 128, 51–60.

Jadhav, A. P., Cho, S.-H. H. and Cepko, C. L. (2006). Notch activity permits retinal cells to progress through multiple progenitor states and acquire a stem cell property. *Proceedings of the National Academy of Sciences of the United States of America* 103, 18998–9003.

Jasnos, L. and Korona, R. (2007). Epistatic buffering of fitness loss in yeast double deletion strains. *Nat Genet* 39, 550–554.

Jennings, B. H., Pickles, L. M., Wainwright, S. M., Roe, S. M., Pearl, L. H. and Ish-Horowicz, D. (2006). Molecular Recognition of Transcriptional Repressor Motifs by the WD Domain of the Groucho/TLE Corepressor. *Mol Cell* 22, 645–655.

Jensen, A. M. and Wallace, V. A. (1997). Expression of Sonic hedgehog and its putative role as a precursor cell mitogen in the developing mouse retina. *Development* 124, 363–371.

Jin, K. and Xiang, M. (2017). Transitional Progenitors during Vertebrate Retinogenesis. *Mol Neurobiol* 54, 3565 3576.

Katoh, K., Omori, Y., Onishi, A., Sato, S., Kondo, M. and Furukawa, T. (2010). Blimp1 suppresses Chx10 expression in differentiating retinal photoreceptor precursors to ensure proper photoreceptor development. *J Neurosci Official J Soc Neurosci* 30, 6515–26.

Kaufman, M. L., Park, K. U., Goodson, N. B., Chew, S., Bersie, S., Jones, K. L., Lamba, D. A. and Brzezinski, J. A. (2019). Transcriptional profiling of murine retinas undergoing semi-synchronous cone photoreceptor differentiation. *Dev Biol* 453, 155–167.

Kim, H.-T. and Kim, J. (2012). Compartmentalization of vertebrate optic neuroephithelium: External cues and transcription factors. 33,.

Kindiakov, B. N. and Koniukhov, B. V. (1986). [Mutant gene expression in murine aggregation chimeras. 5. The ocular retardation and fidget genes]. *Ontogenez* 17, 47–55.

Kokkinopoulos, I., Pearson, R., Macneil, A., Dhomen, N., MacLaren, R., Ali, R. and Sowden, J. (2008). Isolation and characterisation of neural progenitor cells from the adult Chx10(orJ/orJ) central neural retina. *Molecular and cellular neurosciences* 38, 359–73.

Konyukhov, B. and Sazhina, M. (1966). Interaction of the genes of ocular retardation and microphthalmia in mice. *Folia biologica* 12, 116–23.

Krämer, A., Green, J., Pollard, J. and Tugendreich, S. (2014). Causal analysis approaches in Ingenuity Pathway Analysis. *Bioinformatics* 30, 523–530.

Kubo, F., Takeichi, M. and Nakagawa, S. (2003). Wnt2b controls retinal cell differentiation at the ciliary marginal zone. *Development* 130, 587–598.

Kubo, F., Takeichi, M. and Nakagawa, S. (2005). Wnt2b inhibits differentiation of retinal progenitor cells in the absence of Notch activity by downregulating the expression of proneural genes. *Development* 132, 2759–2770.

Kusnadi, E. P., Timpone, C., Topisirovic, I., Larsson, O. and Furic, L. (2021). Regulation of gene expression via translational buffering. *Biochimica Et Biophysica Acta Bba - Mol Cell Res* 1869, 119140.

Laessing, U. and Stuermer, C. A. O. (1996). Spatiotemporal pattern of retinal ganglion cell differentiation revealed by the expression of neurolin in embryonic zebrafish. *J Neurobiol* 29, 65–74.

Lee, A. Y., Perreault, R., Harel, S., Boulier, E. L., Suderman, M., Hallett, M. and Jenna, S. (2010). Searching for Signaling Balance through the Identification of Genetic Interactors of the Rab Guanine-Nucleotide Dissociation Inhibitor gdi-1. *Plos One* 5, e10624.

Lehner, B. (2011). Molecular mechanisms of epistasis within and between genes. *Trends Genet* 27, 323–331.

Levine, E. M. and Green, E. S. (2004). Cell-intrinsic regulators of proliferation in vertebrate retinal progenitors. *Seminars in cell & developmental biology* 15, 63–74.

Levine, E., Hitchcock, P., Glasgow, E. and Schechter, N. (1994). Restricted expression of a new paired-class homeobox gene in normal and regenerating adult goldfish retina. *The Journal of comparative neurology* 348, 596–606.

Levine, E. M., Roelink, H., Turner, J. and Reh, T. A. (1997). Sonic Hedgehog Promotes Rod Photoreceptor Differentiation in Mammalian Retinal Cells In Vitro. *The Journal of Neuroscience* 17,.

Liang, L. and Sandell, J. H. (2007). Focus on molecules: homeobox protein Chx10. *Experimental eye research* 86, 541–2.

Lillien, L. and Cepko, C. (1992). Control of proliferation in the retina: temporal changes in responsiveness to FGF and TGF alpha.

Liu, I. S. C., Chen, J., Ploder, L., Vidgen, D., Kooy, D. van der, Kalnins, V. I. and Mclnnes, R. R. (1994). Developmental expression of a novel murine homeobox gene (Chx10): Evidence for roles in determination of the neuroretina and inner nuclear layer. *Neuron* 13, 377–393.

Liu, H., Xu, S., Wang, Y., Mazerolle, C., Thurig, S., Coles, B. L., Ren, J.-C. C., Taketo, M. M., Kooy, D. van der and Wallace, V. A. (2007). Ciliary margin transdifferentiation from neural retina is controlled by canonical Wnt signaling. *Developmental biology* 308, 54–67.

Locker, M., Agathocleous, M., Amato, M. A., Parain, K., Harris, W. A. and Perron, M. (2006). Hedgehog signaling and the retina: insights into the mechanisms controlling the proliferative properties of neural precursors. *Genes & development* 20, 3036–48.

Love, M. I., Huber, W. and Anders, S. (2014). Moderated estimation of fold change and dispersion for RNA-seq data with DESeq2. *Genome Biol* 15, 550.

Lundberg, A. S. and Weinberg, R. A. (1999). Control of the cell cycle and apoptosis1Reprinted from Eur J Cancer 1999, 35(4), 531–539. Please use this reference when citing this article.1. *Eur J Cancer* 35, 1886–1894.

Luo, H., Jin, K., Xie, Z., Qiu, F., Li, S., Zou, M., Cai, L., Hozumi, K., Shima, D. T. and Xiang, M. (2012). Forkhead box N4 (Foxn4) activates Dll4-Notch signaling to suppress photoreceptor cell fates of early retinal progenitors. *Proceedings of the National Academy of Sciences of the United States of America* 109, E553-62.

Lyu, J. and Mu, X. (2021). Genetic control of retinal ganglion cell genesis. *Cell Mol Life Sci* 78, 4417–4433.

Marquardt, T., Ashery-Padan, R., Andrejewski, N., Scardigli, R., Guillemot, F. and Gruss, P. (2001). Pax6 is required for the multipotent state of retinal progenitor cells. *Cell* 105, 43–55.

Martinez-Morales, J. R. (2016). Organogenetic Gene Networks. *springer* 259–274.

Martinez-Morales, J.-R. R., Bene, F. D., Nica, G., Hammerschmidt, M., Bovolenta, P. and Wittbrodt, J. (2005). Differentiation of the vertebrate retina is coordinated by an FGF signaling center. *Developmental cell* 8, 565–74.

Martinez-Morales, J.-R., Cavodeassi, F. and Bovolenta, P. (2017). Coordinated Morphogenetic Mechanisms Shape the Vertebrate Eye. *Frontiers in Neuroscience* 11, 721.

Masai, I., Stemple, D. L., Okamoto, H. and Wilson, S. W. (2000). Midline Signals Regulate Retinal Neurogenesis in Zebrafish. *Neuron* 27, 251–263.

Matsushima, D., Heavner, W. and Pevny, L. H. (2011). Combinatorial regulation of optic cup progenitor cell fate by SOX2 and PAX6. *Development (Cambridge, England)* 138, 443–54.

McCabe, K. L., Gunther, E. C. and Reh, T. A. (1999). The development of the pattern of retinal ganglion cells in the chick retina: mechanisms that control differentiation. *Development* 126, 5713–5724.

McCabe, K. L., McGuire, C. and Reh, T. A. (2006). Pea3 expression is regulated by FGF signaling in developing retina. *Dev. Dyn.* 235, 327–335.

Merilahti, J. A. M. and Elenius, K. (2019). Gamma-secretase-dependent signaling of receptor tyrosine kinases. *Oncogene* 38, 151–163.

Merilahti, J. A. M., Ojala, V. K., Knittle, A. M., Pulliainen, A. T. and Elenius, K. (2017). Genome-wide screen of gamma-secretase–mediated intramembrane cleavage of receptor tyrosine kinases. *Mol Biol Cell* 28, 3123–3131.

Miale, I. L. and Sidman, R. L. (1961). An autoradiographic analysis of histogenesis in the mouse cerebellum. *Exp Neurol* 4, 277–296.

Miesfeld, J. B., Moon, M., Riesenberg, A. N., Contreras, A. N., Kovall, R. A. and Brown, N. L. (2018). Rbpj direct regulation of Atoh7 transcription in the embryonic mouse retina. *Scientific Reports* 8, 10195.

Mills, E. A. and Goldman, D. (2017). The Regulation of Notch Signaling in Retinal Development and Regeneration. *Current Pathobiology Reports* 5, 323–331.

Miton, C. M., Buda, K. and Tokuriki, N. (2021). Epistasis and intramolecular networks in protein evolution. *Curr Opin Struc Biol* 69, 160–168.

Moore, R. and Alexandre, P. (2020). Delta-Notch Signaling: The Long and the Short of a Neuron's Influence on Progenitor Fates. *J Dev Biology* 8, 8.

Morest, D. K. (1970). The pattern of neurogenesis in the retina of the rat. *Zeitschrift Für Anatomie Und Entwicklungsgeschichte* 131, 45–67.

Mori, M., Ghyselinck, N. B., Chambon, P. and Mark, M. (2001). Systematic immunolocalization of retinoid receptors in developing and adult mouse eyes. *Invest Ophth Vis Sci* 42, 1312–8.

Muhr, J., Andersson, E., Persson, M., Jessell, T. M. and Ericson, J. (2001). Groucho-Mediated Transcriptional Repression Establishes Progenitor Cell Pattern and Neuronal Fate in the Ventral Neural Tube. *Cell* 104, 861–873.

Mui, S. H., Kim, J., Lemke, G. and Bertuzzi, S. (2005). Vax genes ventralize the embryonic eye. *Genes & Development* 19, 1249–1259.

Murali, D., Yoshikawa, S., Corrigan, R. R., Plas, D. J., Crair, M. C., Oliver, G., Lyons, K. M., Mishina, Y. and Furuta, Y. (2005). Distinct developmental programs require different levels of Bmp signaling during mouse retinal development. *Development* 132, 913–923.

Murata, K., Hattori, M., Hirai, N., Shinozuka, Y., Hirata, H., Kageyama, R., Sakai, T. and Minato, N. (2005). Hes1 Directly Controls Cell Proliferation through the Transcriptional Repression of p27 Kip1. *Mol Cell Biol* 25, 4262–4271.

Nelson, B. R., Gumuscu, B., Hartman, B. H. and Reh, T. A. (2006). Notch activity is downregulated just prior to retinal ganglion cell differentiation. *Developmental neuroscience* 28, 128–41.

Nelson, B. R., Hartman, B. H., Georgi, S. A., Lan, M. S. and Reh, T. A. (2007). Transient inactivation of Notch signaling synchronizes differentiation of neural progenitor cells. *Developmental biology* 304, 479–98.

Nerli, E., Rocha-Martins, M. and Norden, C. (2020). Asymmetric neurogenic commitment of retinal progenitors involves Notch through the endocytic pathway. *Elife* 9, e60462.

Nguyen, M. and Arnheiter, H. (2000). Signaling and transcriptional regulation in early mammalian eye development: a link between FGF and MITF. *Dev Camb Engl* 127, 3581–91.

Nie, B., Nie, T., Hui, X., Gu, P., Mao, L., Li, K., Yuan, R., Zheng, J., Wang, H., Li, K., et al. (2017). Brown Adipogenic Reprogramming Induced by a Small Molecule. *Cell Reports* 18, 624–635.

Ohsaki, K., Morimitsu, T., Ishida, Y., Kominami, R. and Takahashi, N. (1999). Expression of the Vax family homeobox genes suggests multiple roles in eye development. *Genes Cells* 4, 267–276.

Ohsawa, R. and Kageyama, R. (2008). Regulation of retinal cell fate specification by multiple transcription factors. *Brain research* 1192, 90–8.

Ohtsuka, T., Ishibashi, M., Gradwohl, G., Nakanishi, S., Guillemot, F. and Kageyama, R. (1999). Hes1 and Hes5 as Notch effectors in mammalian neuronal differentiation. *Embo J* 18, 2196–2207.

Olsauskas-Kuprys, R., Zlobin, A. and Osipo, C. (2013). Gamma secretase inhibitors of Notch signaling. *Oncotargets Ther* 6, 943–955.

Osipov, V. V. and Vakhrusheva, M. P. (1984). [Clonal analysis of the development of the pigment epithelium of the eye in chimeric or/or----AKR mice]. *Ontogenez* 15, 73–80.

Pacal, M. and Bremner, R. (2014). Induction of the ganglion cell differentiation program in human retinal progenitors before cell cycle exit. *Dev Dynam* 243, 712–729.

Pandit, T., Jidigam, V. K., Patthey, C. and Gunhaga, L. (2015). Neural retina identity is specified by lens-derived BMP signals. *Development* 142, 1850–1859.

Percin, E. F., Ploder, L. A., Yu, J. J., Arici, K., Horsford, D. J., Rutherford, A., Bapat, B., Cox, D. W., Duncan, A. M. V., Kalnins, V. I., et al. (2000). Human microphthalmia associated with mutations in the retinal homeobox gene CHX10. *Nat Genet* 25, 397–401.

Perron, M. and Harris, W. A. (2000). Determination of vertebrate retinal progenitor cell fate by the Notch pathway and basic helix-loop-helix transcription factors. *Cell Mol Life Sci Cmls* 57, 215 223.

Philips, G. T., Stair, C. N., Lee, H., Wroblewski, E., Berberoglu, M. A., Brown, N. L. and Mastick, G. S. (2005). Precocious retinal neurons: Pax6 controls timing of differentiation and determination of cell type. *Developmental Biology* 279, 308–321.

Picker, A., Cavodeassi, F., Machate, A., Bernauer, S., Hans, S., Abe, G., Kawakami, K., Wilson, S. W. and Brand, M. (2009). Dynamic Coupling of Pattern Formation and Morphogenesis in the Developing Vertebrate Retina. *PLoS Biology* 7, e1000214.

Planas-Silva, M. D. and Weinberg, R. A. (1997). The restriction point and control of cell proliferation. *Curr Opin Cell Biol* 9, 768–772.

Porter, F. D., Drago, J., Xu, Y., Cheema, S. S., Wassif, C., Huang, S. P., Lee, E., Grinberg, A., Massalas, J. S., Bodine, D., et al. (1997). Lhx2, a LIM homeobox gene, is required for eye, forebrain, and definitive erythrocyte development. *Development* 124, 2935–2944.

Prada, C., Puga, J., Pérez-Méndez, L., López, R. and Ramírez, G. (1991). Spatial and Temporal Patterns of Neurogenesis in the Chick Retina. *Eur J Neurosci* 3, 559–569.

Raay, T. J., Moore, K. B., Iordanova, I., Steele, M., Jamrich, M., Harris, W. A. and Vetter, M. L. (2005). Frizzled 5 signaling governs the neural potential of progenitors in the developing Xenopus retina. *Neuron* 46, 23–36.

Rapaport, D. H., Wong, L. L., Wood, E. D., Yasumura, D. and LaVail, M. M. (2004). Timing and topography of cell genesis in the rat retina. *Journal of Comparative Neurology* 474, 304–324.

Rapaport, F., Khanin, R., Liang, Y., Pirun, M., Krek, A., Zumbo, P., Mason, C. E., Socci, N. D. and Betel, D. (2013). Comprehensive evaluation of differential gene expression analysis methods for RNA-seq data. *Genome Biol* 14, 3158.

Rauscher, R., Bampi, G. B., Guevara-Ferrer, M., Santos, L. A., Joshi, D., Mark, D., Strug, L. J., Rommens, J. M., Ballmann, M., Sorscher, E. J., et al. (2021). Positive epistasis between disease-causing missense mutations and silent polymorphism with effect on mRNA translation velocity. *Proc National Acad Sci* 118, e2010612118.

Reis, L., Khan, A., Kariminejad, A., Ebadi, F. and Tyler, R. (2011). VSX2 mutations in autosomal recessive microphthalmia.

Riesenberg, A. N., Le, T. T., Willardsen, M. I., Blackburn, D. C., Vetter, M. L. and Brown, N. L. (2009a). Pax6 regulation of Math5 during mouse retinal neurogenesis. *genesis* 47, 175–187.

Riesenberg, A. N., Liu, Z., Kopan, R. and Brown, N. L. (2009b). Rbpj cell autonomous regulation of retinal ganglion cell and cone photoreceptor fates in the mouse retina. *J Neurosci* 29, 12865 12877.

Roberts, M. R., Hendrickson, A., McGuire, C. R. and Reh, T. A. (2005). Retinoid X Receptor γ Is Necessary to Establish the S-opsin Gradient in Cone Photoreceptors of the Developing Mouse Retina. *Investigative Opthalmology Vis Sci* 46, 2897.

Rotstein, N. P., Politi, L. E. and Aveldaño, M. I. (1998). Docosahexaenoic acid promotes differentiation of developing photoreceptors in culture. *Invest Ophth Vis Sci* 39, 2750–8.

Rowan, S., Chen, C.-M. A. M., Young, T. L., Fisher, D. E. and Cepko, C. L. (2004). Transdifferentiation of the retina into pigmented cells in ocular retardation mice defines a new function of the homeodomain gene Chx10. *Development (Cambridge, England)* 131,.

Roy, A., Melo, J. de, Chaturvedi, D., Thein, T., Cabrera-Socorro, A., Houart, C., Meyer, G., Blackshaw, S. and Tole, S. (2013). LHX2 Is Necessary for the Maintenance of Optic Identity and for the Progression of Optic Morphogenesis. *J Neurosci* 33, 6877–6884.

Sakagami, K., Gan, L. and Yang, X.-J. (2009). Distinct Effects of Hedgehog Signaling on Neuronal Fate Specification and Cell Cycle Progression in the Embryonic Mouse Retina. *J Neurosci* 29, 6932–6944.

Sameith, K., Amini, S., Koerkamp, M. J. A. G., Leenen, D. van, Brok, M., Brabers, N., Lijnzaad, P., Hooff, S. R. van, Benschop, J. J., Lenstra, T. L., et al. (2015). A high-resolution gene expression atlas of epistasis between gene-specific transcription factors exposes potential mechanisms for genetic interactions. *Bmc Biol* 13, 112.

Sánchez-Sánchez, A. V., Camp, E., Leal-Tassias, A. and Mullor, J. L. (2010). Wnt signaling has different temporal roles during retinal development. *Dev Dynam* 239, 297–310.

Schafer, K. A. (1998). The Cell Cycle: A Review. *Vet Pathol* 35, 461–478.

Schindelin, J., Arganda-Carreras, I., Frise, E., Kaynig, V., Longair, M., Pietzsch, T., Preibisch, S., Rueden, C., Saalfeld, S., Schmid, B., et al. (2012). Fiji: an open-source platform for biological-image analysis. *Nat Methods* 9, 676–682.

Schwarz, M., Cecconi, F., Bernier, G., Andrejewski, N., Kammandel, B., Wagner, M. and Gruss, P. (2000). Spatial specification of mammalian eye territories by reciprocal transcriptional repression of Pax2 and Pax6. *Development (Cambridge, England)* 127, 4325–34.

Sharma, R. K. and Netland, P. A. (2007). Early born lineage of retinal neurons express class III β-tubulin isotype. *Brain Res* 1176, 11–17.

Shendure, J. (2008). The beginning of the end for microarrays? *Nat Methods* 5, 585–587.

Shiau, F., Ruzycki, P. A. and Clark, B. S. (2021). A single-cell guide to retinal development: Cell fate decisions of multipotent retinal progenitors in scRNA-seq. *Dev Biol* 478, 41–58.

Shih, I.-M. and Wang, T.-L. (2007). Notch Signaling, γ-Secretase Inhibitors, and Cancer Therapy. *Cancer Res* 67, 1879–1882.

Sigulinsky, C. L., Green, E. S., Clark, A. M. and Levine, E. M. (2008). Vsx2/Chx10 ensures the correct timing and magnitude of Hedgehog signaling in the mouse retina. *Developmental biology* 317, 560–75.

Sigulinsky, C. L., German, M. L., Leung, A. M., Clark, A. M., Yun, S. and Levine, E. M. (2015). Genetic chimeras reveal the autonomy requirements for Vsx2 in embryonic retinal progenitor cells. *Neural Dev* 10, 12.

Simandi, Z., Horvath, A., Cuaranta-Monroy, I., Sauer, S., Deleuze, J.-F. and Nagy, L. (2018). RXR heterodimers orchestrate transcriptional control of neurogenesis and cell fate specification. *Mol Cell Endocrinol* 471, 51–62.

Sinn, R. and Wittbrodt, J. (2013). An eye on eye development. *Mechanisms of development* 130, 347–58.

Skowronska-Krawczyk, D., Ballivet, M., Dynlacht, B. D. and Matter, J.-M. (2004). Highly specific interactions between bHLH transcription factors and chromatin during retina development. *Development* 131, 4447–4454.

Skowronska-Krawczyk, D., Chiodini, F., Ebeling, M., Alliod, C., Kundzewicz, A., Castro, D., Ballivet, M., Guillemot, F., Matter-Sadzinski, L. and Matter, J.-M. (2009). Conserved regulatory sequences in Atoh7 mediate non-conserved regulatory responses in retina ontogenesis. *Development* 136, 3767–3777.

Smirnov, V. M., Robert, M. P., Condroyer, C., Navarro, J., Antonio, A., Rozet, J.-M., Sahel, J.-A., Perrault, I., Audo, I. and Zeitz, C. (2022). Association of Missense Variants in VSX2 With a Peculiar Form of Congenital Stationary Night Blindness Affecting All Bipolar Cells. *Jama Ophthalmol* 140,.

Soneson, C. and Delorenzi, M. (2013). A comparison of methods for differential expression analysis of RNA-seq data. *BMC Bioinformatics* 14, 1–18.

Steinbuck, M. P. and Winandy, S. (2018). A Review of Notch Processing With New Insights Into Ligand-Independent Notch Signaling in T-Cells. *Front Immunol* 9, 1230.

Steingrímsson, E., Moore, K. J., Lamoreux, M. L., Ferré-D'Amaré, A. R., Burley, S. K., Zimring, D. C., Skow, L. C., Hodgkinson, C. A., Arnheiter, H. and Copeland, N. G. (1994). Molecular basis of mouse microphthalmia (mi) mutations helps explain their developmental and phenotypic consequences. *Nature genetics* 8, 256–63.

Steingrímsson, E., Arnheiter, H., Hallsson, J. H., Lamoreux, M. L., Copeland, N. G. and Jenkins, N. A. (2003). Interallelic Complementation at the Mouse Mitf Locus. *Genetics* 163, 267–276.

Stiemke, M. M. and Hollyfield, J. G. (1995). Cell birthdays in Xenopus laevis retina. *Differentiation* 58, 189–193.

Storti, F., Klee, K., Todorova, V., Steiner, R., Othman, A., Velde-Visser, S. van der, Samardzija, M., Meneau, I., Barben, M., Karademir, D., et al. (2019). Impaired ABCA1/ABCG1-mediated lipid efflux in the mouse retinal pigment epithelium (RPE) leads to retinal degeneration. *Elife* 8, e45100.

Strooper, B. D., Annaert, W., Cupers, P., Saftig, P., Craessaerts, K., Mumm, J. S., Schroeter, E. H., Schrijvers, V., Wolfe, M. S., Ray, W. J., et al. (1999). A presenilin-1-dependent γ-secretase-like protease mediates release of Notch intracellular domain. *Nature* 398, 518–522.

Sun, Y., Hao, M., Luo, Y., Liang, C., Silver, D. L., Cheng, C., Maxfield, F. R. and Tall, A. R. (2003). Stearoyl-CoA Desaturase Inhibits ATP-binding Cassette Transporter A1-mediated Cholesterol Efflux and Modulates Membrane Domain Structure*. *J Biol Chem* 278, 5813–5820.

Svendsen, P. C. and McGhee, J. D. (1995). The C. elegans neuronally expressed homeobox gene ceh-10 is closely related to genes expressed in the vertebrate eye. *Development* 121, 1253–1262.

Svoboda, K. K. and O'Shea, K. S. (1987). An analysis of cell shape and the neuroepithelial basal lamina during optic vesicle formation in the mouse embryo. *Development* 100, 185–200.

Take-uchi, M., Clarke, J. D. and Wilson, S. W. (2003). Hedgehog signalling maintains the optic stalk-retinal interface through the regulation of Vax gene activity. *Development* 130, 955–968.

Tétreault, N., Champagne, M.-P. and Bernier, G. (2009). The LIM homeobox transcription factor Lhx2 is required to specify the retina field and synergistically cooperates with Pax6 for Six6 trans-activation. *Developmental Biology* 327, 541–550.

Truslove, G. M. (1962). A gene causing ocular retardation in the mouse. *Journal of embryology and experimental morphology* 10, 652 660.

Urquiza, A. M. de, Liu, S., Sjöberg, M., Zetterström, R. H., Griffiths, W., Sjövall, J. and Perlmann, T. (2000). Docosahexaenoic Acid, a Ligand for the Retinoid X Receptor in Mouse Brain. *Science* 290, 2140–2144.

Vail, M. M. la, Rapaport, D. H. and Rakic, P. (1991). Cytogenesis in the monkey retina. *Journal of Comparative Neurology* 309,.

Visser, J. A. G. M. de, Cooper, T. F. and Elena, S. F. (2011). The causes of epistasis. *Proc Royal Soc B Biological Sci* 278, 3617–3624.

Vitorino, M., Jusuf, P. R., Maurus, D., Kimura, Y., Higashijima, S. and Harris, W. A. (2009). Vsx2 in the zebrafish retina: restricted lineages through derepression. *Neural Development* 4, 14.

Vorobyov, E. and Horst, J. (2006). Getting the Proto-Pax by the Tail. *J Mol Evol* 63, 153–164.

Wall, D. S., Mears, A. J., McNeill, B., Mazerolle, C., Thurig, S., Wang, Y., Kageyama, R. and Wallace, V. A. (2009). Progenitor cell proliferation in the retina is dependent on Notch-independent Sonic hedgehog/Hes1 activity. *The Journal of cell biology* 184, 101–12.

Walther, C., Guenet, J. L., Simon, D., Deutsch, U., Jostes, B., Goulding, M. D., Plachov, D., Balling, R. and Gruss, P. (1991). Pax: a murine multigene family of paired box-containing genes. *Genomics* 11, 424–34.

Wang, Y., Dakubo, G. D., Thurig, S., Mazerolle, C. J. and Wallace, V. A. (2005). Retinal ganglion cell-derived sonic hedgehog locally controls proliferation and the timing of RGC development in the embryonic mouse retina. *Development* 132, 5103–5113.

Wang, Z., Gerstein, M. and Snyder, M. (2009). RNA-Seq: a revolutionary tool for transcriptomics. *Nat Rev Genet* 10, 57–63.

Wavre-Shapton, S. T., Meschede, I. P., Seabra, M. C. and Futter, C. E. (2014). Phagosome maturation during endosome interaction revealed by partial rhodopsin processing in retinal pigment epithelium. *J Cell Sci* 127, 3852–3861.

Wen, B., Li, S., Li, H., Chen, Y., Ma, X., Wang, J., Lu, F., Qu, J. and Hou, L. (2016). Microphthalmia-associated transcription factor regulates the visual cycle genes Rlbp1 and Rdh5 in the retinal pigment epithelium. *Sci Rep-uk* 6, 21208.

Westenskow, P., Piccolo, S. and Fuhrmann, S. (2009). β-catenin controls differentiation of the retinal pigment epithelium in the mouse optic cup by regulating Mitf and Otx2 expression.

Wightman, B., Ha, I. and Ruvkun, G. (1993). Posttranscriptional regulation of the heterochronic gene lin-14 by lin-4 mediates temporal pattern formation in C. elegans. *Cell* 75, 855–862.

Willardsen, M. I., Suli, A., Pan, Y., Marsh-Armstrong, N., Chien, C.-B. B., El-Hodiri, H., Brown, N. L., Moore, K. B. and Vetter, M. L. (2009). Temporal regulation of Ath5 gene expression during eye development. *Developmental biology* 326, 471–81.

Wright, E. M., Perveen, R., Bowers, N., Ramsden, S., McCann, E., O'Driscoll, M., Lloyd, C. I., Clayton-Smith, J. and Black, G. C. (2010). VSX2 in microphthalmia: a novel splice site mutation producing a severe microphthalmia phenotype. *British Journal of Ophthalmology* 94, 386–388.

Xiang, L., Zhang, J., Rao, F.-Q., Yang, Q.-L., Zeng, H.-Y., Huang, S.-H., Xie, Z.-X., Lv, J.-N., Lin, D., Chen, X.-J., et al. (2022). Depletion of miR-96 Delays, But Does Not Arrest, Photoreceptor Development in Mice. *Invest Ophth Vis Sci* 63, 24.

Xu, S., Witmer, P. D., Lumayag, S., Kovacs, B. and Valle, D. (2007). MicroRNA (miRNA) Transcriptome of Mouse Retina and Identification of a Sensory Organ-specific miRNA Cluster*. *J Biol Chem* 282, 25053–25066.

Yang, S., Zhou, J. and Li, D. (2021). Functions and Diseases of the Retinal Pigment Epithelium. *Front Pharmacol* 12, 727870.

Young, R. (1985). Cell differentiation in the retina of the mouse.

Yun, S., Saijoh, Y., Hirokawa, K. E., Kopinke, D., Murtaugh, L. C., Monuki, E. S. and Levine, E. M. (2009). Lhx2 links the intrinsic and extrinsic factors that control optic cup formation. *Dev Camb Engl* 136, 3895–906.

Zhang, X.-M. and Yang, X.-J. (2001). Temporal and Spatial Effects of Sonic Hedgehog Signaling in Chick Eye Morphogenesis. *Dev Biol* 233, 271–290.

Zhang, H., Zhuang, P., Welchko, R. M., Dai, M., Meng, F. and Turner, D. L. Regulation of retinal amacrine cell generation by miR-216b and Foxn3. *Development* 149,.

Zhao, S., Hung, F.-C., Colvin, J. S., White, A., Dai, W., Lovicu, F. J., Ornitz, D. M. and Overbeek, P. A. (2001). Patterning the optic neuroepithelium by FGF signaling and Ras activation. *Development* 128, 5051–5060.

Zheng, M.-H., Shi, M., Pei, Z., Gao, F., Han, H. and Ding, Y.-Q. (2009). The transcription factor RBP-J is essential for retinal cell differentiation and lamination. *Mol Brain* 2, 38.

Zou, C. and Levine, E. M. (2012). Vsx2 controls eye organogenesis and retinal progenitor identity via homeodomain and non-homeodomain residues required for high affinity DNA binding. *PLoS genetics* 8,.

Zuber, M. E., Gestri, G., Viczian, A. S., Barsacchi, G. and Harris, W. A. (2003). Specification of the vertebrate eye by a network of eye field transcription factors. *Development* 130, 5155–5167.